Implications of a polymer meniscus implant on knee tribology

Sara Ehsani Majd

2016

This research forms part of the Project P2.03 TRAMMPOLIN of the research program of the BioMedical Materials Institute, co-funded by the Dutch Ministry of Economic Affairs.

The purchase of UMT-3 tribometer setup was done using the grant no. 91112026 from the Netherlands Organization for Health Research and Development (ZonMW).

The printing of this thesis was financially supported in part by Bruker Ltd.

Implications of a polymer meniscus implant on knee tribology
By **Sara Ehsani Majd**

University Medical Center Groningen, University of Groningen
Groningen, The Netherlands

Layout and cover design by Manuel N. Melo

Printed by Netzodruk, Groningen

ISBN (printed version): 978-90-367-8814-4
ISBN (electronic version): 978-90-367-8813-7

The cover design was inspired by the traditional Persian handicrafts of inlaid turquoise and copper.

rijksuniversiteit
groningen

Implications of a polymer meniscus implant on knee tribology

Proefschrift

ter verkrijging van de graad van doctor aan de
Rijksuniversiteit Groningen
op gezag van de
rector magnificus prof. dr. E. Sterken
en volgens besluit van het College voor Promoties.

De openbare verdediging zal plaatsvinden op

maandag 30 mei 2016 om 16.15 uur

door

Sara Ehsani Majd

geboren op 23 januari 1983
te Tehran, Iran

Promotor
Prof. dr. ir. H. J. Busscher

Copromotores
Dr. P. K. Sharma
Dr. R. Kuijer

Beoordelingscommissie
Prof. dr. S. K. Bulstra
Prof. dr. ir. E. van der Heide
Prof. dr. ir. N. Verdonschot

To my dear parents

تقدیم به پدر و مادر عزیزم

Paranimfen
Ekaterina Ovchinnikova
Rebecca van der Westen

Contents

Chapter 1

Introduction and Aim of the Thesis

THIS CHAPTER discusses the importance of tribology, and specifically biotribology, in the human body and synovial joints. Understanding of the composition and function of the articular cartilage, synovial fluid and meniscus and their role in the knee joint lubrication leads to a better understanding of this sophisticated, unique tribological system. Meniscal injuries impair the well-functioning of the knee joint. Therefore, these injuries and the current methods to treat them are also covered in this chapter.

Tribology and Biotribology

In 1966 the separate topics of friction, lubrication and wear were unified under the title "tribology"[1] related to the Greek word "tribo" meaning rubbing. In 1973, the title "biotribology" was introduced for tribological processes in the field of biology and medicine.[1] Since then the biotribology of different human tissues and organs has been studied, e.g., synovial joint, skin, hair, oral and ocular tribology.

Tribological (for man-made materials) and biotribological (for natural biological materials) systems differ in many aspects. The most important difference is in the nature of the lubricant used to facilitate low friction and wear. In man-made tribological systems, gears and bearings are mainly lubricated by oil-based lubricants. The viscosity of oil increases under high pressure (shear thickening), making it capable of forming a lubricating film in between the hard surfaces articulating at high speeds.[2] Biotribological systems, on the other hand, are lubricated by water-based lubricants, where water, as a Newtonian fluid, does not show the shear thickening property. It is the presence of large molecular weight biopolymers, e.g., proteins, glycoproteins and polysaccharides, that transforms water from a poor lubricant on its own to an outstanding lubricant in these systems. Glycoproteins like mucins and proteoglycan 4 (PRG4, also known as lubricin) in saliva, tears and synovial fluid play an essential role in oral, ocular and articular joint lubrication. Water-based lubricants are also used in the metal cutting, rolling and mining industry (to provide cooling and avoid fire and explosions) and in the food, textile and pharmaceutical industries (to avoid final product contamination). Another important difference between a tribological and a biotribological system is the hardness of the involved surfaces and contact pressure. In biological systems the contact generally occurs between soft–soft surfaces at low contact pressures; surfaces with low elastic modulus, e.g., tongue, eye and cartilage deform elastically or viscoelastically under heavy loads and reduce the contact pressure due to an increase in the contact area at the sliding interface. The exception is enamel sliding against enamel, where the contact pressures can be as high as 86 MPa.[3] In man-made tribological systems, on the other hand, the contact occurs between hard–hard surfaces, e.g., gears and rolling element bearings, or hard–soft surfaces, e.g., rubber seals and tire–road contact, and they operate at much higher contact pressures compared to biotribological systems. The sliding direction and speed are also different between tribological and biotribological systems. Reciprocating sliding at low speeds is most common for biotribological systems with maximum speeds of 80−100 mm/s,[4] found for eyelid closure during blinking. In tribological systems continuous unidirectional rotation and rolling at high speeds is most commonly observed.

Synovial Joints in the Human Body

Synovial (diarthrodial) joints occur at the articulation of long bones. The movement of these bones is coupled through constrained motion within the joint. The terminal parts of the bones are covered with a thin layer (1–5 mm)[1] of hydrated, avascular articular cartilage and are submerged in synovial fluid. The joint cavity is sealed with the synovial membrane. Synovial joints include hip, knee, shoulder, elbow, ankle and finger joints. Well-functioning joints are essential for human mobility and quality of life. A healthy synovial joint provides a unique articulation between the contacting tissues, with ultralow values of coefficient of friction (COF ~0.001–0.005) and an exceptional protection against wear under high loads.[5,6] The bearing material—cartilage—is composed of chondrocytes and depending on species and joint, it possesses specific structural details.[7] In humans, the articular cartilage consists of 70–80% water. 2% of the cartilage volume consists of chondrocytes and the other 98% is extra-cellular matrix (ECM) produced by the chondrocytes. The dry weight of ECM contains 50–75% collagen, 15–30% proteoglycans and 10% lipids (mainly phospholipids).[7–9] The collagen content of the articular cartilage is predominantly type II collagen (~90%).[8,9] Proteoglycans are composed by a protein core with many glycosaminoglycans (GAGs) attached to it.[9] GAGs are linear polysaccharide chains, consisting of repeating disaccharides.[9] The GAG content of the articular cartilage consists of chondroitin sulfate, keratan sulfate, dermatan sulfate and hyaluronan.[8,9] Chondroitin sulfate and keratan sulfate are the most abundant GAGs in the articular cartilage; hyaluronan (HA) is the only non-sulfated GAG, and the only one not part of a proteoglycan.[8,9] Aggrecan, the most abundant proteoglycan in the ECM, is a large, highly glycosylated macromolecule, consisting of a central protein core of 230 kDa substituted with chondroitin sulfate and keratin sulfate.[8,9] These GAG chains are covalently bound to the aggrecan protein core and form a bottlebrush-like structure.[9,10] Aggrecan molecules are further noncovalently bound to a single long chain of HA, forming large aggrecan aggregates (M_w ~50–100 MDa).[9] In the ECM a gel of hydrated proteoglycans is trapped in a dense network of thin collagen fibers.[9]

Next to the bone there is a tidemark separating the calcified and non-calcified cartilage, which is followed by three distinguishable zones of the articular cartilage towards the joint surface: deep/radial, middle/transitional and superficial/tangential zones (**Figure 1A,B**).[7–9] The latter zone is in contact with the synovial fluid. These zones have different chondrocyte morphology, collagen fiber orientation, biochemical composition and mechanical properties.[7–9] In the deep zone, the collagen fibers are anchored to the bone and are mostly oriented perpendicular to the cartilage surface; the proteoglycan content is much lower than the middle zone

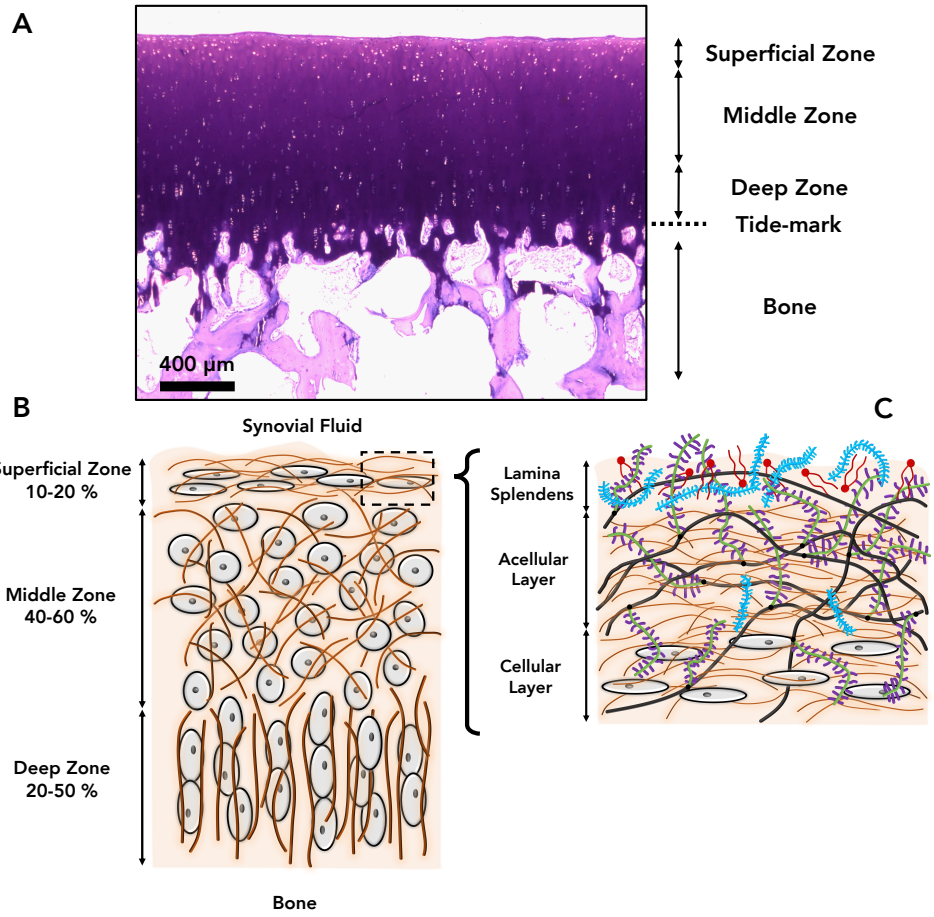

Figure 1. A: A low power image of a section of bovine articular cartilage tissue, stained with thionine. **B:** A schematic illustration of the chondrocytes and collagen fibers orientation within the articular cartilage, organized in three distinguishable zones: superficial, middle and deep zones, containing 10−20%, 40−60% and 20−50% of the overall tissue depth, respectively. **C:** A schematic illustration of three distinguishable zones of the superficial layer of the articular cartilage: cellular layer, acellular layer and lamina splendens; PRG4 (in blue), aggrecan (with green protein core and purple GAGs attached to it), HA (in black) and surface-active phospholipids (in red) are shown next to flattened chondrocytes and collagen fibers. The schematics are not to scale.

and the chondrocyte content is the lowest of the three zones. The slightly elongated chondrocytes are grouped together in columns and oriented parallel to the collagen fibers, i.e., perpendicular to the cartilage surface.[7–9] In the middle zone, the collagen fibers are randomly oriented, proteoglycan content is the highest and chondrocytes become spherical and randomly scattered.[7–9] The superficial zone contains collagen fibers oriented mainly parallel to the surface, has a relatively low proteoglycan content and has chondrocytes with a flattened morphology.[7–9] The superficial zone of the articular cartilage has several distinguishable regions itself (**Figure 1C**):[7–9] its lower section contains flattened chondrocytes with their long axis parallel to the surface; just above lies a thin acellular layer consisting of collagen fibers and rich in hyaluronan; the topmost part is a thin layer called lamina splendens, containing high amounts of PRG4 and phospholipids. The origin and function of this top layer is not yet fully understood.[7–9] In the superficial zone of the articular cartilage the chondrocytes synthesize a superficial zone protein (SZP, also known as PRG4) which has an important role in the lubrication and surface properties of the articular cartilage. The SZP has a large, highly glycosylated mucin-like main core ending in globular domains—the C-terminal region is a hemopexin-like domain whereas the N-terminal region consists of two somatomedin B domains and a heparin binding domain.[7–9]

Synovial fluid, a dialysate of blood plasma with water as a major component (~85% of the total weight), lubricates the bearing surfaces. Beside blood plasma components,[11] synovial fluid contains a high concentration of HA (1−4 mg/mL)[12,13] —responsible for the high viscosity of the fluid with a relative viscosity >300[14]—, PRG4 (0.052−0.350 mg/mL)[15,16] and surface-active phospholipids (SAPL, 0.1−0.2 mg/mL).[17–19] A healthy human knee joint contains approximately 2 mL of synovial fluid.[20]

The meniscus is a unique element of the knee joint and is essential for its proper functioning. Medial and lateral menisci are crescent-wedge-shaped, fibrocartilaginous tissues, located in between the weight-bearing surfaces of tibia and femur (**Figure 2**).[21] Water is their major component (63−75% of the total weight). 75% of the dry weight of meniscus consists of collagen (mostly type I collagen) (**Figure 3**) and 2.5% consists of proteoglycan (mainly aggrecan).[22] In humans, the medial meniscus is 40.5−45.5 mm long and 27 mm wide, and the lateral meniscus is 32.4−35.7 mm long and 26.6−29.3 mm wide.[21] The mobility of the medial and lateral menisci is limited by ligaments. Menisco-tibial ligaments connect both menisci to the tibia plateau. Menisco-femoral ligaments (the Wrisberg and Humphry ligaments) connect the lateral meniscus to the femur.[23] The total incidence of at least one of the menisco-femoral ligaments existing is 92%, while the

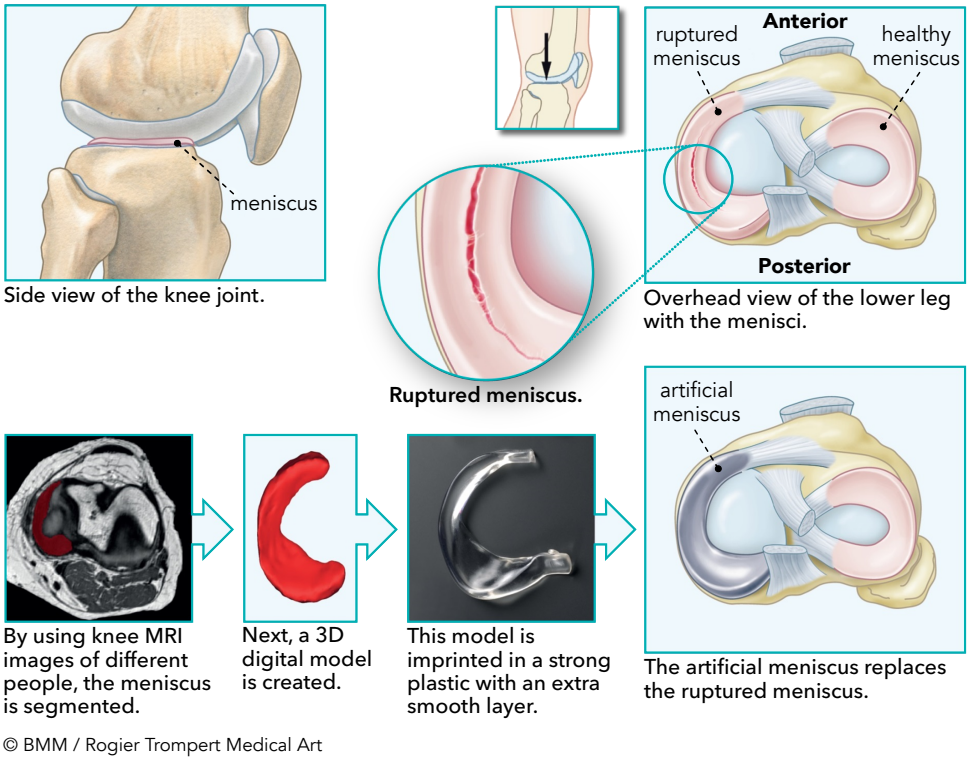

Figure 2. A summary of the TRAMMPOLIN project showing the anatomy of the knee joint, menisci and meniscal tear, and TRAMMPOLIN meniscus implant.

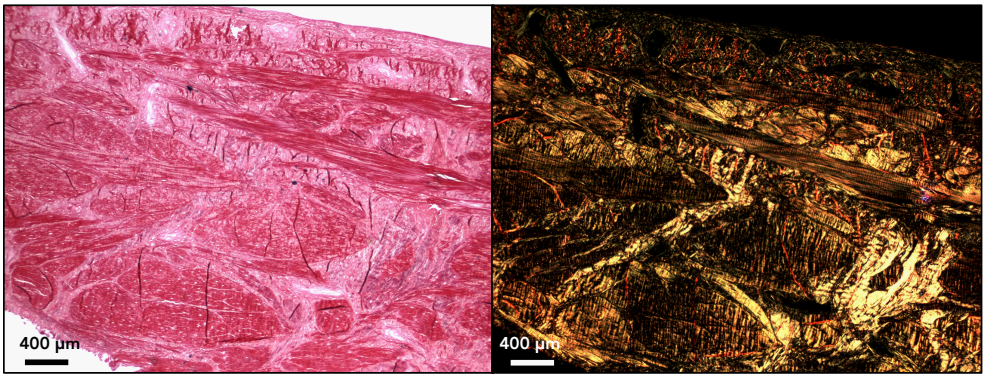

Figure 3. Low power images of sections of bovine meniscus tissue. Collagen fibers have been stained with Sirius red and photographed with white light (left) and polarized light (right).

incidence of both menisco-femoral ligaments existing in one knee is 32%.[23] In infants the meniscus is fully vascularized.[21] Vascularization decreases with aging[21] and in adults only the peripheral one-third of the meniscus is vascular (called red zone), the rest being avascular.[24]

The water-based tribological system of the joint provides a unique lubrication which is still very difficult to achieve in any artificial aqueous or non-aqueous system.[25] The constituents of synovial fluid are absorbed into/onto the articular cartilage and meniscus tissue, and lubricate the joint's movements. HA, PRG4 and SAPL are the main components believed to be responsible in the joint lubrication.[12,26,27] In addition, the synovial fluid constituents exchange oxygen and nutrients with carbon dioxide and other cellular waste products.[12,26,27]

Lubrication Mechanisms in Synovial Joints

Theories of the lubrication mechanism in the synovial joints have been discussed and developed since the 1930s. In 1932 MacConaill proposed hydrodynamic lubrication as a theory of joint lubrication.[28] In 1936 Jones also proposed the equivalent fluid film lubrication mechanism as a common form of the lubrication in human joints.[29] These models propose that the sliding surfaces are kept apart by a fluid layer of lubricant. The geometry of the surfaces and the physical properties of the lubricant, most importantly its viscosity, define the thickness of the lubricating film and are essential parameters in the hydrodynamic lubrication mechanism. Yet, the suggestion that synovial fluid, as a lubricant, can make a fluid film in between the articulating surfaces, keep them apart and provide hydrodynamic lubrication has been under debate since the proposition of the hydrodynamic lubrication theory. In addition, the complex reciprocating movement of the knee joint in different directions, comparatively low speeds, high loads and the relatively rough surface of articular cartilage do not support the hydrodynamic lubrication theory.[1,30]

In 1960, Charnley questioned the hydrodynamic lubrication theory as the acting mechanism in the joints and instead proposed the boundary lubrication mechanism, which is based on opposite concepts:[5] Charnley suggested that the lubricant has an affinity for the surface it is lubricating, thus it forms mono-molecular films and chemically bound to the surface. While moving, the sliding then takes place not between the surfaces themselves but between these adsorbed lubricant films.[1] Contrary to hydrodynamic lubrication, in boundary lubrication it is the molecular structure, chemical properties and mutual interactions of the lubricant molecules and surfaces that play the main role in lubrication.[1,31]

Throughout the 1960s, the debate between supporters of the hydrodynamic lubrication theory and those in favor of boundary lubrication continued. Attempts to identify the boundary lubricant components of the synovial fluid were conducted through biochemical and biotribological studies. At the same time, attempts to confirming the hydrodynamic lubrication mechanism were based on rheological studies.[1]

In 1963 Dintenfass claimed that neither the theory of hydrodynamic lubrication nor the theory of boundary lubrication completely explained the lubrication mechanisms in a synovial joint, and formulated the elastohydrodynamic theory.[32] This model is a mode of hydrodynamic lubrication, but it happens at higher loads and considers the effect of surface elastic deformation.[33] In 1966 Dowson presented support for this theory of joint lubrication.[30]

In 1962 McCutchen proposed the weeping lubrication mechanism, a completely new model for joint lubrication taking into consideration the porous and hygroscopic nature of cartilage.[34] This mechanism has since been called different names such as self-pressurized hydrostatic lubrication,[34] biphasic lubrication,[35,36] or interstitial fluid pressurization.[37] In this lubrication mechanism of the joints the articular cartilage and meniscus secrete, upon loading, lubricating fluid into the loaded interface creating a fluid film that provides lubrication. This is a consequence of the unique flexible and permeable structure of cartilage and meniscus.

In the following years, alongside the development of the boundary[38–41] and hydrodynamic[30,42] lubrication theories, a wide range of lubrication mechanisms were proposed such as gels,[43] boosted,[44] squeeze-film,[45,46] micro-elastohydrodynamic[47] and mixed-regime lubrication.[30,48]

A greater knowledge of the properties and composition of the articular cartilage and synovial fluid has led to a better understanding of the lubrication mechanism of synovial joints. Current views are that, depending on the dynamic conditions in the joint (sliding/shearing velocity and contact pressure), interstitial fluid pressurization and weeping (IFPW) and boundary lubrication mechanisms, or a mixture thereof, are responsible for the joint lubrication. In different studies PRG4, HA and SAPL have been proposed to play important roles in this lubrication mechanism of synovial joints.[12,26,27,49] HA and PRG4 are of particular relevance; the one by increasing synovial fluid viscosity, the other by adsorbing onto surfaces and providing boundary lubrication.[50] Some studies further suggest that PRG4–HA interactions are important for the boundary lubrication function of PRG4,[12,26,51] but it is still unclear how PRG4 is maintained on the surface of the cartilage in a configuration that provides ultralow friction.

Role of Meniscus in the Health of the Knee Joint

Menisci are responsible for load distribution, load bearing, proprioception and lubrication of the knee joint. Furthermore, they act as secondary stabilizers in the knee joint and support the exchange of nutrients and waste products through the articular cartilage matrix.[52] Although under debate, they are also believed to function as shock absorbers due to their viscoelastic structure.[53] Meniscal injuries include 14.5% of all the knee injuries.[54] A meniscal injury can easily happen in the form of a tear, especially in young individuals, and is often the result of sport-related activities. In these cases, the external rotation of the tibia on the flexed femur causes a posterior displacement of the medial meniscus resulting in a tear.[52,55] Most tears originate in the avascular part of the meniscus, which has a very limited ability to regenerate.[24,56] Besides these acute tears, the natural aging process is responsible for the degeneration of the tissue, which may result in degenerative tears.[21] Both types of injury lead to changes in the cartilage load distribution and result in premature osteoarthritis.[57,58]

Current Methods to Treat the Injured Meniscus

Different techniques have been developed for the treatment of injured menisci (**Figure 2**), to avoid development of premature osteoarthritis and the subsequent total knee arthroplasty. All these techniques have their own drawbacks. Repairing meniscal tears with sutures, staples and anchors preserves the native meniscus but has shown to be unsuccessful for tears in the avascular sides. The procedure is only suitable for repairing tears in the vascular regions of the meniscus. A technique that has been broadly used is total or partial meniscectomy. Many clinical studies have shown that meniscectomy interferes with the stress distribution in the knee joint and significantly increases the risk of osteoarthritis.[21,58,59] Instead, some surgeons have chosen to replace the injured meniscus to protect the articular cartilage from further damage.[60] Transplantation of a meniscal allograft is an option that has shown a satisfactory survival rate. It lessens pain and improves the function of the joint,[61,62] but it has drawbacks such as limited availability, size mismatching, high costs, post-implantation graft shrinkage and risk of transmission of disease.[63,64] Thus far allografts have not been used as a primary treatment for meniscal injury, but rather for relieving symptoms of knee joint degeneration as consequence of meniscal injury.

Given this background, meniscus prostheses are considered to have clinical potential and certainly deserve serious attention. Several groups have been working on an anatomically shaped implant with right characteristics made out of

various materials. A currently explored alternative is to replace the damaged meniscus tissue with biodegradable scaffolds made of synthetic or natural polymers to regenerate the meniscal tissue.[65–71] These implants also have disadvantages such as lack of durability under high loads or lack of mechanical strength.[65,66,68–71] Another alternative is the replacement of the native meniscus by a permanent synthetic implant.[60,72–75] The challenge is to find a biomaterial with right biomechanical and biotribological properties, and that ensures the integrity of implant and cartilage. Furthermore, the design of the implant should match the native meniscus. Recently, a freely floating medial meniscus implant made out of polycarbonate urethane—reinforced circumferentially with ultrahigh molecular weight polyethylene fibers (NUsurface® by Active Implants)—has been developed.[54,76] The results after six months in a sheep model were promising.[60] For human use, the design was changed to a freely floating, disk-shaped implant, for which the presence of peripheral rim of the native meniscus is a requirement. This requirement precludes the use on patients with total meniscectomy.[77] Preliminary clinical results in 61 patients after one year have shown considerable pain relief, although there are major complications due to the implant dislocation, fracturing or tearing and inflammation or progression of osteoarthritis.[78,79]

A material must fulfill a number of requirements to be considered as a biomaterial for meniscus implant or scaffold. The material must have mechanical properties similar to the healthy meniscus, i.e., a compressive modulus of 75 to 150 kPa and a tensile modulus of 75 to 150 MPa at 33 °C. The implant design must provide a proper transferring of the applied loads through the knee joint and avoid peak stresses in the articular cartilage. The tribological properties should be close to the properties of the healthy meniscus, i.e., coefficient of friction of 0.05 or less. The size of the implant should match the size of the counterpart and anatomic limitations of the host. This makes a custom-made implant preferable; otherwise, one should select from pre-sized implants. The material of interest and its degradation products have to be biocompatible. If the material serves as a scaffold aimed at growth of a new, natural meniscus, it should allow cell adhesion and function as a skeleton to promote tissue ingrowth. The scaffold degradation time must be long enough to allow enough tissue ingrowth, formation and organization. Implantation should preferably be performed using a minimal invasive surgical procedure, such as arthroscopy, because an arthrotomy may damage the articular cartilage.[80] We chose to use polycarbonate urethane in the TRAMMPOLIN project since it fulfills most of the above-mentioned conditions and has already been tested and used as a disk-shaped implant by Active Implants.

The natural meniscus is porous; it absorbs the molecules of synovial fluid

into/onto its surface and provides the lubricating properties through the IFPW and boundary lubrication mechanisms. The artificial meniscus implant studied in this thesis is made of non-porous biomaterials (different modifications of polycarbonate urethane), and will not be able to provide lubrication through IFPW from its side. In order for the implant to become lubricated it needs to adsorb lubricant molecules from the synovial fluid, e.g., PRG4 or SAPL, on its surface. The properties of the adsorbed layer of molecules, such as its thickness, molecular composition and stability in the presence of synovial fluid components, will depend on the chemical and physical properties of the surfaces of the materials and are subject of the studies presented in this thesis.

The changes that a meniscus implant will bring in the tribology of the knee joint need to be well understood. This, in turn, requires a good understanding of the tribology of the intact knee, i.e., friction and wear at the cartilage–meniscus interface. Thus far there are no tribological studies on either subject. This thesis pioneers the direct *in vitro* characterization of the tribological properties of cartilage–meniscus system. The studies described in this thesis are part of the TRAMMPOLIN project of the Dutch BioMedical Materials program. TRAMMPOLIN aimed to develop a permanent meniscus prosthesis anatomically shaped like a natural meniscus (**Figure 2**).

Structure of the Thesis

The technique of quartz crystal microbalance with dissipation (QCM-D) was used to study adsorption of relevant molecules to different polycarbonate urethane surfaces at the molecular level. QCM-D is an instrument that employs acoustic sensing technique to measure adsorption kinetics of the studied molecules, and to quantify and structurally characterize the adsorbed layer at solid–liquid interfaces. This technique operates in a nondestructive and noninvasive manner by monitoring in real time the changes in frequency and dissipation energy of a resonating piezoelectric gold-coated quartz crystal, itself coated with the substrate under study. In **Chapter 2**, QCM-D and atomic force microscope (AFM) with colloidal probe were used to gain more insight into the function of molecules of the synovial fluid and articular cartilage in joint lubrication. In particular, the roles of surface-bound hyaluronan and type II collagen in adsorbing PRG4, dependent on the presence or absence of albumin, were investigated in an *in vitro* model. The QCM-D and AFM techniques were used to describe the interactions between these molecules, as well as their effects on the coefficient of friction (COF).

In **Chapter 3**, a study is described using the same techniques as in **Chapter 2**

to compare the effects of different adsorbed proteins on polycarbonate urethane substrates, with modified surfaces, differing in wettability.

Besides the above-mentioned nano-scale biotribological characterizations, the macro-scale biotribological behavior of the biomaterials was also analyzed. This is presented in **Chapter 4**, using simulated physiological conditions in the presence of synovial fluid components. A Bruker UMT-3 tribometer (universal mechanical tester) was used to first establish a cartilage–meniscus reciprocating, sliding model. This model was then used to measure the COFs between articular cartilage and the studied biomaterials. The COF values were compared to those obtained from articulating natural meniscus against cartilage. Wear of cartilage due to articulation against the biomaterial was further evaluated using histological techniques.

Aim of the Thesis

The first aim of this thesis was to clarify the open discussion on synovial joint lubrication and the importance of the molecules that keep PRG4 on the surface in a configuration that provides optimal boundary lubrication.

The second aim was to understand the adsorption of synovial fluid components on the biomaterials and relate it to the nano- and macro-tribology of these materials by comparing them to the tribology of an intact knee joint via a cartilage–meniscus sliding model. The biomaterials used were polycarbonate urethane materials without surface modifications (Bionate 80A, PCU) or with surface-tethered C18 chains (Bionate II 80A, mPCU-c), with mono-functional polydimethylsiloxane (PDMS) groups (Bionate 80A S, mPCU-s) or with mono-functional polytetrafluoroethylene (PTFE) groups (Bionate 80A 2F, mPCU-f) as surface modifications.

Chapter 2

Both Hyaluronan and Type II Collagen Keep Proteoglycan 4 (Lubricin) at the Cartilage Surface in a Condition that Provides Low Friction during Boundary Lubrication

This chapter is an edited version of the manuscript:
Sara Ehsani Majd, Roel Kuijer, Alexander Köwitsch, Thomas Groth, Tannin A. Schmidt and Prashant K. Sharma
Langmuir, 2014, 30 (48), 14566−14572

Abstract

Wear resistance and ultralow friction in synovial joints are the outcome of a sophisticated synergy between the major macromolecules of the synovial fluid, e.g., hyaluronan (HA) and proteoglycan 4 (PRG4), with type II collagen fibrils and other non-collagenous macromolecules of the cartilage superficial zone (SZ). This study aimed at better understanding the mechanism of PRG4 localization at the cartilage surface. We show direct interactions between surface bound HA and freely floating PRG4 using the quartz crystal microbalance with dissipation (QCM-D). Freely floating PRG4 was also shown to bind with surface bound type II collagen fibrils. Albumin, the most abundant protein of the synovial fluid, effectively blocked the adsorption of PRG4 with HA, through interaction with C and N termini on PRG4, but not that of PRG4 with type II collagen fibrils. The above results indicate that type II collagen fibrils strongly contribute in keeping PRG4 in the SZ during cartilage articulation *in situ*. Furthermore, PRG4 molecules adsorbed very well on mimicked SZ of absorbed HA molecules with entangled type II collagen fibrils and albumin was not able to block this interaction. In this last condition PRG4 adsorption resulted in a coefficient of friction (COF) in the same order of magnitude as the COF of natural cartilage, measured with an atomic force microscope in lateral mode.

Introduction

Healthy diarthrodial or synovial joints (e.g., hip, knee and shoulder) are unique water-based tribological systems which facilitate both ultralow friction between the articulating surfaces (coefficient of friction ~0.0005–0.04) and very low wear, thus allowing the joints to endure millions of loading cycles during a lifetime.[5,81] A wide range of lubrication mechanisms have been proposed: hydrodynamic,[28] elasto-hydrodynamic,[82] squeeze-film,[46] weeping,[34] boosted,[44] biphasic[36] and boundary lubrication.[83] Although the main mechanisms remain controversial, there is a general agreement that under high loads and low sliding speeds, boundary lubrication is the most important mechanism in play.[49,84]

The major components that play a role in joint lubrication are the opposing articular cartilage surfaces and the synovial fluid. The articular cartilage surface mainly consists of type II collagen fibrils aligned parallel to the surface. In between the fibrils, hyaluronan (HA), synthesized by chondrocytes and synoviocytes, is present. The proteoglycan content in the superficial zone (SZ) of cartilage is relatively low.[7,8] The chondrocytes in the SZ are flattened and synthesize a superficial zone protein, known as proteoglycan 4 (PRG4; also known as lubricin), which has been shown to be very important for boundary lubrication.[50]

Synovial fluid is basically an ultrafiltrate of blood plasma, with albumin as major component (~4–10 mg/mL, M_w ~67 kDa).[11] It is supplemented with several synovial fluid and cartilage molecules such as HA (~1–4 mg/mL, M_w ~0.5–6 MDa),[12,13] PRG4 (~52–350 μg/mL, M_w ~0.230–0.460 MDa)[15,16] and surface-active phospholipids (SAPL) (~0.1–0.2 mg/mL, M_w ~0.73 kDa),[17–19] which all play a role in joint lubrication.[12,26,27] These molecules interact with each other in the SZ of articular cartilage and provide lubrication by keeping the opposing sliding surfaces spaced apart.[12,26,27] In addition, synovial fluid contains 133–139 mmol/L sodium.[14]

In a recent model for boundary lubrication,[12,85] HA is considered to be responsible for holding and trapping PRG4 at the sliding interface of the articular cartilage. In this model part of the HA molecule is physically held inside the cartilage SZ and part of it is dangling outside, where it is cross-linked and complexed with the PRG4 molecule at the cartilage surface. Upon loading, HA keeps PRG4 at the interface, thus providing boundary lubrication. Since the superficial layer also contains type II collagen along with HA and the surrounding synovial fluid contains a high concentration of albumin, it is possible that PRG4 also interacts with type II collagen, and albumin either interacts with these molecules or interferes with PRG4 in its interactions. To better understand the mechanism of PRG4 localization at the cartilage–cartilage interface, in the present study we directly measured the inter-

action of PRG4 with HA and type II collagen individually and simultaneously and studied the effects of albumin on these interactions.

Quartz crystal microbalance with dissipation (QCM-D) equipped with gold-coated QCM-D crystals was used to first allow deposition of either thiolated hyaluronan (t-HA) or type II collagen, followed by interactions of these basal layers with PRG4 or albumin, applied either individually or simultaneously. t-HA was used to allow a stable covalent bonding of hydrophilic HA to the gold surface. Non-thiolated HA did not adsorb. Furthermore, we mimicked the articular cartilage SZ by first depositing t-HA on the gold-coated crystal followed by deposition of type II collagen fibrils as a basal layer and then investigating the interaction between this layer with PRG4, albumin and a mixture of both. Lateral atomic force microscopy (AFM) was used to measure the coefficient of friction (COF), i.e., the ratio of the friction force and the applied normal force, of the different surfaces.

Experimental Section

Materials. Type II collagen from human articular cartilage (stock concentration of 2 mg/mL in 0.5 M acetic acid) of adult patients was isolated as described previously.[86] 5% thiolated hyaluronan (t-HA 5; every 20th HA disaccharide unit was thiolated, M_w = 14 kDa, PDI = 1.4) and 25% thiolated hyaluronan (t-HA 25; every 4th HA disaccharide unit was thiolated) were prepared as described previously.[87] Proteoglycan 4 (PRG4) was isolated, purified and characterized as described previously.[16,88] Bovine serum albumin (98−99%) was purchased from Sigma-Aldrich, Ltd. (St. Louis, MO). Ammonia solution 28−30%, hydrogen peroxide 30% and acetic acid (100%) were from Merck (Darmstadt, Germany).

QCM-D. The adsorption of molecules to the gold crystal assessed in QCM-D was visualized by plotting the changes in dissipation (ΔD) against the changes in frequency (Δf) for different substrates. The higher the negative frequency shift ($-\Delta f$), the higher the adsorbed mass; on the other hand, the higher the dissipation or the slope of the lines, the more viscous or hydrated the molecular films were.[89] The QCM-D (Q-Sense E4) as well as the gold-coated QCM-D crystals were from QSense AB (Västra Frölunda, Sweden). Prior to measurements, the gold sensors were cleaned, as follows: the crystals were rinsed with ultrapure water (Milli-Q), dried with nitrogen gas, treated with UV/ozone treatment for 10 min and kept in a freshly prepared solution of 3:1:1 mixture of ultrapure water, ammonia solution (NH_3) and hydrogen peroxide (H_2O_2) at 70−80 °C for 16 min. Then, the sensors were rinsed with ultrapure water, dried with nitrogen gas and received a final UV/ozone treatment for an additional 10 min. Inside the QCM-D, 10 mM

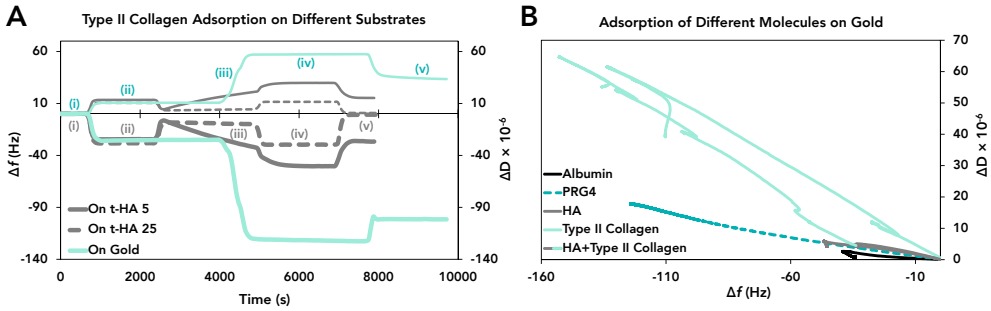

Figure 1. A: Kinetics of type II collagen interaction with t-HA 5 (gray solid lines), type II collagen interaction with t-HA 25 (gray dashed lines) and type II collagen interaction with gold (light blue lines) measured with QCM-D. Thicker lines represent Δf and thinner $\Delta D \times 10^{-6}$. Region **iii** corresponds to adsorption of type II collagen on the three substrates from 250 mM PBS, regions **i** and **v** correspond to rinsing with 10 mM PBS and regions **ii** and **iv** correspond to rinsing with 250 mM PBS. **B:** $\Delta D \times 10^{-6}$ vs Δf curves showing interaction of synovial fluid and cartilage superficial zone components with gold-coated QCM-D sensor surface.

phosphate-buffered saline (PBS) was flowed through the system and passed over the crystals in order to create a baseline for the measurements. All of the QCM-D measurements were conducted with the flow rate of 50 µL/min at 22 °C. Application of the substrates to the crystals was performed in the QCM-D. The following solutions were flowed to create three substrates: (1) t-HA 5 (2 mg/mL PBS); (2) type II collagen fibrils (24 µg/mL); (3) first t-HA 5 solution, followed by type II collagen solution.

The type II collagen fibril suspension was prepared as follows: 2 mg/mL of type II collagen in 0.5 M acetic acid was diluted 50 times with ultrapure water (Milli-Q), giving a concentration of 40 µg/mL in 10 mM acetic acid. The molecules were converted to fibrils, 10 min before flowing into the QCM-D, by adding 66% v/v of 250 mM PBS resulting in a pH of 7.3. The type II collagen substrate was formed through the following steps (**Figure 1A**): (**i**) 10 mM PBS was flowed through the system and passed over the crystals to create a baseline for the measurements, (**ii**) 250 mM PBS was flowed through the system, (**iii**) the suspension of type II collagen fibrils in 250 mM PBS was flowed over the crystal and allowed to adsorb. As the adsorption of type II collagen did not reach a plateau by itself, i.e., no saturation was obtained, the flowing of the solution was stopped after achieving a desired amount of adsorption ($-\Delta f$ ~100 Hz), (**iv**) the crystals were rinsed by 250 mM PBS to remove unattached molecules and (**v**) the crystals were rinsed with 10 mM PBS to obtain the type II collagen layer in physiological state and for further experimentation.

To mimic physiological concentrations in synovial fluid, PRG4 was dissolved in 10 mM PBS at 100 μg/mL,[15,16] and bovine serum albumin was dissolved in 10 mM PBS at 5 mg/mL;[11] the mixture of PRG4 and albumin consisted of 100 μg/mL PRG4 and 5 mg/mL albumin in 10 mM PBS. PBS contained 150 mmol/L NaCl, similar to synovial fluid.

To summarize, three different substrates were made on gold: HA, type II collagen and the combined layer of HA and type II collagen. Then the interactions between these substrates and three protein solutions—albumin, PRG4 and the mixture of albumin and PRG4—were studied.

QCM-D data are presented as ΔD versus Δf plots, which all have a hook-like shape at the end (**Figures 1B** and **3A–C**) due to the rinsing step at the end of the adsorption phase of the procedure. Both albumin and PRG4 showed affinity to gold and adsorbed well with negative frequency shifts at saturation (i.e., $-\Delta f/\Delta t <$ 2 Hz/10 min) of respectively 34 ± 4 and 124 Hz (**Figure 1B**) (time to achieve saturation = 45 and 60 min, respectively). The thiolated disaccharide of t-HA 5 bound well with the gold surface with a $-\Delta f$ at saturation of 48 ± 11 Hz (time to achieve saturation = 40 min). Type II collagen adsorbed well on both gold and HA but did not attain saturation as easily as HA. Thus, the flow of the type II collagen solution was stopped when $-\Delta f$ was 123 ± 27 and 102 ± 35 Hz respectively on gold and HA (adsorption time = 20 and 45 min, respectively). The superficial zone of articular cartilage was mimicked by first flowing the solution of t-HA over the gold surface, followed by the solution of type II collagen. On all the substrates (i.e., HA, type II collagen and HA combined with type II collagen) PRG4 adsorbed as layers with very similar viscoelasticity behavior, $\Delta D/\Delta f = (0.23 \pm 0.03) \times 10^{-6}$, $(0.24 \pm 0.00) \times 10^{-6}$ and $(0.19 \pm 0.01) \times 10^{-6}$ s, respectively. As compared with PRG4, albumin made a more viscoelastic layer on type II collagen and HA combined with type II collagen, $(0.33 \pm 0.00) \times 10^{-6}$ and $(0.59 \pm 0.00) \times 10^{-6}$ s, respectively. Adsorption of the mixture of PRG4 and albumin resulted in a layer possessing an intermediate viscoelasticity as compared with albumin alone or PRG4 alone (**Table 1**), $\Delta D/\Delta f = (0.51 \pm 0.49) \times 10^{-6}$ on HA, $(0.25 \pm 0.02) \times 10^{-6}$ on type II collagen and $(0.22 \pm 0.03) \times 10^{-6}$ s on HA+type II collagen.

The adsorption of type II collagen on gold was very fast, but the adsorption of type II collagen on HA (t-HA 5) was much slower, indicating that the mechanisms of interaction of type II collagen with gold and with HA are different (**Figure 1A**). In the interaction of type II collagen with gold, hydrophobic interactions could be playing an important role whereas much slower mechanical interactions, e.g. entanglement, could be more prominent when type II collagen flows over the loops of HA (**Figures 1A** and **3D**), and small part of HA loops was still shining through

type II collagen. Mechanical entanglement as mechanism of interaction was indicated by the observation that type II collagen did not interact with t-HA 25, which has a very small loop size (4 disaccharides compared to 20 disaccharides in t-HA 5). All the efforts to mimic the SZ by first adsorbing type II collagen on gold and then allowing adsorption of HA (not thiolated) to the coated type II collagen failed (data not shown).

AFM. A Veeco (New York, NY) atomic force microscope (AFM) (NanoScope IV Dimension 3100), equipped with the Dimension Hybrid XYZ SPM scanner, was used in contact mode to measure the coefficient of friction (COF) of each sample in the presence of 10 mM PBS. Using AFM Tune IT v2.5 software, the exact normal and torsional spring constants of rectangular, tipless cantilevers (CSC12/tipless/no Al) with the length, width and thickness of respectively 250/300, 35 and 1 μm and a stiffness of 0.02−0.05 N m^{-1} (MikroMasch, Estonia) were determined. Then, a single silica bead with the diameter of 4.87 μm (SS05N) (Bangs Laboratories, Fishers, IN) was glued to the edge of the cantilever with an epoxy glue (Pattex, Brussels, Belgium), using the micromanipulator (Narishige Group, Tokyo, Japan), to make a colloidal probe, which was ready for use after 24 h drying. Prior to AFM measurements, the deflection sensitivity (α) of each probe was quantified on a bare clean glass slide in ultrapure water.

Immediately after the QCM-D assessment, the crystal with substrate and adsorbed protein was taken to the AFM to measure the COF.

During friction measurements the colloidal probe approached the substrate in contact mode and slid over it in a reciprocating motion at a sliding distance of 20 μm and a tip speed of 20 μm/s. The tip moved against the substrate at increasing normal load in steps of few nanonewtons in the range of 1−40 nN and then unloaded backward. Friction forces, during loading and unloading, were plotted against the applied normal forces, and linear least-squares fitting in the whole normal force range of 1−40 nN provided the COF values.[90,91] For each sample, COF was measured at two to four different locations. All the measurements were performed in PBS.[91–94]

AFM was also used to determine the stiffness of the substrates, represented by the Young's modulus (E). The stiffness of the layers was obtained by approaching the layer with a colloidal probe of radius R = 2.44 μm, pressing the layer with 1 nN force and then retracting the probe away from the layer with the help of the indentation module of the NanoScope Analysis software from Bruker. Stiffness of the layer was determined by fitting equation 1 to the plot between applied force (F) against deformation of the layer (δ) and by assuming the Poisson's ratio (ν) of

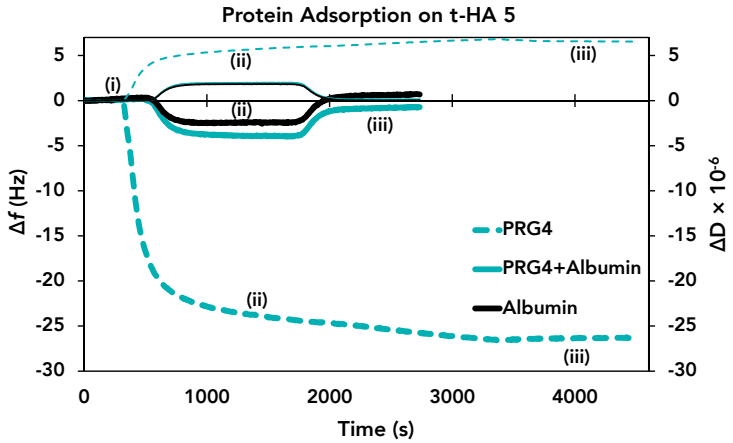

Figure 2. Kinetics of protein adsorption (PRG4, albumin and their mixture) with HA measured with QCM-D. Thicker lines represent Δ*f* and thinner ΔD × 10^{-6}. Regions **i** and **iii** correspond to rinsing with 10 mM PBS, and region **ii** corresponds to protein adsorption with HA.

0.4 for the layers. The Hertzian contact model (sphere on flat) is used to derive equation 1.

$$F = \frac{4}{3}\frac{E}{1-\nu^2}\sqrt{R}\delta^{3/2} \quad (1)$$

Statistical analysis. Two-tailed, unpaired, Student's t-tests were performed to judge statistical significance. Differences were deemed significant when $p \leq 0.05$.

Results and Discussion

The Δ*f* and ΔD versus time plots for the adsorption of PRG4, albumin and the mixture of PRG4 and albumin on a HA-coated crystal are shown in **Figure 2**. The adsorption time at the saturation was 30 min for albumin, 60 min for PRG4 and 60 min for the mixture of albumin and PRG4. **Figures 3A–C** were generated based on original QCM-D plots similar to **Figure 2**. PRG4 adsorbed to HA was not washed off during the final rinsing step; i.e., it was adsorbed in an irreversible manner (**Figures 2** and **3A** and **Table 1**). On the other hand, albumin caused a mass increase when it was allowed to flow over a HA-coated surface but was completely washed away during the final rinsing with PBS (**Figures 2** and **3A**), indicating that the interaction of albumin with HA was reversible. The synergistic effect of PRG4 and HA in lowering the COF and providing wear protection has been known for some time,

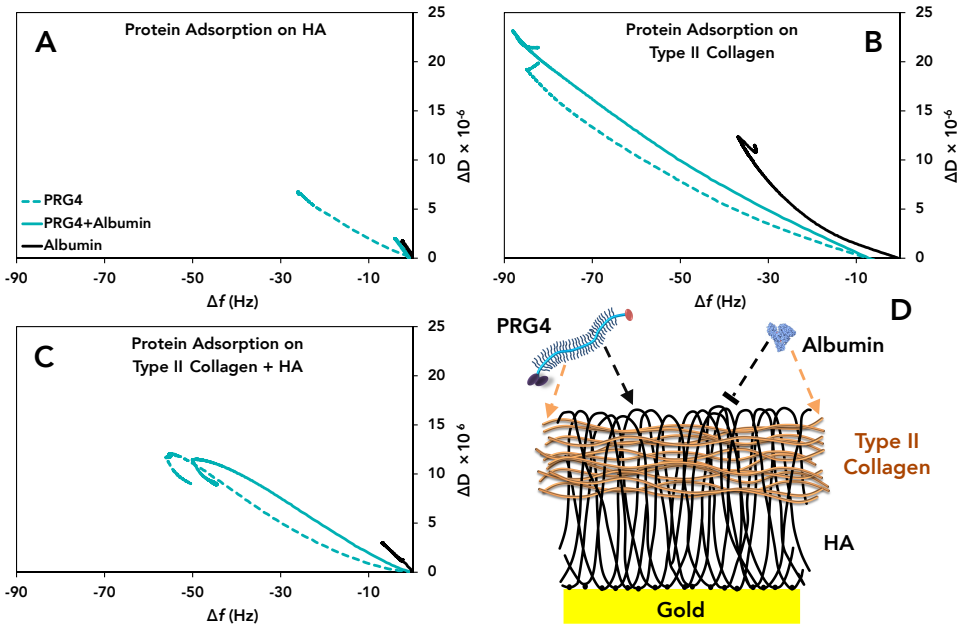

Figure 3. Interaction of synovial fluid protein with the components of cartilage superficial zone studied using the QCM-D. Frequency and dissipation shift signal (Δf and $\Delta D \times 10^{-6}$) from typical measurements on the QCM-D during the adsorption of albumin (5 mg/mL) alone, PRG4 (100 µg/mL) alone and their mixture on **A:** HA, **B:** type II collagen and **C:** mimicked superficial zone (first HA and then type II collagen). **D:** Cartoon summarizing the interaction of synovial fluid protein with the components of cartilage superficial zone.

Table 1. Substrate stiffnesses measured by AFM, the total frequency shift ($-\Delta f$, indicating adsorbed mass) and the ratio of dissipation to frequency shift ($-\Delta D/\Delta f \times 10^{-6}$, indicating the viscoelasticity of the layer) during the adsorption of synovial fluid protein on the constituents of the superficial zone. Values are the mean and SD (n = 2–3).

Substrate	Young's Modulus (kPa)	$-\Delta f$ (Hz)			$-\Delta D/\Delta f \times 10^{-6}$ (s)		
		PRG4	Albumin	PRG4 + Albumin	PRG4	Albumin	PRG4 + Albumin
HA	24±15	–	16±13	0.67±0.28	–	0.23±0.03	0.51±0.49
Type II Collagen	542±181	46±19	80±3	76±8	0.33±0.00	0.24±0.00	0.25±0.02
HA + Type II Collagen	58±4	2±0	43±10	29±22	0.59±0.00	0.19±0.01	0.22±0.03

but only recently a study showed a direct interaction between PRG4 and HA.[85,95] Albumin did adsorb on the naked Au surface (**Figure 1B**) but no longer on the HA-coated Au surface (**Figures 2** and **3A**), indicating that the HA layer was homogeneous and confluent without any pores and with all its thiolated groups bound to the Au surface. The mixture of albumin and PRG4 did adsorb on HA (**Figures 2** and **3A**), but the presence of albumin caused a large decrease in the $-\Delta f$ (by 96%, **Figure 3A** and **Table 1**) as compared to adsorption of PRG4 alone; i.e., albumin interfered and blocked the PRG4–HA interaction to a very large extent.

Adsorption of PRG4 alone on type II collagen (**Figure 3B**), as compared to HA, resulted in a much higher negative frequency shift ($-\Delta f$), indicating a high affinity of PRG4 toward type II collagen as described previously.[96] Albumin, which did not adsorb to HA, did interact with type II collagen and gave rise to the high values of $-\Delta D/\Delta f$. The ΔD vs Δf curve for albumin adsorption on type II collagen (**Figure 3B**) was very different from albumin adsorption on gold (**Figure 1B**), indicating that albumin is only interacting with type II collagen and not with underlying gold meaning the type II collagen layer is thick and homogeneous. A mixture of albumin and PRG4 over type II collagen also showed a very high $-\Delta f$ with the same slope of the adsorption curve as with PRG4, indicating that albumin did not interfere at all with the adsorption of PRG4 on type II collagen (**Figure 3B** and **Table 1**).

There are two possible causes for the blockage of the PRG4–HA interaction: (1) albumin interacts with HA reversibly and blocks sites on the HA molecule that are necessary for interaction with PRG4, or (2) albumin nonspecifically interacts with the C and N termini of PRG4, therewith blocking its interaction with HA. We did observe a reversible interaction of albumin with HA (**Figure 3A**, black line), and the fact that albumin was able to block PRG4 interaction to HA but not to type II collagen strongly indicates that albumin nonspecifically and reversibly interacts with the HA molecule. In order to investigate the second possibility, albumin was first adsorbed on the clean gold and then PRG4 was allowed to interact with albumin. **Supplementary Data Figure 1** shows that PRG4 molecules did interact with sessile albumin. Furthermore, upon rinsing with buffer no detachment was observed, indicating that the interaction was irreversible under these experimental conditions and in absence of any other competing molecule, e.g., HA or type II collagen. The saturation of the gold surface with albumin was confirmed by allowing albumin adsorption from twice concentrated albumin solution without finding any additional adsorption (**Supplementary Data Figure 2**). To make sure that the C and N termini of the PRG4 molecules are involved in this interaction, PRG4 was adsorbed on HA first and then albumin was brought to the system, but no interaction was observed (compare regions **v** and **vii** in **Supplementary Data Figure 3**). Thus, albu-

min reversibly interacts with HA but irreversibly with the C and N termini of PRG4, preventing the PRG4–HA interaction in its presence.

For mimicking the superficial zone of articular cartilage in the QCM-D, first HA was adsorbed on gold in the form of a confluent nonporous layer and then type II collagen was allowed to interact with the loops of HA and interacts via entanglement as described in the Experimental Section. Good adsorption of PRG4 was observed on the mimicked superficial zone (**Figure 3C**), but less PRG4 was adsorbed than when PRG4 was adsorbed on type II collagen alone. Adsorption of albumin to the mimicked superficial zone was suppressed compared to its adsorption to type II collagen substrate (**Figure 3C** and **Table 1**). Putting these facts together, we conclude that not only type II collagen fibrils, mechanically entrapped between the HA loops, but also HA loops, exposed out of the type II collagen fibril layer, are responsible for the limited adsorption of albumin as compared to albumin adsorption on type II collagen alone (**Figure 3B** and **Table 1**). The presence of type II collagen prevented albumin to block PRG4 adsorption to the mimicked SZ (**Figure 3C** and **Table 1**).

Measurement of Young's modulus using the AFM on different substrates showed that HA layer was the softest, type II collagen layer was the stiffest and HA and type II collagen layer had an intermediate stiffness (**Table 1**). AFM also showed that there was no measurable adhesion force between the colloidal probe (SiO_2) and the substrates or the proteins adsorbed on the substrates. A typical adhesion force curve is presented in **Supplementary Data Figure 4**. The COF of the combination of HA and type II collagen (0.12 ± 0.05) was significantly higher than the COF of adsorbed HA (0.01 ± 0.005) ($p = 6 \times 10^{-6}$) and the COF of adsorbed type II collagen (0.05 ± 0.2) ($p = 0.006$) (**Figure 4**). Adsorption of albumin on HA and type II collagen both significantly increases the COF, whereas its adsorption on the combination of HA and type II collagen fibrils did not change the COF. This observation confirms that albumin does not play an important role in the reduction of the COF in natural joints. Adsorption of PRG4 to HA or to type II collagen caused significant increases in COF, 0.03 ± 0.008 ($p = 0.0005$) and 0.19 ± 0.03 ($p = 9 \times 10^{-7}$), respectively. These increases in COF are surprising, but a similar increase was shown before,[97] and it is even proposed that PRG4 on its own is unable to lubricate an interface at high contact pressures.[25] On the other hand, the adsorption of PRG4 on the combination of HA and type II collagen, showed a decrease in COF (0.01 ± 0.004), and the measured value is close to the one observed *in vivo*.[81] The lubricating capability of PRG4 appears to depend on the underlying layer; HA and type II collagen individually could not harness this capability, but combined they did. The lubricating capability of PRG4 appears to depend on its

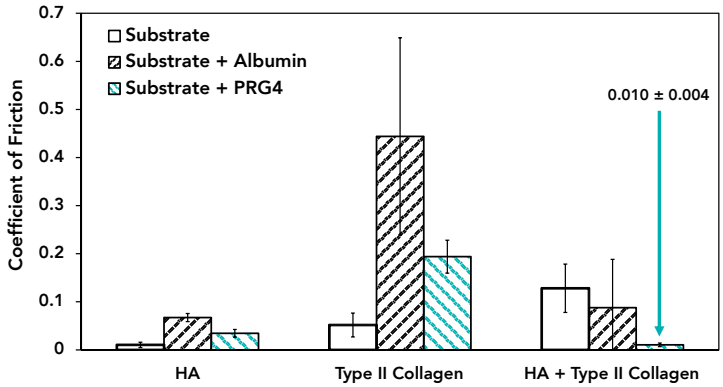

Figure 4. Coefficients of friction on different substrates measured by colloidal probe and AFM techniques in the absence or presence of albumin or PRG4. Error bars indicate SD of the mean over COF measurements on 2–3 separately prepared surfaces and each surface measured at 2–4 different spots.

binding to the substrate. Both HA and type II collagen are needed to allow PRG4 to obtain the structural freedom needed for proper boundary lubrication.

Another important factor that affects the assessed COF is the stiffness of the substrates (**Table 1**). The lowest COF was observed when PRG4 was adsorbed on a soft substrate of the combination of HA and type II collagen. The soft substrate of HA (E ~24 kPa, giving rise to a contact pressure of 7 kPa at 40 nN normal load) on its own could not provide this low COF probably due to very low amounts of PRG4 adsorption. PRG4 adsorbed on hydrophilic and negatively charged substrates have either shown an increase in COF[97] or very high COFs[98] at contact pressures above 1000 kPa. In both these cases, PRG4 was directly adsorbed on substrates with high stiffness values. In our study, the combined HA and type II collagen layer with a stiffness of ~58 kPa, giving rise to a contact pressure of 13 kPa (at normal load of 40 nN), allowed PRG4 to lubricate the substrate very well. Type II collagen alone with a stiffness of 542 kPa giving rise to a contact pressure of 55 kPa was probably too stiff. Further investigation is necessary to elucidate whether molecular interactions, substrate stiffness or both are essential for the observed tribological properties of PRG4.

Finally, it is necessary to emphasize that this is an *in vitro* study. This set up, using QCM-D, enabled the study of protein adsorption in a controlled way and allowed for the subsequent measuring of the COF under boundary lubrication conditions between a silica bead and the different molecules deposited on the QCM-D sensor surfaces. Certainly, the ideal measurement would have been

between articular cartilage and the prepared substrates, but that is not possible with the current nanoscale techniques. Therefore, these *in vitro* COF values may differ from the exact *in vivo* ones; however, the differences between different combinations of molecules would remain as they are reported.

Conclusions

PRG4 elicits a COF similar to the one for articular cartilage after adsorption to a soft surface containing both type II collagen fibrils and HA. Adsorption to surfaces coated with either component alone resulted in high COF. Albumin interacts irreversibly with the C and N termini of PRG4, thus interfering in PRG4 interaction with HA. Albumin did not interfere with the interaction of PRG4 with type II collagen; thus, type II collagen plays an important role in keeping PRG4 at the cartilage–cartilage interface. Besides the requirement of both type II collagen and HA at the surface, also the stiffness of the layer plays a role in the observed low COF.

Acknowledgments

This research forms part of the Project P2.03 TRAMMPOLIN of the research program of the BioMedical Materials institute, co-funded by the Dutch Ministry of Economic Affairs. We also acknowledge Grant no. 355591-2009 from Natural Sciences and Engineering Research Council of Canada.

Supplementary Data

In order to investigate the type of interaction between albumin and PRG4, albumin was first adsorbed on the clean gold and then PRG4 was allowed to interact with albumin in the QCM-D. **Supplementary Data Figure 1** shows that PRG4 molecules did interact with sessile albumin. Furthermore, upon rinsing with clean buffer no detachment was observed, indicating that the interaction is irreversible under these experimental conditions and in absence of any other competing molecule, e.g., HA or type II collagen. To make sure that the C and N termini of the PRG4 molecules are involved in this interaction, PRG4 was adsorbed on HA first and then albumin was brought to the system, but no interaction was observed (compare regions **v** and **vii** in **Supplementary Data Figure 3**).

To clarify that the interaction took place between PRG4 and albumin in **Supplementary Data Figure 1** and not between PRG4 and free gold spot on the QCM-D sensor surface, another experiment was preformed (**Supplementary Data Figure 2**). In this experiment, albumin with the concentration that we used in this study (5 mg/mL) was allowed to adsorb on the clean gold surface. Then albumin with twice the concentration (10 mg/mL) was flowed over the crystal, but no additional adsorption of albumin was observed, indicating that already at 5 mg/mL the gold-coated QCM-D surface is saturated with albumin molecules.

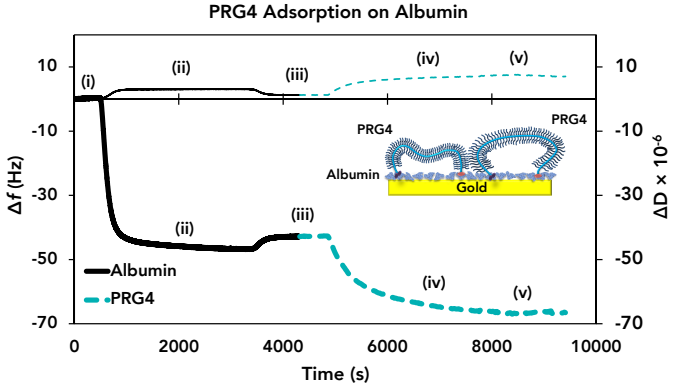

Supplementary Data Figure 1. Kinetics of PRG4 adsorption with albumin measured with QCM-D. Thicker lines represent Δ*f* and thinner ΔD × 10^{-6}. Region **ii** corresponds to albumin adsorption on gold, region **iv** corresponds to PRG4 adsorption on albumin and regions **i**, **iii** and **v** correspond to rinsing with 10 mM PBS.

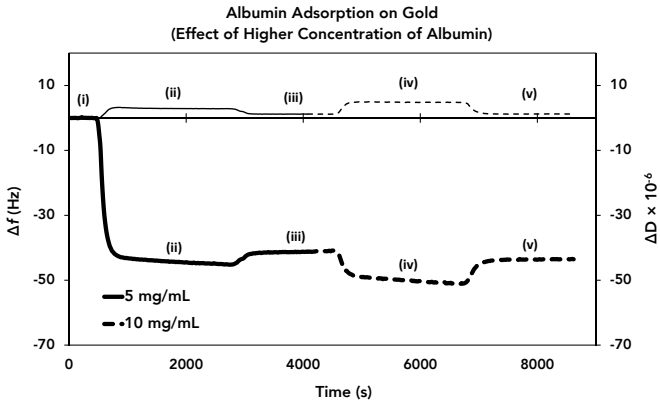

Supplementary Data Figure 2. Adsorption of albumin on gold at two different concentrations, i.e., 5 and 10 mg/mL measured with QCM-D. No additional adsorption at the concentration of 10 mg/mL shows that the gold surface is saturated with albumin already at the concentration of 5 mg/mL. Thicker lines represent Δ*f* and thinner ones $\Delta D \times 10^{-6}$. Region **ii** corresponds to albumin (5 mg/mL) adsorption on gold, region **iv** corresponds to albumin brought in at 10 mg/mL and regions **i**, **iii** and **v** correspond to rinsing with 10 mM PBS.

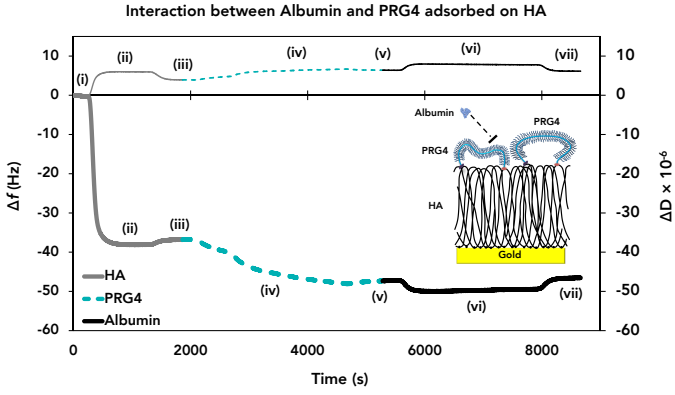

Supplementary Data Figure 3. Kinetics of interaction between albumin and PRG4, which is already adsorbed on HA, measured with QCM-D. Thicker lines represent Δ*f* and thinner $\Delta D \times 10^{-6}$. Region **ii** corresponds to HA adsorption on gold, region **iv** corresponds to PRG4 adsorption on HA, region **vi** corresponds to albumin interaction with PRG4 and regions **i**, **iii**, **v** and **vii** correspond to rinsing with 10 mM PBS.

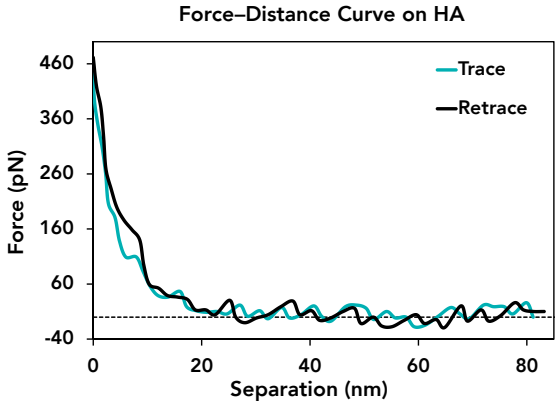

Supplementary Data Figure 4. Force–distance curve between a silica colloidal probe and HA as a substrate measuring with AFM. The blue line represents the colloidal probe approaching the substrate upon the applied external loading force and the black line represents the retracting of the probe, which shows no adhesion between the probe and the substrate.

Chapter 3

Role of Hydrophobicity on the Adsorption of Synovial Fluid Proteins and Biolubrication of Polycarbonate Urethane: Materials for Permanent Meniscus Implants

This chapter is an edited version of the manuscript:
Sara Ehsani Majd, Roel Kuijer, Tannin A. Schmidt and Prashant K. Sharma
Materials & Design, 2015, 83, 514–521

Abstract

Both absorption and release of synovial fluid components lubricate the porous natural meniscus, whereas only adsorption can lubricate non-porous meniscus prostheses. The aim of this study was to establish the adsorption characteristics of the synovial fluid proteoglycan 4 (PRG4) and albumin on modified and unmodified polycarbonate urethane (PCU) and determine the effects on the coefficient of friction. PCU was modified with surface-tethered C18 chains (mPCU-c). Self-assembled monolayers (SAM) on gold were also used to generate higher and lower hydrophobicities. Protein adsorption and coefficients of friction were measured by quartz crystal microbalance and atomic force microscope with colloidal probe. PRG4 formed a thick viscoelastic layer and significantly decreased the coefficient of friction on PCU and mPCU-c, with an exceptionally low coefficient of friction measured on mPCU-c (0.02 ± 0.02) due to its soft surface. Albumin formed a thin rigid layer with a much higher coefficient of friction on mPCU-c (1.14 ± 0.19). Albumin blocked PRG4 adsorption when simultaneously added to PCUs, and coefficients of friction of 0.48 ± 0.24 (PCU) and 0.49 ± 0.17 (mPCU-c) were measured. Albumin adsorption on hydrophobic substrates (water contact angle ≥70° ± 4°) dramatically increased the coefficient of friction (3.41 ± 1.21 on hydrophobic SAM), indicating that increased hydrophobicity through hydrocarbon surface modification of PCU carries tribological risks.

Introduction

Meniscal injury in the form of a tear is one of the most common sports-related injuries in young patients. Meniscal tears often occur due to the posterior displacement of the medial meniscus as a response to the external rotation of the tibia on the flexed femur.[99] Left untreated, the injury may lead to cartilage damage and signs of early arthritis. Considering the fact that menisci have a very limited ability to regenerate and heal, once damaged, they cause serious problems.[99] The menisci in the knee joint play important roles in load bearing, load distribution, shock absorption, proprioception and lubrication of the joint. Furthermore, this tissue also acts to provide nutrition to the articular cartilage and behaves as secondary stabilizers.[52] The loss of menisci function leads to degeneration of the joint due to changes in the cartilage load distribution.[58] In the synovial joints the terminal portion of bone is covered with a thin layer (1–5 mm)[100] of hydrated, avascular hyaline tissue called articular cartilage which plays an important role in lubrication during articulation and load distribution in the joint.[101] Articular cartilage consists of 70–80% water, and its dry weight contains 2% chondrocytes and 98% extra-cellular matrix (ECM) produced by the chondrocytes. ECM is composed of 50–75% collagen (90% type II collagen), 15–30% proteoglycans (mainly aggrecan) and 10% lipids (mainly phospholipids).[9,101] Meanwhile, menisci are crescent-shaped, biphasic composite materials which play many important roles in the knee joint. The fibro-cartilaginous tissue of the meniscus consists of water as a major component (63–75% of the total weight). The dry weight consists of 75% collagen (mostly type I collagen) and 2.5% proteoglycan.[22]

As a treatment for meniscal injury, total or partial meniscectomy is commonly performed. Clinical studies show that both types of meniscectomy increase the risk of osteoarthritis in the knee due to the decreased stress distribution.[58,59] Therefore, surgeons prefer to repair the injured meniscus. However, when this is not possible, the meniscus is replaced with an allograft to protect the articular cartilage from damage.[60] An allograft meniscus transplant alleviates pain and improves function as well as having a satisfactory survival rate.[61,62] Drawbacks of these allografts are limited availability, size mismatching, high costs, graft shrinkage after implantation and risk of transmission of disease.[63,64] Alternatively, there are several biodegradable implants based on synthetic and natural polymers available, but these implants demonstrate other disadvantages such as lack of durability in loading conditions.[102–104]

The development of permanent meniscus prostheses is a promising alternative to the above treatments. Such a prosthesis needs to remain in place and perform for many years. The challenge is thus to find a biomaterial that is able to

withstand the loading forces in the joint, is chondroprotective and yields effective tribological properties in the presence of synovial fluid.

Healthy diarthrodial or synovial joints provide ultralow coefficients of friction (0.001–0.005) and excellent wear protection between the articulating surfaces during lifetime in the body.[81] These sophisticated tribological properties are due to unique lubrication mechanisms inside the joints which are difficult to achieve in artificial systems.[25] Several descriptions of these mechanisms have been proposed: hydrodynamic lubrication,[28,42] boundary lubrication,[5,39] elastohydrodynamic lubrication,[30,32] weeping lubrication,[34] boosted lubrication,[44] squeeze-film lubrication[45,46] and biphasic lubrication.[36] The lubrication mechanisms are not mutually exclusive, and the predominant form will depend upon the loads and speed. There is now a general agreement that under high load and low sliding speeds boundary lubrication is the most important mechanism in play.[49,84]

In the knee joint the porous nature of the cartilage and meniscus tissue and the presence of viscous synovial fluid play critical roles in the lubrication process. Water is the major component of synovial fluid along with different inorganic (**Table 1**) and organic (**Table 2**) components. A high concentration of hyaluronan (HA) is responsible for the high viscosity of the fluid.[12,13] A glycoprotein proteoglycan 4 (PRG4, also known as lubricin) mainly secreted by superficial layer chondrocytes[15,16] and surface-active phospholipids (SAPL) are known to be involved in the joint lubrication.[27,81] Albumin, a globular protein, is the most abundant protein present in synovial fluid.[11] Despite this fact albumin does not play a key role as a boundary lubricant on the natural cartilage or meniscus surface,[26,105] but it is known to decrease the wear rate of ultrahigh molecular weight polyethylene (UHMWPE) acetabular cups against metallic heads used in the artificial joints.[106] However, joint diseases, such as osteoarthritis and rheumatoid arthritis, or injuries could change the chemical environment in the joint which influences cells and the secretion of the lubricant molecules (HA, PRG4 and SAPL) by them.[107] Joint diseases and injuries also change synovial membrane permeability, and consequently the filtration of plasma proteins (albumin).[108] Therefore, the composition of rheumatoid or osteoarthritic synovial fluid changes.[107,108] Clinical studies have shown that in humans, HA concentration could decrease down to 0.1 g/L due to arthritis, while albumin, PRG4 and SAPL concentrations could increase up to 20 g/L, 0.762 g/L and 0.8 g/L, respectively.[26,108]

As per the fluid pressurization and weeping model the porous, natural meniscus absorbs synovial fluid and releases it upon loading keeping the opposing sliding surfaces spaced apart.[12,26,27] Meanwhile, the proteic components of the synovial fluid adsorb onto both meniscus and cartilage surfaces providing bound-

Table 1. Concentrations of the major inorganic components of healthy synovial fluid.

Component	Concentration (mmol/L)
Sodium[14]	133–139
Potassium[14]	3.5–4.5
Chloride[14]	87–138

Table 2. Concentrations and molecular weights of some of the major organic components of healthy synovial fluid.

Component	Molecular weight (kDa)	Concentration (g/L)
HA[12,13]	500–6000	1–4
PRG4[15,16]	230–460	0.052–0.350
SAPL[17,18]	0.73	0.100–0.200
Albumin[11]	70	4–10

ary lubrication under high loads and low sliding velocities.[12,26,27] For an artificial nonporous meniscus, the only way to achieve effective lubrication at points of high contact pressures is through the adsorbed layer of lubricating molecules, e.g., PRG4, HA and SAPL.

Polycarbonate urethane (PCU) is currently used for making a synthetic meniscus implant (NUsurface® by Active Implants) to replace the damaged meniscus.[54,76] The PCU meniscus is very well studied for its biomechanical characteristics,[76] but the tribological characteristics in the synovial joint milieu still require attention.

The first aim of this study was to investigate the adsorption of synovial fluid proteins, i.e., PRG4 and albumin, on PCU as well as the resulting biolubrication. HA was not included in the study, because preliminary experiments demonstrated that HA did not adsorb to any of the surfaces. Albumin has been shown to decrease wear of UHMWPE and it is important to be considered due to its abundance in synovial fluid. Especially since in salivary lubrication albumin is known to interfere with the adsorption of mucin to surfaces.[109]

The second aim of this study was to investigate the role of hydrophobicity of the material on the protein adsorption and resulting biolubrication. PRG4 molecules are known to adsorb very well on hydrophobic surfaces[98,110] and are thus expected to do the same on PCU, which is moderately hydrophobic. To enhance this effect, a modified PCU (mPCU-c) with surface-tethered C18 chains has been studied as well. To further increase the range of hydrophobicity, self-assembled monolayers (SAM) terminating in hydroxyl or methyl groups were made over gold sensors to create a very hydrophilic and a very hydrophobic substratum respectively.

Quartz crystal microbalance with dissipation (QCM-D) was used to investi-

gate the adsorption mechanisms and kinetics of PRG4 and albumin, applied individually or simultaneously, on surfaces of PCU, mPCU-c, the hydrophobic SAM and the hydrophilic SAM on gold. QCM-D is a non-destructive and non-invasive, acoustic sensing technique. It provides real-time information of the adsorption process *in situ*, such as the adsorption kinetics of the molecules (PRG4 and albumin in this study), the quantity of the adsorption and the structure of the adsorbed layer at solid–liquid interfaces.[111] Afterwards the samples with adsorbed molecules were subjected to atomic force microscopy (AFM) to measure the coefficient of friction (COF), i.e., the ratio of the friction force and the applied normal force, on the different surfaces. AFM is a principal tool to study the boundary lubrication phenomena at the molecular level, which occur at high loads and low sliding speeds.[112] Due to the small sizes involved, AFM is a very suitable device to study the phenomena where high local pressures squeeze out the lubricant liquid at the contacting asperities and result in solid–solid contact, while a (mono)layer of lubricant molecules prevents the interpenetration or adhesion at the asperities. The combination of QCM-D and AFM has been used to study the molecular adsorption and biolubrication of the proteic lubricant films.[90, 91, 105, 113]

Experimental Section

Materials. Polycarbonate urethanes (PCU) were used in the form of Bionate 80A. The modified polycarbonate urethane (mPCU-c) was Bionate II 80A; both materials were obtained from DSM Biomedical (Geleen, The Netherlands). The difference between PCU and mPCU-c is the presence of C18 chains at the surface of mPCU-c. Bovine proteoglycan 4 (PRG4) was isolated, purified and characterized as described previously.[16, 88] Bovine serum albumin (98−99%), 1-octadecanethiol 98% ($HS(CH_2)_{17}CH_3$) and 11-mercapto-1-undecanol 97% ($HSCH_2(CH_2)_9CH_2OH$) were from Sigma–Aldrich, Ltd. (St. Louis, MO). Tetrahydrofuran (THF), ammonia solution 28−30% and hydrogen peroxide 30% were from Merck (Darmstadt, Germany).

Quartz Crystal Microbalance with Dissipation. The QCM-D (Q-Sense E4) as well as the gold-coated QCM-D sensors were from QSense AB (Västra Frölunda, Sweden). The 14 mm-diameter sensors have a fundamental frequency of 5 MHz. Prior to measurements, the gold-coated sensors were cleaned as follows: the sensors were rinsed with ultrapure water (Milli-Q), dried with nitrogen gas, treated with UV/ozone for 10 min and incubated in a freshly prepared solution of 3:1:1 ultrapure water (Milli-Q), ammonia (NH_3) and hydrogen peroxide (H_2O_2) at 70−80 °C for 16 min. Subsequently, the sensors were rinsed with ultrapure water, dried with nitrogen gas and treated with UV/ozone for an additional 10 min. The clean sen-

sors were either spin coated with the PCU and mPCU-c solutions or immersed in SAM solutions.

Spin coating was used to apply a smooth, even, thin layer of PCU and mPCU-c over the clean gold-coated QCM-D sensor surface (14 mm in diameter). The rotation rate of the spin coater was preset at 50 revolutions/s for 120 s. Polymer solutions were prepared by dissolving PCU and mPCU-c in tetrahydrofuran (THF) for 24 h at a concentration of 40 g/L. Spin coating would allow individual polycarbonate urethane molecules to adsorb on the gold surface. In order to bring the polymers more into the bulk state a heat treatment was performed in which the coated sensors were heated to 75 °C for 2 h. Prior to use, the polymer-coated gold sensors were hydrated by ultrapure water (Milli-Q) for an hour to allow swelling.

The SAMs were created by immersing clean sensors in 1 mM solution of either $HS(CH_2)_{17}CH_3$ (1-octadecanethiol) or $HSCH_2(CH_2)_9CH_2OH$ (11-mercapto-1-undecanol) in absolute ethanol, for 18 h while mildly shaking. The 1-octadecanethiol created the hydrophobic SAM and the 11-mercapto-1-undecanol created the hydrophilic SAM.

Prior to the QCM-D measurements contact angles of 1 µL sessile Milli-Q water droplets were measured on all surfaces using a home-made contour monitor, to confirm whether the surface coating on each coated sensor was applied properly.[114] On each sample, three droplets were placed on different spots; their average values were reported.

Inside the QCM-D, to create a baseline for the measurements, 10 mM phosphate-buffered saline (PBS) was flowed through the system and passed over the sensors. All the measurements were conducted on the coated sensors with a flow rate of 50 µL/min at 22 °C. The molecules in solutions were then allowed to flow over the sensor surface. Thus, the interaction between the substrates and three protein solutions albumin, PRG4 and the mixture of albumin and PRG4 were studied. At the end the sensors were rinsed with PBS to remove nonspecifically adsorbed molecules and only allow the irreversibly adsorbed molecules to remain.

During the protein adsorption in the QCM-D, both the frequency shift (Δf) and dissipation shift (ΔD) are presented in **Figure 1** as a function of time. The adsorption of molecules to the substrates assessed in QCM-D is visualized by plotting the changes in dissipation against the changes in frequency for different substrates. The higher the negative frequency shift ($-\Delta f$), the higher the adsorbed mass; on the other hand, the higher the dissipation shift or the slope of the lines ($-\Delta D/\Delta f$) (**Figure 2**), the more viscous or hydrated the molecular films are.[89] Both adsorption and rinsing are defined as stopped when the plateau region is obtained, i.e.,

$-\Delta f/\Delta t < 2$ Hz/10 min. Plotting ΔD against Δf (**Figure 2**) demonstrates that each adsorption line ends in a hook shape, signifying the drop in frequency and dissipation shifts corresponding to the rinsing step.[91,105]

In this study we tried to mimic the physiological ratio of the synovial fluid molecules in a healthy joint since meniscal injuries are predominantly sports-related and occur in otherwise non-arthritic and healthy joints. PRG4 was dissolved in 10 mM PBS at 100 μg/mL,[15,16] and bovine serum albumin was dissolved in 10 mM PBS at 5 mg/mL;[11] the mixture of PRG4 and albumin consisted of 100 μg/mL PRG4 and 5 mg/mL albumin in 10 mM PBS. PBS contained 150 mmol/L NaCl, similar to synovial fluid.[105]

Atomic Force Microscopy and Colloidal Probe Technique. The atomic force microscope (AFM) (NanoScope IV Dimension 3100), equipped with Dimension Hybrid XYZ SPM scanner head, was from Veeco (New York). In contact mode, it was used to measure the coefficient of friction of each sample in the presence of 10 mM PBS. Rectangular, tipless cantilevers (CSC12/tipless/no Al) with length, width and thickness of 250/300, 35 and 1 μm respectively and a normal stiffness of 0.02−0.05 N m^{-1} were from MikroMasch (Estonia). Using AFM Tune IT v2.5 software, the exact normal and torsional spring constants of each cantilever were determined.[94] Subsequently, a silica bead with the diameter of 4.87 μm (SS05N) (Bangs Laboratories, Fishers, IN) was glued to the edge of the cantilever using epoxy glue (Pattex, Brussels, Belgium) and a micromanipulator (Narishige groups, Tokyo, Japan), to make a colloidal probe,[92] which was ready for use after 24 h drying. The deflection sensitivity (α) of each probe was quantified, prior to AFM measurements, on a bare clean glass slide in ultrapure water.[90,91,93,105,115] A silica bead was used to articulate against the PCU as using biological material has yet to be proven accurate enough to mimic naturally hydrophilic cartilage and thus has yet to become a common technique.

Immediately after the QCM-D assessment, the coated sensors with adsorbed protein were taken to the AFM to measure the coefficient of friction.[90,91,105]

During friction measurements the colloidal probe approached the substrate in contact mode and slid over it in a reciprocating motion at a sliding distance of 20 μm and a tip speed of 20 μm/s. The tip moved against the substrate at an increasing normal load in steps of a few nanonewtons in the range of 1−40 nN and then unloaded backward. Friction forces, during loading and unloading, were plotted against the applied normal forces, and linear least-squares fitting in the whole normal force range of 1−40 nN provided the coefficient of friction values.[116] For

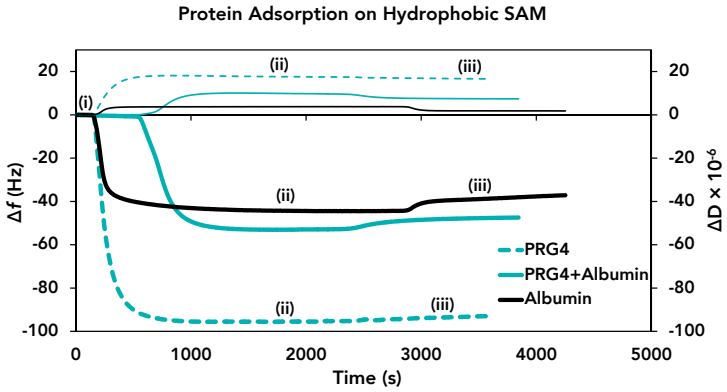

Figure 1. Kinetics of protein (PRG4, albumin and PRG4+albumin) adsorption on hydrophobic SAM measured with QCM-D. Thicker lines represent Δ*f* and thinner lines ΔD. Regions **i** and **iii** correspond to rinsing with 10 mM PBS and region **ii** corresponds to adsorption of protein.

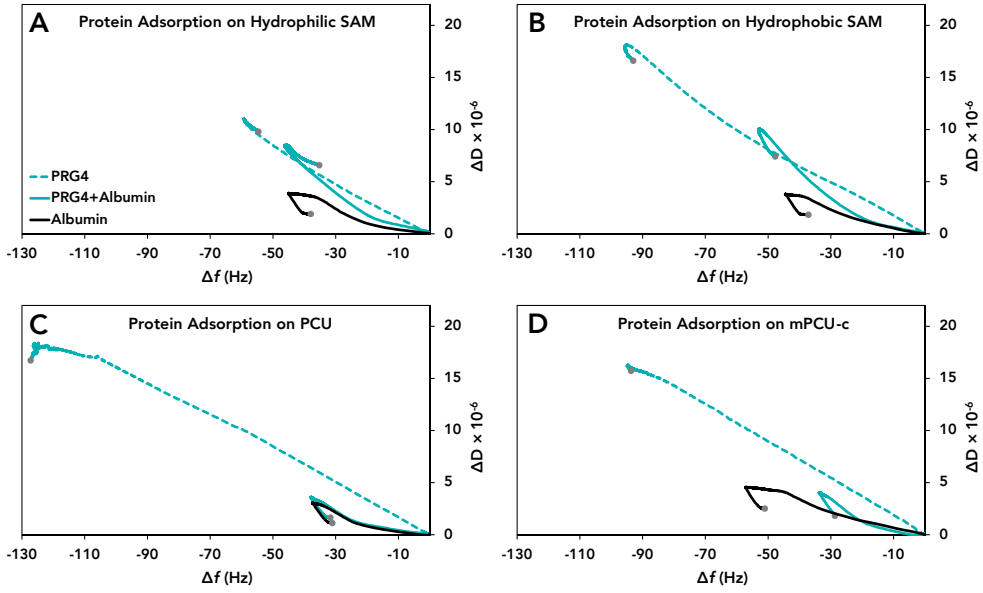

Figure 2. Plots of the changes in dissipation versus the frequency shift as measured by QCM-D, representing adsorption characteristics of PRG4, albumin and PRG4+albumin at **A:** hydrophilic SAM, **B:** hydrophobic SAM, **C:** PCU and **D:** mPCU-c.

each sample, coefficient of friction was measured at two to four different locations. All the measurements were performed in PBS.[90, 91, 93, 105, 115]

Statistical Analysis. Unpaired, two-tailed, Student's t-tests were performed to assess statistical significance. Differences were deemed significant if $p \leq 0.05$.

Results

Prior to QCM-D measurements, water contact angles were measured on coated sensors to confirm that the coatings were properly applied. The results are presented in **Table 3**. The hydrophilic SAM coated sensors had a water contact angle of 11° ± 8°. The PCU and mPCU-c coated sensors were both hydrophobic with water contact angles of 70° ± 4° and 76° ± 3°, respectively. Their hydrophobicity is significantly different from each other ($p < 0.001$). The hydrophobic SAM coated sensors had a water contact angle of 9° ± 4°.

At PCU, mPCU-c and the hydrophobic SAM surfaces, adsorption of PRG4 was significantly higher compared to the adsorption of albumin alone or to albumin mixed with PRG4. At the hydrophilic SAM substrate, adsorption of PRG4 and the mixture of PRG4 and albumin did not differ significantly ($p = 0.095$) (**Figure 2** and **Table 3**). At mPCU-c, PRG4 adsorption caused a frequency shift ($-\Delta f$) of 92 ± 1 Hz, whereas the frequency shifts of albumin and PRG4+albumin adsorption were significantly lower, i.e., $-\Delta f = 40 \pm 14$ Hz ($p < 0.001$) and $-\Delta f = 26 \pm 7$ Hz ($p < 0.0012 \times 10^{-6}$), respectively. The frequency shift due to PRG4 adsorption on the hydrophilic SAM ($-\Delta f = 55 \pm 15$ Hz) was significantly smaller than on the more hydrophobic PCU ($-\Delta f = 135 \pm 15$ Hz) ($p = 0.008$), mPCU-c ($-\Delta f = 92 \pm 1$ Hz) ($p = 0.003$) and hydrophobic SAM ($-\Delta f = 91 \pm 8$ Hz) ($p < 0.001$). The highest value of PRG4 adsorption was observed at the PCU coating. The frequency shifts caused by albumin adsorption at the four different surfaces did not differ significantly. The frequency shift due to PRG4+Albumin adsorption at the hydrophobic SAM coating ($-\Delta f = 46 \pm 5$ Hz) was significantly higher compared to PCU or mPCU-c coatings ($p = 0.009$ and $p = 0.01$, respectively) but not compared to the hydrophilic SAM coating ($p = 0.16$).

Table 3 and **Figure 2** also contain values of $-\Delta D/\Delta f$ resulting from adsorption of the molecules at the different substrates. A higher value of $-\Delta D/\Delta f$ indicates higher hydration of the adsorbed layer or a more viscous structure of the layer. On all four surfaces, adsorption of PRG4 provided $-\Delta D/\Delta f$ values which were significantly higher than those related to adsorption of albumin, i.e., adsorption of PRG4 formed a viscous, fluffy layer ($-\Delta D/\Delta f = 0.14 \times 10^{-6}$ to 0.20×10^{-6} s), whereas adsorption of albumin gave rise to a more rigid layer ($-\Delta D/\Delta f = 0.03 \times 10^{-6}$ to 0.05×10^{-6} s). When a mixture of PRG4 and albumin was allowed to

Table 3. Hydrophobicity of all the substrates and QCM-D data for adsorption of PRG4 and albumin individually and simultaneously, in terms of $-\Delta f$ and $-\Delta D/\Delta f$, on different substrates. The $-\Delta f$ and $-\Delta D/\Delta f$ values reported here correspond to the end points marked with gray dots in **Figure 2**. Values are the mean and SD (n = 3–5).

Substrate	Water Contact Angle (°)	$-\Delta f$ (Hz)			$-\Delta D/\Delta f \times 10^{-6}$ (s)		
		PRG4	Albumin	PRG4 + Albumin	PRG4	Albumin	PRG4 + Albumin
Hydrophilic SAM	11±8[†]	55±15	36±7[$]	38±4	0.20±0.02	0.05±0.02[$]	0.16±0.04
PCU	70±4[*†]	135±15[*]	33±5[$]	34±3[$‡]	0.14±0.01	0.03±0.03[$]	0.08±0.02
mPCU-c	76±3[*]	92±1[*]	40±14[$]	26±7[$‡]	0.17±0.01	0.05±0.01[$]	0.05±0.02
Hydrophobic SAM	92±4[*†]	91±8[*]	35±4[$]	46±5[$]	0.17±0.01	0.04±0.01[$]	0.14±0.01

[*] Significantly different ($p < 0.05$) as compared to hydrophilic SAM.
[†] Significantly different ($p < 0.05$) as compared to mPCU-c.
[‡] Significantly different ($p < 0.05$) as compared to hydrophobic SAM.
[$] Significantly different ($p < 0.05$) in QCM-D signal as compared to PRG4 adsorption.

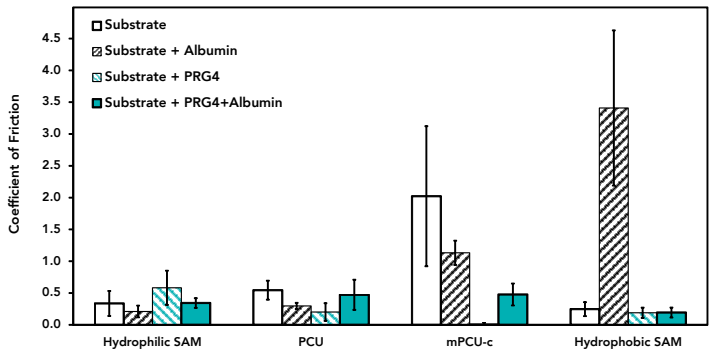

Figure 3. Coefficient of friction on different substrates in the absence or presence of different molecules, measured by colloidal probe and AFM techniques. Error bars indicate SD of the mean of coefficient of friction (COF) measurements, comprising two to four separately prepared coatings and each coating measured at two to five different spots.

adsorb onto SAMs, irrespective of their hydrophobicity, a viscous and fluffy layer ($-\Delta D/\Delta f \geq 0.14 \times 10^{-6}$ s) was formed similar to an adsorbed PRG4 layer. In contrast, adsorption of the mixture of PRG4 and albumin onto PCU or mPCU-c resulted in rigid layers ($-\Delta D/\Delta f \leq 0.08 \times 10^{-6}$ s and $-\Delta D/\Delta f \leq 0.05 \times 10^{-6}$ s, respectively) similar to an adsorbed albumin layer. The adsorption curve resulting from adsorption of PRG4+albumin to the SAMs indicates that first albumin was adsorbed (until a Δf of ~−20 Hz) followed by PRG4 (rise of the curve to the level of PRG4). The adsorp-

tion curves of PRG4+albumin on PCU and mPCU-c were similar to the curves of adsorption of albumin alone to these materials, indicating that adsorption of albumin blocked adsorption of PRG4. Apparently, the avidity of albumin for the PCU surfaces was so high that albumin could not be replaced (**Figure 2C,D**) by PRG4.

The coefficients of friction of the control surfaces without any adsorbed protein (white bars in **Figure 3**) were 0.26 ± 0.11 for the hydrophobic SAM and 0.35 ± 0.20 for the hydrophilic SAM (no significant difference), indicating that the coefficients of friction were independent of the hydrophobicity of the substrates. The coefficient of friction of PCU was significantly higher compared to hydrophobic SAM ($p = 0.003$) but not compared to hydrophilic SAM. The coefficient of friction of mPCU-c was 2.03 ± 1.10, significantly higher than PCU, hydrophilic and hydrophobic SAM ($p = 0.01$, $p < 0.001$ and $p < 0.001$, respectively). Adsorption of albumin (hatched black bars) slightly decreased the coefficient of friction on PCU; on hydrophobic SAM an increase from 0.26 ± 0.11 to 3.42 ± 1.22 was observed. Adsorbed PRG4 (alone) on both PCU and mPCU-c significantly decreased the coefficient of friction (0.21 ± 0.14 and 0.02 ± 0.02, respectively) (hatched blue bars) compared to the values of the bare surfaces ($p = 0.001$ and $p < 0.001$, respectively). On hydrophilic and hydrophobic SAMs, adsorbed PRG4 or PRG4+albumin did not decrease the coefficient of friction relative to the bare surfaces. Adsorbed PRG4+albumin at the PCU surface resulted in coefficients of friction as high as those of the bare surface or the albumin-covered surface. On mPCU-c with adsorbed PRG4+albumin the coefficient of friction values were significantly higher than the values for adsorbed PRG4 alone ($p < 0.001$) but significantly lower than the coefficient of friction of the bare substrate ($p = 0.001$) or adsorbed albumin ($p < 0.001$). In the presence of PRG4 and albumin, both PCU and mPCU-c had similar coefficients of friction of 0.48 ± 0.24 and 0.49 ± 0.17, respectively. Increasing the hydrophobicity of the substrates consistently led to an increase in the coefficient of friction values in the presence of albumin.

Discussion

In this study, we evaluated the tribological properties of polycarbonate urethanes (PCU) that are clinically used as meniscus prosthesis (NUsurface® by Active Implants) in the knee joint since 2008. The prosthesis presently is undergoing a clinical trial in the US and the outcomes are not yet known, but some preliminary MR images show restoration of joint space and maintenance of cartilage signal intensity at 12 months post-surgery.[54, 117]

The QCM-D data (**Table 3**, **Figures 1** and **2**) showed that the adsorbed mass of PRG4 is higher (larger $-\Delta f$) than that of albumin. The adsorbed PRG4 appears

as a fluffy and highly hydrated (large $-\Delta f$) viscoelastic layer on all the substrates as opposed to the adsorbed albumin, which forms a relatively rigid layer. The fluffy nature is likely due to the large hydrated polysaccharide content of PRG4 as opposed to the not-glycosylated albumin. The higher mass of PRG4 on the three hydrophobic surfaces compared to the hydrophilic SAM surface has also been observed elsewhere;[98,110] in contrast, albumin adsorption was not affected by surface hydrophobicity. Surprisingly, it appeared that not the hydrophobicity but the composition of the underlying substrate was important during the simultaneous adsorption of PRG4 and albumin. On the SAMs, irrespective of hydrophobicity, albumin was the first to adsorb. Over time PRG4 either adsorbed onto the albumin layer or replaced it due to the Vroman effect[118] (**Figure 2A,B** and **Table 3**). On PCU and mPCU-c the $-\Delta D/\Delta f$ values (**Table 3**) and ΔD vs Δf curves (**Figure 2C,D**) show that only albumin adsorbed and that PRG4 adsorption was completely blocked. Future studies may reveal the reason for the preference of the PCU surfaces for albumin over PRG4. If this property is related to the avidity of albumin, modifications of PCU to weaken this interaction should be topic for future research.

Adsorption of synovial fluid proteins had a great effect on the tribological behavior of the biomaterials. **Figure 3** shows that PRG4 adsorption on the biomaterials (PCU and mPCU-c) significantly decreased the coefficient of friction as compared to the bare surfaces, which will protect the cartilage against high friction in the knee joint. But on the SAMs, PRG4 adsorption did not show any lubricating effect. Difference in contact pressure could be playing an important role in causing this difference because the PCUs have Young's moduli of 5.6 to 8.8 MPa,[119] which will provide a low contact pressure of 0.4 MPa, whereas SAMs are created on gold surface thus their Young's modulus is an order of magnitude higher, i.e., 79 GPa,[120] giving rise to contact pressures up to 90 MPa. PRG4 has previously been shown to be ineffective when adsorbed on substrates with high stiffnesses.[97,98] The presence of surface-tethered C18 chains could have made mPCU-c locally softer than PCU giving rise to a coefficient of friction of 0.02 ± 0.02, the lowest value measured in this study. In the same fashion, the SAM molecules (similar length as that of mPCU-c surface chains) could have provided local softness to PRG4 molecules that apparently was not enough to counteract a very stiff base layer of gold. If we only consider the effect of substrate hydrophobicity (water contact angle) on the coefficient of friction after adsorption of PRG4 then we see a decreasing trend (**Figure 4**), the outlier being mPCU-c due to its local softness.

Figure 4 shows that the coefficient of friction after adsorption of albumin positively correlates with the water contact angle; beyond an angle of about $70° \pm 4°$, i.e., for mPCU-c and hydrophobic SAM, this increase is sharp and results in

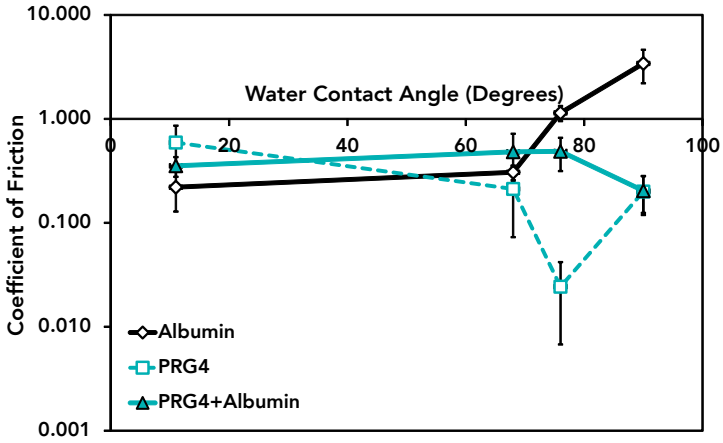

Figure 4. Coefficient of friction, measured using the AFM on substrates after the adsorption of different synovial proteins, as a function of the substrate hydrophobicity (water contact angle). Vertical error bars indicate SD of the mean of coefficient of friction (COF) measurements, comprising two to four separately prepared coatings and each coating measured at two to five different spots. Horizontal error bars indicate SD of the mean of water contact angle measurements, comprising two to four separately prepared coatings and each coating measured at two to three different spots.

high coefficients of friction (1.14 ± 0.19 and 3.42 ± 1.22, respectively), which might affect knee joint lubrication. The albumin molecule is known to change its orientation and configuration upon adsorption to hydrophobic surfaces[121] giving rise to much thinner layers[122] which could cause this drastic increase in coefficient of friction. Interestingly, albumin shows this effect both at high and low contact pressures; thus, hydrophobicity of the surface appears to be the dictating variable here.

Albumin did block PRG4 adsorption on the biomaterials, although ultimately both PCU and mPCU-c show a similar coefficient of friction ~0.5 (0.48 ± 0.24 and 0.49 ± 0.17, respectively), which is comparable to the coefficient of friction of bare PCU and one fourth of the coefficient of friction of bare mPCU-c. A coefficient of friction of 0.5 is orders of magnitude higher than the coefficient of friction of meniscus articulating with articular cartilage in a healthy knee joint and should be considered a matter of concern. **Figure 4** shows that the coefficient of friction was not affected by the slight increase in hydrophobicity (mPCU-c vs PCU) when PRG4 and albumin were allowed to adsorb simultaneously. Thus, the advantage of higher PRG4 adsorption on more hydrophobic biomaterials modified with sur-

face hydrocarbons is abrogated by the abundantly present albumin. Making PCU more hydrophobic by hydrocarbon surface modification is probably not a good strategy to develop an ideal material for articulation in synovial joints unless we can weaken the interaction of albumin with the biomaterial. Hydrophobic biomaterials may even carry an added risk for patients with Sjögren's syndrome[123] or patients having reduced PRG4 secretions because then albumin adsorption could drastically increase the coefficient of friction and may cause faster degradation of the joint tissues.

It is important to note that all the experiments for this study were performed *in vitro*. Ideally the coefficient of friction should have been measured between articular cartilage and the adsorbed protein layer on bulk biomaterials, instead, due to challenges and difficulties of using biological colloidal probes in AFM, it was decided to use hydrophilic silica bead colloidal probes simulating cartilage. The *in vitro* setup was required to make controlled protein adsorption studies possible; using QCM-D in a controlled fashion and then measure the coefficient of friction under boundary lubrication conditions best mimicked using the AFM. Since the coefficient of friction were measured against silica beads *in vitro*, in our opinion the exact values might differ from what would happen *in vivo* but the differences observed under various conditions would remain the same and important lessons can be learned towards the choice of biomaterials and their surface physico-chemistry for meniscus implants and probably other biotribological applications. It must be noticed that there are other molecules and macromolecules in synovial fluid that may play a role in the joint lubrication, however in this study we focused on PRG4 and albumin.

Conclusions

Our study showed that PRG4 molecules adsorbed in high amounts as a highly hydrated viscoelastic layer on all the substrates in comparison to albumin molecules. Adsorption of PRG4 on hydrophobic surfaces was significantly higher than on the hydrophilic surface. In contrast, no effect of surface hydrophobicity was observed on the adsorption of albumin. During the simultaneous adsorption of PRG4 and albumin, the influential factor was the composition of the underlying substrate and not its hydrophobicity, i.e., on PCU and mPCU-c the PRG4 adsorption was completely blocked and only albumin was adsorbed irrespective of hydrophobicity.

In the absence of albumin, PRG4 adsorption on the soft surfaces of PCU and mPCU-c significantly decreased the coefficient of friction as compared to the bare surfaces, resulting in the lowest coefficient of friction (0.024 ± 0.018) being measured on mPCU-c with adsorbed PRG4. This was most likely due to the increased

local softness by the surface-tethered C18 chains. Altered orientation and configuration of adsorbed albumin were likely to be the cause of the high coefficient of friction on mPCU-c and hydrophobic SAM as both surfaces had water contact angles above 70° ± 4°, independent of substrate's stiffness. The coefficient of friction after simultaneous adsorption of PRG4 and albumin on PCU and mPCU-c was found to be 0.48 ± 0.24 and 0.49 ± 0.17 respectively, higher than that measured on PRG4 adsorbed surfaces. The presence of albumin negated the advantage of higher PRG4 adsorption on more hydrophobic biomaterials that are modified with surface hydrocarbons. Increasing the hydrophobicity of the biomaterial by hydrocarbon surface modification is probably not a good strategy to develop a material suitable for articulation in a synovial joint.

Acknowledgments

This research forms part of the Project P2.03 TRAMMPOLIN of the research program of the BioMedical Materials Institute, co-funded by the Dutch Ministry of Economic Affairs. We also acknowledge grant no. 355591-2009 from the Natural Sciences and Engineering Research Council of Canada. We also like to thank Dr. Edward Rochford from the Department of Biomedical Engineering, UMCG, Groningen, The Netherlands for proof reading the article.

Chapter 4

An *in vitro* Study of Cartilage–Meniscus Tribology to Understand the Changes Caused by a Meniscus Implant

This chapter is an edited version of the manuscript:
Sara Ehsani Majd, Aditya Iman Rizqy, Hans J. Kaper, Tannin A. Schmidt, Roel Kuijer and Prashant K. Sharma
(submitted for publication)

Abstract

Active lifestyles increase the risk of meniscal injury. A permanent meniscus implant of polycarbonate urethane (PCU) is a promising solution to prevent total knee arthroplasty. Study of the changes in articular cartilage tribology in the presence of PCU is essential in developing the optimum meniscus implant. The purpose of this study is to examine changes in cartilage tribology caused by meniscus replacement with a permanent implant. A cartilage–meniscus reciprocating, sliding model was developed mimicking the stance and swing phases of the gait cycle, to evaluate its tribological properties in simulated physiological conditions. The meniscus was replaced with PCU to study the changes. Coefficient of friction (COF) was measured during sliding, and wear of cartilage was determined histologically and quantified according to a custom-made scoring system. In addition to PCU itself, three surface modifications of PCU were evaluated: PCU with C18 chains, with mono-functional PDMS (polydimethylsiloxane) and with mono-functional PTFE (polytetrafluoroethylene) groups. Cartilage–meniscus sliding resulted in low COF during both stance and swing ($0.01 < COF < 0.12$) and low wear of cartilage (scores < 1). Cartilage–PCU sliding, during stance, revealed similar low COFs. But during swing, the COFs were high (~1) with a maximum value of 1.6. COF increased with increasing the sliding time and decreased with increasing the contact pressure (according to a power equation) up to 1 MPa. The tested biomaterials and meniscus occasionally damaged the cartilage. No systematic correlation was found between the damage and the experimental condition. Changes in the lubricant solution or surface modification of PCU did not affect PCU's tribological performance. Therefore, Replacement of native meniscus with PCU resulted in an increase of the COF during the swing phase of the gait cycle, which is indicative of breakdown in interstitial fluid pressurization lubrication and therefore non-effective activation of the boundary lubrication. The wear of cartilage against biomaterial was not higher than its wear against meniscus under experimental conditions. To be concluded, permanent meniscus implants made of PCU, which show high COF during the swing phase of the gait cycle, may result in patient discomfort and wear of cartilage in the long term.

Introduction

Meniscal injuries are associated with active life styles[124] and professions.[125] Age, gender (male) and activity increase the chances of such injuries.[124,126] Of all knee injuries 14.5−38% are meniscal injuries.[124,126] The incidence of sports-related meniscal lesions leading to a meniscectomy is 60−70 per 100,000 patients per year.[124] Additionally, the natural aging process causes degenerative tears of the meniscus.[21]

The medial and lateral menisci in the knee joint are crescent-wedge-shaped fibro-cartilaginous tissues, located in between the weight bearing surfaces of the tibia and femur.[21] Menisci play an essential role in the load distribution and stability of the knee joint. The lateral meniscus is much more mobile as compared to the medial meniscus, which can explain the higher risks of generating medial meniscal tears.[21]

The porous and permeable meniscus tissue consists mainly of water, i.e., 63−75% of the total weight.[127] Two types of cells are recognized in the meniscus, fibro-chondrocytes (in the inner and middle part of the meniscus) surrounded by an extra-cellular matrix (ECM) and fibroblast-like cells (in the outer part of the meniscus) surrounded by a dense connective tissue.[127] The dry weight of the matrix is composed of 75% collagen (90% type I collagen and 10% type II, III and V collagens) and 2.5% proteoglycans (mainly aggrecan).[127] The regenerative capability of the meniscus is limited due to vascularization in only the peripheral one-third of its volume.[21,24]

The menisci rub against a thin layer (1−5 mm)[1] of avascular articular cartilage, which covers the ends of the femoral condyle and tibia plateau. Articular cartilage consists of 70−80% water. Collagens make up to ~60% of the dry weight (90% of which is type II collagen) and proteoglycans ~30%. The final 10% is made up of non-collagenous proteins, chondrocytes and lipids. The chondrocytes at the superficial zone synthesize a superficial zone protein (SZP, also known as proteoglycan 4, PRG4 or lubricin), which plays an important role in the lubrication of the articular cartilage.[9]

Articular cartilage and menisci are surrounded by synovial fluid. Synovial fluid components—hyaluronan (HA), albumin, proteoglycan 4 (PRG4, also known as lubricin) and surface-active phospholipids (SAPL)—absorb in/on the cartilage and meniscus surfaces and provide lubricating properties there.[26]

In a healthy knee joint, articular cartilage, meniscus and synovial fluid, together, provide coefficient of friction (COF) as low as 0.005 as well as excellent

wear protection.[25] A variety of lubrication mechanisms have been proposed to be responsible for this unique tribological system.[28,34,36,82] "Interstitial fluid pressurization and weeping" (IFPW)[34,128] in combination with boundary[39,105] lubrication mechanisms are considered to be active.

A meniscus has a limited capacity to regenerate.[21,24] Untreated tears and consequently loss of function change the load distribution inside the knee, resulting in early signs of degenerative arthritis.[58] Repairing strategies, e.g., sutures, anchors or staples, are only applicable on the vascularized zone of meniscus, even so it is not often reliable.[129] Meniscectomy (partial or total) immediately relieves pain and improves the knee function, yet 50% of the patients show symptoms of premature osteoarthritis.[58] The current treatment for symptomatic patients (post-meniscectomy) is the transplantation of meniscal allografts—from a donor meniscus—which also relieves pain and improves the knee function.[61] The limited availability of allografts of appropriate size, the risk of transmission of disease and the shrinkage of allograft post-implantation are major drawbacks of this approach.[61]

Therefore, developing a meniscus implant is a viable option. Implants based on biodegradable scaffolds, made of natural or synthetic polymers, aiming for the regeneration of the meniscus[65,66,68–71] or permanent synthetic implants replacing the native meniscus[60,72–75] have been developed. An anatomically shaped, polycarbonate urethane medial meniscus implant—reinforced circumferentially with ultrahigh molecular weight polyethylene fibers—(NUsurface® by Active Implants) showed promising results after six months in a sheep model.[60] For human use, the design was changed to a freely floating, disk-shaped implant, which requires the presence of the peripheral rim of the native meniscus. Therefore, it is not an appropriate choice for patients having a total meniscectomy.[77] Preliminary clinical results showed considerable pain relief, although there were major complications due to implant dislocation, fracturing or tearing and inflammation or progression of osteoarthritis.[78,79] Recently, a project (TRAMMPOLIN) was funded by the Dutch BioMedical Materials program to design an anatomically shaped permanent meniscus implant made of polycarbonate urethane.[130]

On the fundamental level, there is still little known about the tribology of cartilage and meniscus or the effects on the knee tribology upon replacing the meniscus with an implant. As opposed to a native meniscus, an artificial meniscus implant, being non-porous, is incapable of contributing to the joint lubrication through IFPW.[34,128] Therefore, once it is implanted, the artificial meniscus can only provide boundary lubrication on its surface with the help of adsorbed synovial fluid molecules.[131]

The first aim of this study was to examine the native cartilage–meniscus tribology in simulated physiological conditions. The second aim was to clarify the tribological changes that occur when the native meniscus is replaced with an artificial one: introduction of a biomaterial (polycarbonate urethane used for NUsurface®) in an otherwise healthy knee joint. The third aim was to speculate the operative lubrication mechanism when an artificial permanent meniscus is implanted in a knee joint and to study whether surface modifications, aimed to enhance boundary lubrication, would improve COF and decrease wear of cartilage. Therefore, a cartilage–meniscus model, with a reciprocating unidirectional movement was developed to measure the friction and wear at the interface. One part of the reciprocating cycle was loaded, mimicking the stance phase of the gait cycle during normal walking, while the other part was low-loaded, mimicking the swing phase. The same model was used to study the cartilage–biomaterial interface and to understand the operative type of lubrication mechanism. The polycarbonate urethane materials with surface modifications were used to see whether the modifications were able to affect the tribology of the cartilage–biomaterial interface.

Experimental Section

Materials. Polycarbonate urethane (Bionate 80A, PCU) and PCUs with surface modifications—Bionate II 80A (mPCU-c, with C18 chains), Bionate 80A S (mPCU-s, with mono-functional PDMS groups) and Bionate 80A 2F (mPCU-f, with mono-functional PTFE groups)—were provided by DSM Biomedical (Geleen, The Netherlands). The samples were injection-molded disks (diameter ≈ 37 mm and thickness ≈ 4 mm; **Figure 1A**). Hyaluronic acid sodium salt (hyaluronan, HA) (average M_w of 3.0 × 10^6 Da) was purchased from Kraeber & Co GMBH, (Ellerbek, Germany). Bovine serum albumin (98−99%) (BSA) and 1-palmitoyl-2-oleoyl-sn-glycero-3-phosphocholine (POPC) were from Sigma-Aldrich, Ltd. (St. Louis, MO). Bovine proteoglycan 4 (PRG4) was isolated, purified and characterized as described previously.[16] n-Hexane was from Acros Organics (Geel, Belgium). Formaldehyde solution 4% was from Klinipath (Deventer, The Netherlands). Chloroform and Titriplex® III (EDTA, ethylene-di-nitrilotetraacetic acid disodium salt dihydrate) were from Merck (Darmstadt, Germany).

Preparation of POPC vesicles. POPC was first dissolved in chloroform. Then, chloroform was evaporated by blowing filtered nitrogen gas over the solution, completed by 45 min of vacuum drying at room temperature. The dried POPC film was resuspended in 10 mM phosphate-buffered saline (PBS) resulting in a suspension of POPC vesicles of different sizes. To obtain a mono-dispersed, homogeneous vesicle size distribution the suspension was filtered using a mini-extruder

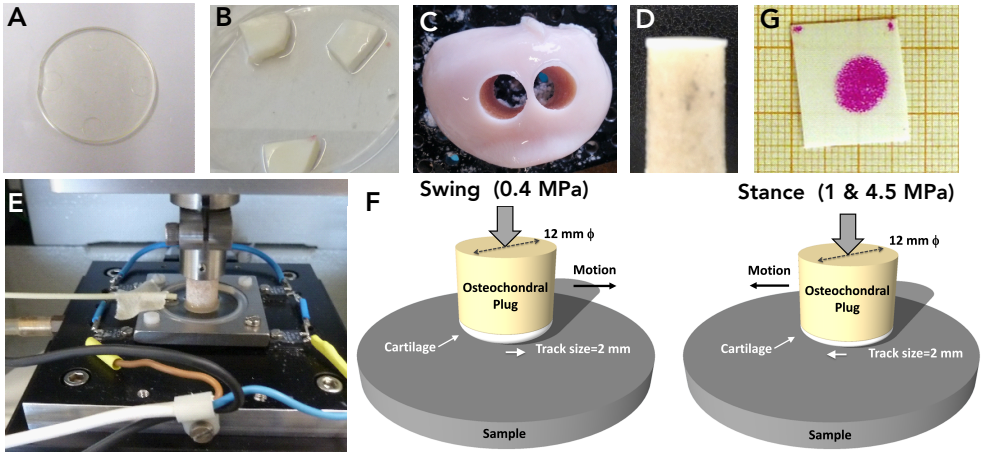

Figure 1. A: PCU disk. **B:** Bovine meniscus samples. **C:** Bovine femoral head with 2 holes from which **D:** osteochondral plugs were harvested. **E:** Experimental set-up (UMT-3). **F:** Schematic illustration of loading and low-loading part of the cycles (stance and swing phases of the gait cycle) during the friction measurements with UMT-3. **G:** Pre-scale film with a contact area mark.

(Avanti Polar Lipids, Inc., Alabaster, USA), in three steps using membranes with decreasing pore diameter—1000, 400 and 100 nm (Whatman, Nuclepore Track-Etch Membrane, St. Louis, MO). The solution was forced through each membrane for 11 times.[132] The size of the vesicles in the suspension (138 ± 24 nm) was measured using light scattering (Zetasizer, Malvern Instruments Ltd., Worcestershire, UK), to assure the mono-dispersity of the solutions.

Preparation of lubricant solutions. Four different solutions in 10 mM PBS were prepared: BSA+HA, BSA+HA+PRG4, BSA+HA+POPC and BSA+HA+PRG4+POPC. The concentrations of the components were: 5 mg/mL BSA,[11] 2 mg/mL HA,[13] 100 μg/mL PRG4[16] and 150 μg/mL POPC[19] to mimic the physiological concentrations in healthy synovial fluid.[105,131] HA molecules were mixed with PBS 24 hours prior to measurements to allow complete dissolution.

Cleaning of polymer disks. All the PCU disks were cleaned with n-hexane, rinsed with ultrapure water (Milli-Q) and then hydrated in sterile ultrapure water for at least 2 weeks prior to experimentation, to allow for swelling.

Preparation of osteochondral plugs and meniscus samples. Bovine stifle joints (~2 year-old and males) were purchased from a local slaughterhouse (Kroon Vlees, Groningen, The Netherlands). The joints were dissected 1 day after slaughter and

delivered intact (unopened with surrounding tissues) and vacuum-packed. To prepare osteochondral plugs and meniscus samples, the joint was opened at room temperature (20−24 °C). All the visibly damaged or arthritic joints were excluded.

Meniscus samples were cut off from the menisci—from the side in contact with the tibial surface—using a scalpel (sample thickness ≈ 3 mm and surface ≈ 15 × 15 mm^2) (**Figure 1B**). Immediately prior to the test, meniscus samples were fixed onto a silicon rubber slab using pins to stay well-stretched and in-place during the experiment.

Osteochondral plugs of 12 and 6 mm in diameter were drilled out of the femoral condyles (**Figure 1C,D**) using hollow drill bits. The 6 mm plugs were used for cartilage–meniscus as well as for high contact pressure cartilage–PCUs tests. The 12 mm plugs were used for low contact pressure cartilage–PCUs tests.

Sample preparation was done under continuous wetting and cooling with PBS. Touching the surfaces intended for sliding was carefully avoided. Samples were rinsed with PBS and stored in PBS at 4 °C and used at the same day.

Tribology tests. A CETR-UMT-3 (Universal Mechanical Tester) (Bruker Corporation, USA) (**Figure 1E**) was used in a reciprocating configuration to measure the COF —the ratio of the friction force and the applied normal force—at the cartilage–meniscus and cartilage–biomaterial interfaces. An osteochondral plug was mounted at the load cell and slid against meniscus or one of the PCUs at a speed of 4 mm/s and frequency of 1 Hz,[27] at 33 °C—the temperature inside a healthy human knee joint.[133] Experiments were done in one of the indicated lubricant solutions. A specific loading/low-loading condition was used to simulate the gait cycle during normal walking. The load during the low-loaded part of the cycle (swing phase of the gait cycle) was kept constant at 4 N (0.4 MPa), while the load during the loaded part of the cycle (stance phase of the gait cycle) was varied according to the experiment (**Figure 1F**). For experiments longer than 1 hour ultrapure water was added using a peristaltic pump at a flow rate of 0.13 μL/s to compensate for evaporation.

During the first phase COFs were measured at the cartilage–meniscus, cartilage–PCU, cartilage–mPCU-c, cartilage–mPCU-s and cartilage–mPCU-f interfaces, for 1 hour (simulating 9 hours of normal activity), at a P_c of 1 MPa (40 N) during stance, in the presence of one of the solutions, BSA + HA, BSA + HA + PRG4, BSA + HA + POPC or BSA + HA + PRG4 + POPC. During the second phase COFs were measured at the interfaces of cartilage–meniscus, cartilage–PCU, cartilage–mPCU-c, cartilage–mPCU-s and cartilage–mPCU-f, for 4 hours (simulating 36 hours of normal activity), at a P_c of 1 MPa (40 N) during stance, in the solution containing BSA +

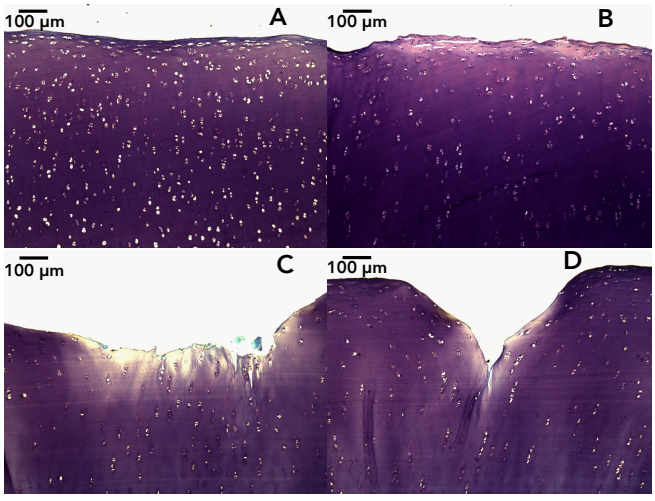

1	Surface abrasion	Scores to be given
	None	0
	Minor	1
	Moderate	2
	Severe	3
2	Clefts up to the radial zone	Scores to be given
	None	0
	1–2	4
	≥ 3	5
3	Clefts up to the tidemark	Scores to be given
	None	0
	1	6
	≥ 1	7
	Total Score	Summation of all

Figure 2. Pictures of the histological sections showing the surface of the articular cartilage **A:** without damage on the surface, corresponds to score = 0, **B:** with surface abrasion, corresponds to score = 1–3, in this case a minor damage corresponds to score = 1, **C:** with severe surface abrasion, corresponds to score = 3 and **D:** clefts up to the radial zone, corresponds to score = 4. The table explains of the scoring system in details. No clefts up to the tidemark were observed in this study.

HA + PRG4 + POPC. During the final phase COFs were measured at the interfaces of cartilage–meniscus and cartilage–PCU, for 1 hour, at the P_c of 4.5 MPa (170 N) during stance, in the solution containing BSA + HA + PRG4 + POPC.

A custom-made MATLAB program was used to extract the mean and standard deviation from each cycle for each experiment. Care was taken to only consider COFs that were measured at an applied load within ± 50% of the target load.

Contact area measurement. After each experiment, the contact area between the plug and sample was visualized using pre-scale films (Extreme Low Pressure 4LW, Fujifilm, Tokyo, Japan) by inserting the film in between the cartilage and meniscus/biomaterial (**Figure 1G**) and then applying the desired load. The contact area and aspect ratio (the ratio between the major and minor axes) were determined using a custom-made MATLAB program. The contact area was used to calculate the contact pressure (P_c) of each experiment.

Histology. All the osteochondral plugs were prepared for histological examinations to assess damage of the cartilage during the friction tests. The plugs were fixated in 4% paraformaldehyde solution for at least 48 hours, then rinsed thoroughly with running water and once with PBS. Most of the bony part of the plugs

was removed before the remaining subchondral bone was decalcified using 10% EDTA (10% Titriplex in ultrapure water) for at least 2 weeks while being shaken. EDTA solution was refreshed every 2–3 days. The samples were then dehydrated in a series of ethanol solutions, cleared in xylol and embedded in paraffin. Sections of 5–7 µm were cut using a microtome (Leica RM2235, Leica Microsystems, Rijswijk, The Netherlands). Three slides with sections of each sample were dewaxed, rehydrated and stained with thionine, hematoxylin/eosin and Syrius Red, respectively, and studied using a light microscope.

Quantifying the cartilage wear. Cartilage damage was quantified using a custom-made scoring system explained in the inset table of **Figure 2** which related to cartilage damage as shown in **Figure 2**. The damage was scored in three categories: (1) surface abrasion, (2) clefts up to the deep zone and (3) clefts up to the tidemark, and the final score is the summation from the three categories. Scoring was performed by two evaluators (SEM, RK), which were blinded for the experimental settings.

Statistical analysis. Unpaired, two-tailed Student's t-test was performed to assess the significance of differences between groups. Differences were deemed significant if $p \leq 0.05$. Histological scores were analyzed using a Kruskal-Wallis one way analysis of variance on ranks. If appropriate a Dunn's post hoc test was used for differences between individual samples.

Results

Friction

– *Correlation between the Stance and Swing Phases*

Figure 3A shows a typical plot of COF versus cycle number measured during the first phase of the experiments (explained in experimental section) between the interfaces of cartilage–meniscus (control) and cartilage–biomaterial. At the cartilage–meniscus interface, COF remained low and was similar during both stance and swing (**Figure 3A**, black lines). At the cartilage–biomaterial interface, on the other hand, the COF was low only during stance, during swing the COF increased with increasing cycle number (**Figure 3A**, blue lines).

In the experimental setup, each loaded part of the cycle (stance) was followed by the low-loaded part (swing) and vice versa. Thus, the interfacial changes occurring during one part of the cycle affect the other part as well. **Figure 3B** shows that if the swing COF increased after 1-hour measurement, the stance COF increased linearly too. For the cartilage–PCUs interface, the COF at stance remained

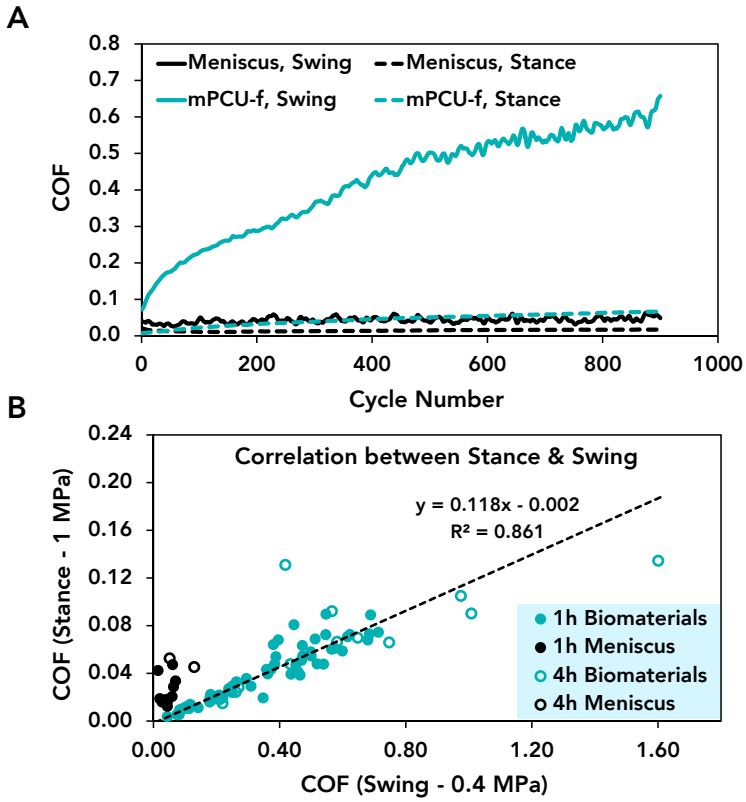

Figure 3. A: COF versus cycle number measured at the cartilage–meniscus (black lines) and cartilage–mPCU-f (blue lines) interfaces, in the presence of BSA+HA+POPC in PBS, for 1 hour, at 1 MPa during stance (dashed lines) and 0.4 MPa during swing (solid lines). **B:** The COF during the last cycle of each measurement was plotted to show the correlation between the COF of the stance (1 MPa) versus the swing (0.4 MPa), for meniscus (black) and all the PCU materials (blue), measured in the presence of all the lubricant solutions, for 1 hour (filled circles) and measured in the presence of BSA+HA+PRG4+POPC, for 4 hours (empty circles).

~one-tenth of the COF at swing (0.118 times lower). At the cartilage–meniscus interface, the COFs at stance and swing did not follow the same linear relation. **Figure 3B** shows that during the first 1 hour of swing, COF at the cartilage–meniscus interface (control) was lower than 0.07 (with a minimum value of 0.01), whereas the COF at the cartilage–PCUs interface increased up to 0.71. The COF at stance remained below 0.05 and 0.09, for the cartilage–meniscus and cartilage–PCUs interfaces, respectively.

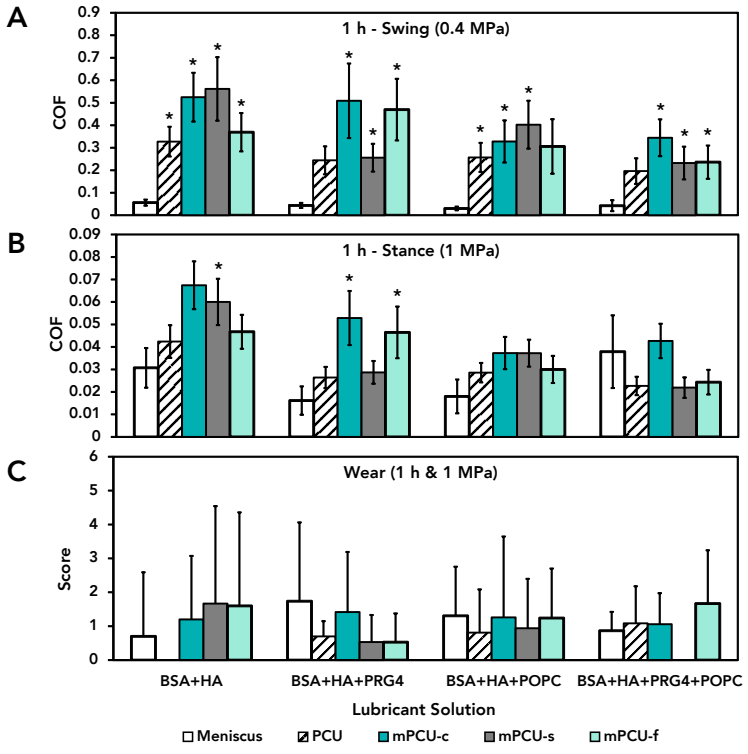

Figure 4. Average COF measured in the presence of different lubricant solutions during **A:** swing (0.4 MPa) and **B:** stance (1 MPa), in 1-hour experiments, on PCU material, with different surface modifications (plots **A** and **B** have different scales). Error bars indicate SD of the mean of COFs over 2–6 separate measurements. **C:** Scores of wear of cartilage at the end of the friction experiments reported in **A** and **B**. Error bars indicate SD of the mean of the scores. Asterisks (*) denote significant differences ($p < 0.05$) as compared to meniscus in that specific solution.

– Effect of Surface Modification and Lubricant Molecules

Average COF at the cartilage–meniscus interface (control), including stance and swing, remained low, 0.06 ± 0.01, irrespective of the lubricant used. The lowest measured COFs were 0.016 ± 0.006 and 0.030 ± 0.008 and the highest measured COFs were 0.037 ± 0.016 and 0.050 ± 0.013 during stance and swing phases, respectively (**Figure 4A,B**).

Replacing meniscus with PCU significantly increased the COF only during swing in solutions containing BSA+HA ($p = 0.039$) and BSA+HA+POPC ($p = 0.021$) (**Figure 4A**). The maximum COF measured at the cartilage–PCU interface in 1 hour was 0.33 ± 0.07.

Replacing meniscus tissue with mPCU-c, mPCU-s and mPCU-f significantly increased the COF during swing in all lubricant solutions. The only exception was mPCU-f in BSA+HA+POPC (p = 0.060) (**Figure 4A**). The highest COF (0.56 ± 0.14) was measured at the cartilage–mPCU-s interface, in the presence of BSA+HA. During stance, replacing meniscus with mPCU-s in BSA+HA (p = 0.051) solution or mPCU-c (p = 0.005) and mPCU-f (p = 0.021) in BSA+HA+PRG4 solution significantly increased the COF (**Figure 4B**). All the PCU materials behaved as well as meniscus in BSA+HA+POPC and BSA+HA+PRG4+POPC, during stance (**Figure 4B**).

Comparing all PCU materials, the lowest average COF was found with PCU, 0.023 ± 0.004, in BSA+HA+PRG4+POPC (the most complete lubricant solution) (**Figure 4B**). Comparing individual measurements, then the lowest measured COF at cartilage–biomaterial interface was 0.0035 which was 3.5 fold lower than 0.012, the lowest measured COF at a cartilage–meniscus interface.

No significant differences were found between modified and unmodified PCUs with respect to the COFs measured while sliding against cartilage in different lubricant solutions.

– Effect of Sliding Duration

The effect of sliding duration was evaluated in BSA+HA+PRG4+POPC as a lubricant solution only.

A relative increase in COF with increasing the sliding duration was observed (**Figures 3B**, **5A,B** and **6B**). The maximum COF measured after 4 hours was 0.90 ± 0.44 on mPCU-s during swing. The average COF at the cartilage–meniscus interface during swing appeared to double, from 0.04 ± 0.02 after 1 hour to 0.09 ± 0.03 after 4 hours (**Figure 5A**). Nevertheless, the differences between 1-hour and 4-hour measurements during both stance and swing for each specific material were not significant (**Figure 5A,B**). The only exception was mPCU-s for which the COF during stance significantly increased (p=0.028) with increasing the sliding duration from 1 to 4 hours (**Figure 5B**).

Similar to the 1-hour experiments in experiments lasting 4 hours no significant differences were found between modified and unmodified PCUs with respect to the COFs measured while sliding against cartilage. The only exception was mPCU-s during stance (p = 0.048) (**Figure 5B**).

After 4 hours of sliding, all COFs measured during swing, at cartilage–PCU (all) interfaces were significantly higher than the ones measured for cartilage–meniscus interfaces (**Figure 5A**). During stance, on the other hand, the only significant

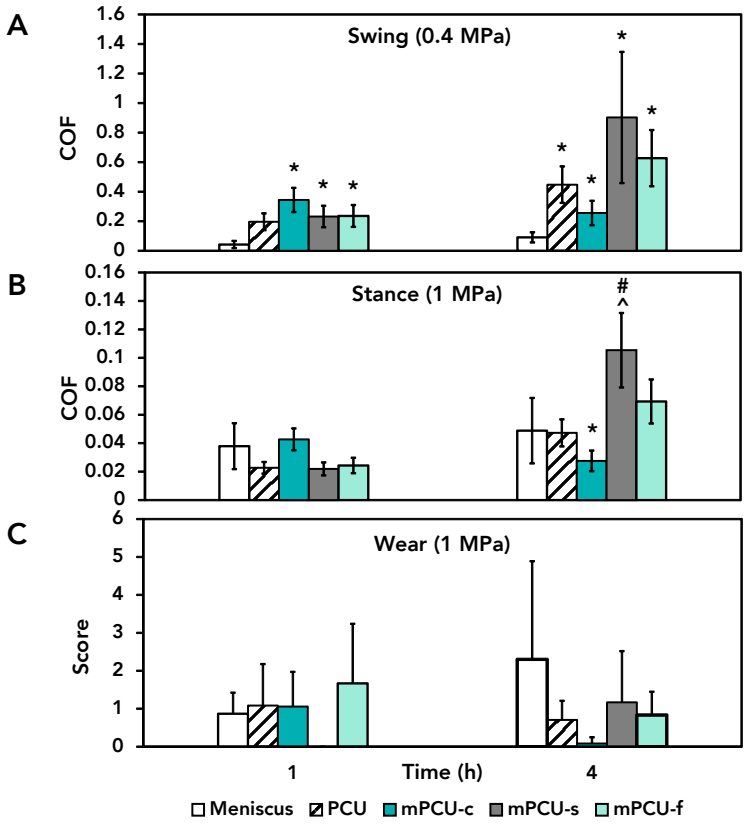

Figure 5. Average COF measured at different sliding duration during **A:** swing (0.4 MPa) and **B:** stance (1 MPa), in the presence of BSA+HA+PRG4+POPC in PBS for 1 hour or 4 hours (plots have different scales). Error bars indicate SD of the mean of COFs over 2–4 separate measurements. **C:** Scores of wear of cartilage at the end of the friction experiments reported in **A** and **B**. Error bars indicate SD of the mean of the scores. Significant differences ($p < 0.05$) are indicated by asterisks (*; as compared to meniscus in that specific solution), the hash sign (#; as compared to the same biomaterial in 1-hour experiment) and the caret (^; as compared to PCU in that specific solution).

difference (p = 0.029) was observed at the cartilage–mPCU-c interface, where a lower COF as compared to cartilage–meniscus was assessed (**Figure 5B**).

– Effect of Contact Pressure (P_c)

It is clear that the COFs during the stance phase were much lower than those measured during the swing phase (**Figures 3–5**). This identifies P_c as an important variable influencing the COF. The P_c of individual measurements was correlated to the measured COF (**Figure 6A**). Negative correlations were found for both cartilage–

PCU materials interface (blue circles) and cartilage–meniscus interface (black circles). Within the first 1 hour of the experiments and in the for $0.15 < P_c < 1.6$ MPa, a rough approximation of the COF can be made via a power equation 1, if the P_c is known.

$$COF = \alpha P_c^{\beta} \quad (1)$$

In this equation β is the contact pressure exponent and α is a multiplication factor, with values of −1.56 and 0.03 for cartilage–PCUs and −0.55 and 0.02 for cartilage–meniscus interface, respectively.

As the measurement time changed from 1 to 4 hours (filled black vs empty black circles), the COF increased during both stance and swing for cartilage–PCUs interface (**Figure 6B**). An equation of the form (1) can also be used to relate the COF to P_c for 4-hour experiments for cartilage–PCU materials interface (**Figure 6B**, dashed black line), in which β decreased very slightly to −1.58 and α increased to 0.06 (2 fold), compared to the blue line in **Figure 6A**. For cartilage–meniscus interface (**Figure 6C**), β increased to 0.08 and α increased to 0.07 (3.5 fold), compared to the black line in **Figure 6A**.

When the P_c increased from 1 to 4.5 MPa, during swing, at the cartilage–PCU interface, the COF increased significantly from 0.20 ± 0.06 to 0.49 ± 0.16 (2.5 fold) (**Figure 7A**); however, the COF at the cartilage–meniscus interface did not increase significantly. During stance, increasing the P_c to 4.5 MPa did not cause any further decrease in the COF, with an average COF smaller than 0.06, neither at the cartilage–PCU nor at the cartilage–meniscus interfaces (filled blue circles in **Figure 6B,C**).

When the sliding duration increased from 1 to 4 hours at 4.5 MPa for cartilage–PCU interface (**Figure 6B**, gray circles), the COF increased slightly with average values of 1.1 ± 0.5 and 0.08 ± 0.03 for swing and stance, respectively.

Wear

The damage to the cartilage surface of the osteochondral plugs was quantified at the microscopic level (**Figures 4C**, **5C** and **7C**). The scores varied between 0 and 2. No significant differences in the scores were found between cartilage that slid against meniscus and cartilage that slid against PCUs. Also, surface modification of PCUs, lubricant solution chemistry, sliding duration for 1 hour up to 4.5 MPa and 4 hours up to 1 MPa contact pressure did not result in differences in damage scores. Only the combination of 4-hour experiments at 4.5 MPa for cartilage–PCU interface increased the wear to 4.3 ± 1.2.

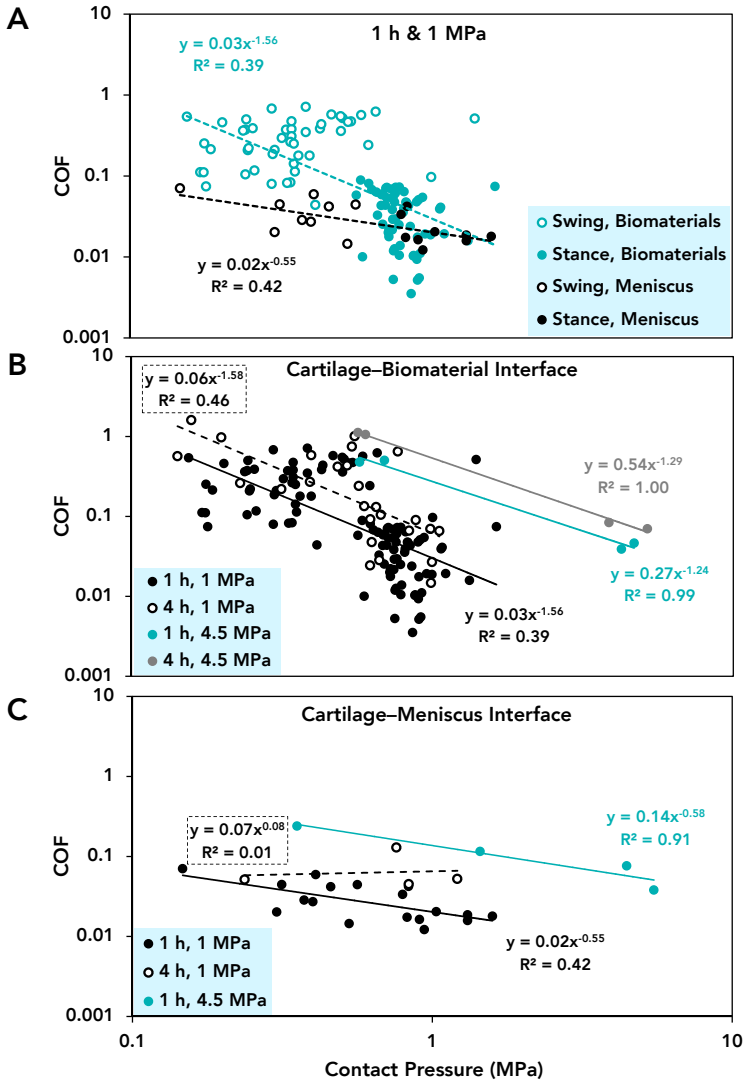

Figure 6. COF versus P_c plots measured: **A:** during the swing (0.4 MPa) (empty circles) and stance (1 MPa) (filled circles), at the cartilage–meniscus (black circles) and cartilage–PCU materials (blue circles) interfaces, irrespective of surface modifications, **B:** at the cartilage–PCU materials interface; filled black circles are related to all materials and all lubricant solutions; empty black circles are related to all materials tested in BSA+HA+PRG4+POPC; blue and gray circles are related to cartilage–PCU interface, in the presence of BSA+HA+PRG4+POPC and **C:** at the cartilage–meniscus interface, filled black circles are measured in the presence of all lubricant solutions; empty black and blue circles are measured in the presence of BSA+HA+PRG4+POPC.

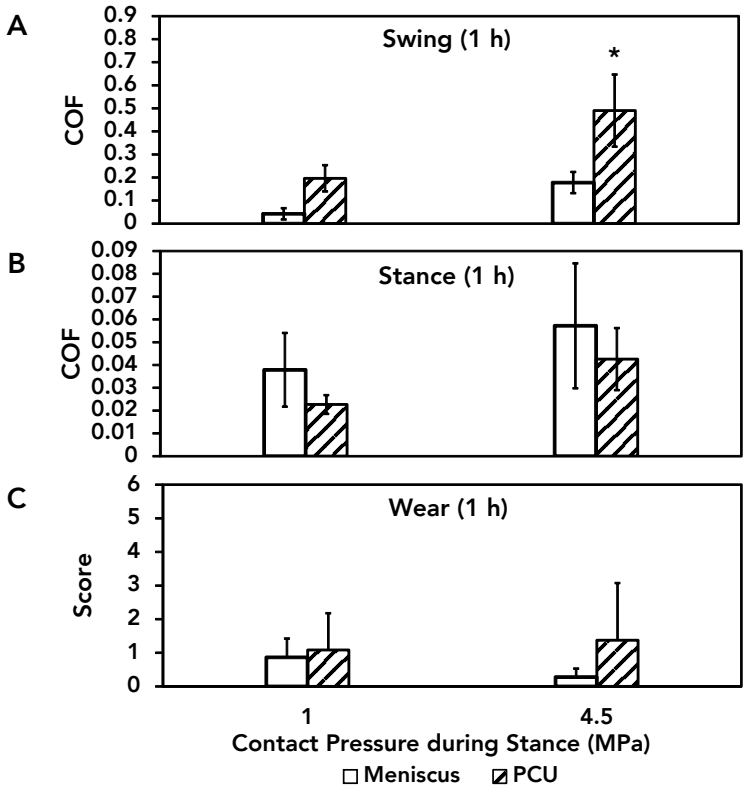

Figure 7. Average COF measured for different P_c's during stance at the cartilage–meniscus (white bars) and cartilage–PCU (hatched bars) interfaces, for 1 hour, in the presence of BSA+HA+PRG4+POPC, at the P_c of **A:** 0.4 MPa during swing and **B:** 1 and 4.5 MPa during stance (plots have different scales). Error bars indicate SD of the mean of COFs over 2–4 separate measurements. **C:** Scores of wear of cartilage at the end of the friction experiments reported in **A** and **B**. Error bars indicate SD of the mean of the scores. The asterisk (*) denotes significant differences ($p < 0.05$) as compared to 1 MPa.

Discussion

This work is the first *in vitro* study describing friction and wear at the cartilage–meniscus interface. The results are used to further explore the tribological changes occurring when meniscus tissue is replaced with a PCU biomaterial, mimicking replacement of meniscus with meniscus prosthesis in an otherwise healthy knee joint. We aimed at performing measurements at P_c's of 0.4, 1 and 4.5 MPa.[134] The effective average P_c values were 0.4 ± 0.2, 0.9 ± 0.2 and 4.6 ± 0.8 MPa. The measurements were performed for 1 and 4 hours at 1 Hz mimicking the same duration of continuous walking or 9 and 36 hours of normal activity, respectively, assuming

one million steps taken per year.

The COF at the cartilage–meniscus interface at 1 MPa after 36 hours of normal activity (0.05 ± 0.02) was twice the highest value (0.023) measured by Charnley in 1960 for a human knee joint with intact cartilage.[5] Cartilage and meniscus are porous tissues. When compressed at 1 MPa, the interstitial fluid weeps out of the pores and creates a thick fluid film at the interface according to the IFPW mechanism. This lubricates the sliding surfaces for hours, resulting in such low COF values. Conversely, during swing (at 0.4 MPa, after 36 hours of normal activity) the COF was 0.09 ± 0.03, almost 5 times higher than the maximum COF measured by Charnley. These high COFs indicate that at low P_c's not enough interstitial fluid weeps out to the interface to create a thick fluid film. On the other hand, the COF lower than 0.1 excludes pure boundary lubrication,[1] indicating a mixed IFPW and boundary lubrication mechanism to be active.

At the cartilage–meniscus interface, within the first 9 hours of normal activity, the COF decreased with increasing P_c according to power equation 2 (for $0.15 < P_c < 1.6$ MPa) (**Figure 6C**, filled black circles).

$$COF_{Cartilage-Meniscus} = 0.02\, P_c^{-0.55} \qquad (2)$$

Such a decrease in COF in a similar pressure range for cartilage against a hard surface or cartilage–cartilage interface has been reported before.[27] However, it appears that higher P_c's (as observed for 4.5 MPa in this study) do not further decrease the COF, i.e., a P_c of around 1 MPa completely harnesses the IFPW lubrication mechanism.[34,128] In order to confirm this statement, extra measurements were performed at a P_c of 2.4 ± 0.4 MPa, and the average COF measured for cartilage–meniscus was 0.04 ± 0.03, which was not lower than the average COF measured at 1 MPa (data not shown).

When meniscus tissue was replaced with PCUs, increased COFs were expected. This did occur during the swing phase, but did not occur during the stance phase.

During the stance phase COFs for cartilage–PCUs interface were lower or as low as cartilage–meniscus interface (the lowest COF measured was 0.0035), indicating that IFPW lubrication mechanism is still active at the cartilage–PCU materials interface, even though the bulk PCU material is not porous. Thus, during stance the cartilage surface would be well protected from wear against biomaterials by a thick fluid film, mainly derived from the cartilage itself. The reason for measuring much lower COF (0.0035) during stance at the cartilage–PCUs interface as compared to

cartilage–meniscus interface (**Figure 6A**) could be the difference in quality of PCU materials and meniscus used here. The polymer disks were homogeneously thick, plane-parallel, pressure molded and flat. Whereas the meniscus samples were manually sliced from the whole meniscus, where the top side was smooth and untouched but the lower side could be rough and in some cases having irregular thickness along the sliding direction.

During the swing phase of the gait cycle, the cartilage–PCUs interfaces revealed significantly higher COFs (10 fold) than cartilage–meniscus interfaces, with the highest COF being 0.71 as compared to 0.07. COF values close to 1 during swing indicate complete breakdown of the IFPW lubricating mechanism. Under these conditions boundary lubrication (complete contact between cartilage and biomaterial) must facilitate the sliding process. If so, the surface modifications of PCU were supposed to result in lower COF values, but that was not observed (**Figures 4A** and **5A**). A possible reason may be the presence of albumin in the lubricant solution. Albumin blocks the adsorption of PRG4, an important boundary lubricant, to the surface of the biomaterials.[131] Phospholipids, another important molecules in the joint lubrication, did not adsorb on the surface of the PCUs when brought in the form of vesicles (**Supplementary Data Figure 1**).

The COF at the cartilage–PCUs interface (for $0.16 < P_c < 1.6$ MPa) can be roughly estimated by power equation 3 (**Figure 6B**, filled black circles).

$$COF_{Cartilage-Meniscus} = 0.03\, P_c^{-1.56} \quad (3)$$

The sensitivity to P_c (β) is threefold higher than the one of cartilage–meniscus interface (Equation 2).

After 36 hours of normal activity, the COF of cartilage–PCUs interfaces during the swing phase even becomes 10 fold larger than at the cartilage–meniscus interface, with a maximum measured value of 1.6 (**Figures 3B** and **5A**).

The standard deviations in **Figures 4**, **5** and **7** and the spread in points shown in **Figure 6** indicate that besides P_c's other variables also affect the COFs. One would be the aspect ratio (AR) of the contact zone taken (**Figure 1G**). Ideally we expect a round circular contact area (AR = 1) between the cartilage and PCU materials/meniscus, but that was not always the case. We observed $1 < AR < 2$, caused by misalignment or lack of roundness of the femoral head. The AR appeared not to be related to COF (**Figure 8**). Thus, variability in data cannot be explained using AR.

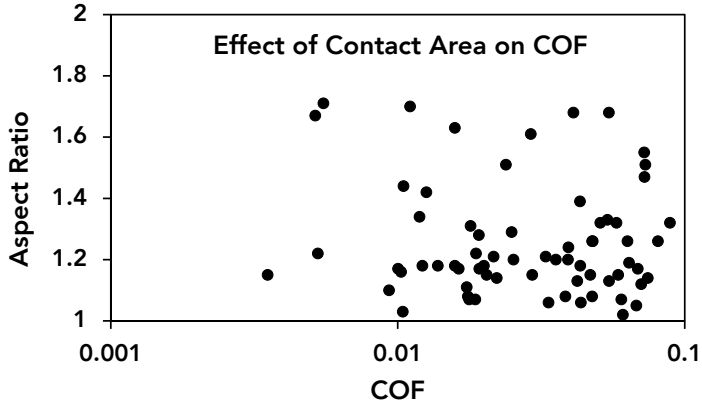

Figure 8. Correlation between aspect ratio and COF during stance (1 MPa), for 1 hour, of all the PCUs and meniscus, in all the solution chemistries.

In the present study, the cartilage–meniscus and cartilage–PCUs sliding did not result in differences in damage to the cartilage surface, independent of the duration of sliding or the applied contact pressures. This indicates that the PCU biomaterials appear suitable for replacement of an articulating surface in the knee joint, at least for a limited period of time. Systematic experiments are required to reveal how these materials will behave in the long term. A small number of pilot experiments showed an increase in cartilage wear at high contact pressures—in 60-hour experiments a P_c of 1 MPa during stance did not increase the cartilage wear but a P_c of 4.5 MPa did (**Figure 9**). Additionally, monitoring the tribological performance of these implants *in vivo* is required. *In vivo* experiments aiming at elucidating the effects of inflammatory factors and the foreign-body reaction are relevant as well.

Conclusion

The use of mimicking stance and swing phases of the gait cycle during friction measurement illustrated the role of IFPW lubrication and mixed IFPW and boundary lubrication mechanisms at the cartilage–meniscus interface. At the cartilage–meniscus interface very low friction ($0.01 < COF < 0.12$) and wear (scores < 1) were observed. When meniscus tissue was replaced with a PCU material, the IFPW remained active during stance, resulting in comparable COFs. During the swing phase approximately 10 fold higher COFs were found as compared to cartilage–meniscus interface because the IFPW mechanism fails and the boundary lubrication mechanism involving PRG4 and POPC was not activated. Since none of the

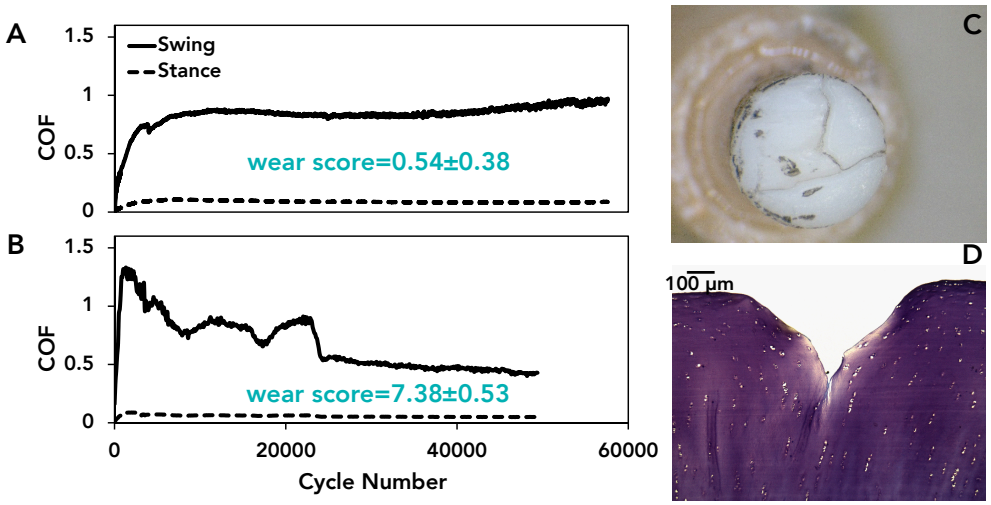

Figure 9. COF versus cycle numbers measured on PCU, for 60 hours, using UMT-3, at the contact pressure of 0.4 MPa during swing and **A:** 1 MPa and **B:** 4.5 MPa, during stance, in the presence of BSA+HA+PRG4+POPC. **C:** Damaged osteochondral plug at the end of the experiment at 4.5 MPa, related to plot **B**. **D:** The histology picture of the damage at the cartilage surface, related to plot **B**.

surface modifications of PCU was able to adsorb PRG4 and POPC, these lubricants remained ineffective in improving friction but there was a decrease in COF with increasing P_c up to ~1 MPa according to a power law, but any further increase in P_c does not decrease COF. Wear of cartilage against PCU materials was not higher than its wear against meniscus up to 36 hours at 1 MPa and for 9 hours up to 4.5 MPa.

Acknowledgments

This research forms part of the Project P2.03 TRAMMPOLIN of the research program of the BioMedical Materials Institute, co-funded by the Dutch Ministry of Economic Affairs. We acknowledge grant no. 91112026 from the Netherlands Organization for Health Research and Development (ZonMW) for the purchase of UMT-3 tribometer setup. We also acknowledge grant no. 355591-2009 from the Natural Sciences and Engineering Research Council of Canada. We also like to thank Bachelor's students Simone van der Hulst and Erik Jan Westerman from the Department of Biomedical Engineering, UMCG, Groningen, The Netherlands for their partial contribution in the experimental section of this study.

Supplementary Data

The adsorption mechanism of POPC vesicles on the PCU materials was investigated using quartz crystal microbalance with dissipation (QCM-D) with the same method explained elsewhere.[131] **Supplementary Data Figure 1A–D** shows that POPC vesicles (the gray curves) did not adsorb on any of the PCU materials. Furthermore, the adsorption mechanism of PRG4, albumin and PRG4+albumin on mPCU-s and mPCU-f was studied with the same method (explained elsewhere).[131] **Supplementary Data Figure 1C, D** shows that PRG4, albumin and PRG4+albumin have a similar adsorption trend as compared to PCU and mPCU-c (studied elsewhere[131]). PRG4 (dashed blue curves) adsorbed a lot and made a viscoelastic layer, as opposed to albumin (black curves), which adsorbed less and made a rigid layer on mPCU-s and mPCU-f. In a mixture (blue curves), albumin blocked PRG4 adsorption. The data for PRG4, albumin and PRG4+albumin adsorption on PCU and mPCU-c is not shown here to avoid repetition from **Chapter 3**.

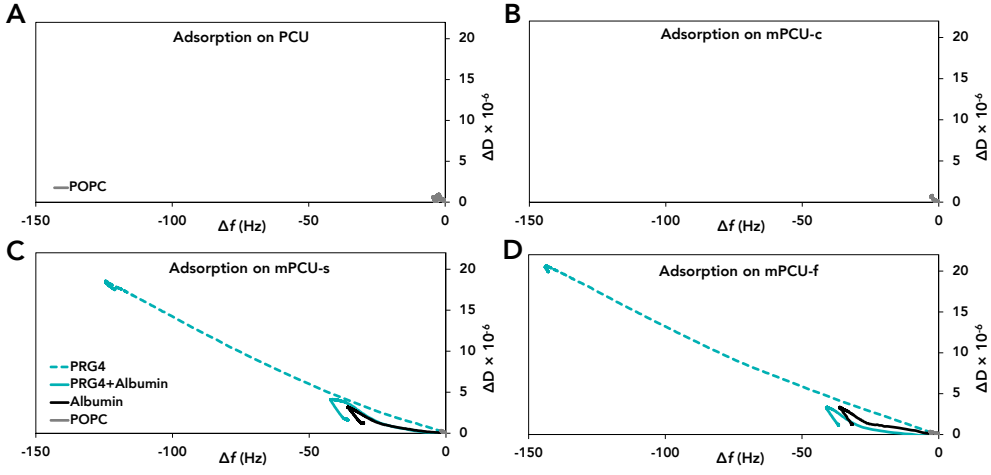

Supplementary Data Figure 1. The dissipation shift versus frequency shift measured using QCM-D during the adsorption of PRG4, albumin, PRG4+albumin and POPC at **A:** PCU, **B:** mPCU-c, **C:** mPCU-s and **D:** mPCU-f.

Chapter 5

General Discussion

In the knee joint, the menisci support articular cartilage throughout its main functions: providing the unique lubrication and load distribution of the joint. Failure of the meniscus results in quick adaptation in the subchondral bone tissue and gradual degeneration of the articular cartilage. To prevent this, replacement of a failing meniscus with an artificial meniscus implant is a promising solution. The TRAMMPOLIN project aimed to develop an anatomically shaped, permanent meniscus implant (**Figure 1A**); the work in this thesis was carried out within the scope of that project. Given the important role of the meniscus in the joint lubrication, different chapters in this thesis dwell upon the changes in the tribology (friction and wear) of the articular cartilage when the meniscus is replaced with a permanent (bulk) polymer material, both at nano- and macro-scale. This thesis pioneers: (1) the measurement of the direct interaction between PRG4 and HA molecules (**Chapter 2**), (2) the development of a protocol to mimic the superficial layer of the articular cartilage *in vitro* using QCM-D (**Chapter 2**) and (3) the *in vitro* characterization of the tribological properties of the native cartilage–meniscus interface (**Chapter 4**).

The dilemma of simplicity of an experimental model versus direct applicability of research results affects the research area of biotribology in general, and is present in this thesis as well. A simplified, far from anatomical reality, experimental set-up, using QCM-D and AFM with colloidal probe, clarified the molecular mechanisms involved in boundary lubrication of the articular cartilage and their effect on the cartilage tribology when a biomaterial is present (**Chapters 2** and **3**). At the

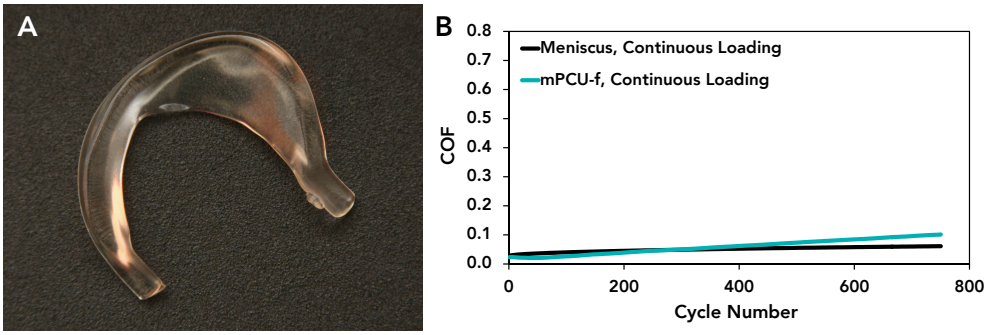

Figure 1. A: The TRAMMPOLIN meniscus implant made from mPCU-c. **B:** Plot representing the similar COF versus cycle number, measured using UMT-3, under continuous loading at 1 MPa, at the cartilage–meniscus interface (black line) and cartilage–mPCU-f interface (blue line) (representing all PCU surfaces), in the presence of BSA+HA, for 1 hour. As seen in **Chapter 4**, this similar behavior of meniscus and biomaterial was not the case when the stance and swing phases of the gait cycle were mimicked.

same time a cartilage–meniscus reciprocating, sliding set-up was used to study friction and wear during the stance and swing phases of the gait cycle on a meniscus tissue or a biomaterial (**Chapter 4**). The following paragraphs summarize the major findings in this thesis and discuss the solution and future work to improve the biomaterial and its lubrication.

In **Chapter 2**, using a QCM-D protocol, it was shown that albumin, the most abundant synovial fluid protein, blocks the interaction of PRG4 molecules with HA, which is a part of the superficial layer of the articular cartilage. But type II collagen, another essential component of the superficial layer, readily interacts with PRG4 molecules and keeps them on the surface despite the presence of albumin. In **Chapter 2**, a protocol was developed using QCM-D to mimic the cartilage superficial layer by first adsorbing loops of thiolated HA and then mechanically entangling collagen in-between them. This creates a soft layer, and adsorption of PRG4 on that provides COFs on the same order of magnitude as the COF of natural cartilage. **Chapter 3** showed that PRG4 molecules adsorb in high amounts on biomaterials and form a highly hydrated viscoelastic layer, as opposed to the thin, rigid layer formed by albumin. Undesirably, presence of albumin completely blocks the adsorption of PRG4 on the biomaterial surfaces.

According to our expectations the PRG4 adsorption on the surface of the biomaterial is necessary to provide the sufficient boundary lubrication. Thus, the surface of polycarbonate urethane has to be modified to be able to adsorb PRG4 molecules despite the presence of albumin. For instance, a specific surface modification using a synthetic molecule with a similar structure (triple helical) and properties as type II collagen can be used, or a specific surface modification with a higher affinity for PRG4 molecules has to be developed. However, according to **Chapters 2** and **3**, adsorption of PRG4 molecules alone is not enough to provide low COF values, and presence of a soft underlying substrate is an important factor as well. On the other hand, surface-active phospholipids have been speculated to play an essential role in the joint lubrication. Unfortunately, the configuration of these molecules in the synovial fluid and the superficial layer of the articular cartilage is not clear and definitely deserves to be studied. As future nano-scale work, the role of SAPL in tribological properties of the joint and their possible interactions with PRG4, albumin, HA and type II collagen have to be extensively studied. In this thesis the adsorption of POPC molecules on the biomaterials was examined; however, no adsorption was observed when POPC in the form of mono-dispersed vesicles solution was flowed over the surfaces using QCM-D (**Chapter 4**). In fact, there are other molecules such as aggrecan or chondroitin sulfate presenting in cartilage but not studied in the current work. The key is that synergistic interactions

between all the molecules present in the cartilage, meniscus and synovial fluid as a whole system provide the unique tribological properties in the joint. Characterizing this synergism will be a complex process. The choice of HA, type II collagen, PRG4 and albumin was just the beginning; the work is far from being complete.

In **Chapter 4** a reciprocating, siding set-up mimicking the stance and swing phases of the gait cycle during normal walking presents more accurate tribological data of cartilage–meniscus/biomaterial system, as compared to continuous loading set-ups, which are mostly used in other studies (comparing **Figure 3A** in **Chapter 4** and **Figure 1B** in the present chapter). Clear differences were present when meniscus was replaced with PCUs. During the stance phase, the COF is low for both cartilage–meniscus and cartilage–biomaterial interfaces, independent of the surface modification of the biomaterial. The reason is the IFPW lubricating mechanism. During the swing phase, the COF is still low for the cartilage–meniscus interface, but 10 fold higher for the cartilage–biomaterial interface. The IFPW lubricating mechanism is fully active at contact pressures higher than 1 MPa. At lower contact pressures, boundary lubrication mechanism also comes into play, gradually raising the COF (**Figure 2**). An ascending COF with time (1 and 4 hours of sliding) is observed. However, after about 10 hours of sliding the COF stabilizes due to stabilization of the lubrication mechanism (**Figure 9A**, **Chapter 4**). In the examined experimental conditions, replacing the meniscus with biomaterial does not show any additional wear of cartilage.

The findings of this thesis indicate two possible reasons why during the swing phase of the gait cycle the cartilage–meniscus interface showed 10 fold lower COF as compared to the cartilage–biomaterial interface:

1. the IFPW lubricating mechanism only partially breaks down due to the meniscus porosity; and
2. the PRG4 molecules provides an efficient boundary lubrication on the meniscus surface.

Therefore, improvement of both boundary lubricating properties (as mentioned earlier) and the IFPW lubricating properties of the biomaterial is necessary. Improving the IFPW lubrication of polycarbonate urethane can be facilitated considering the fact that this mechanism is a unique property of soft, porous materials —biphasic materials—such as cartilage and meniscus. Thus, making the biomaterial porous may be helpful, although the porosity risks the mechanical properties of the implant. The solution can be superficial holes on the surface of the implant

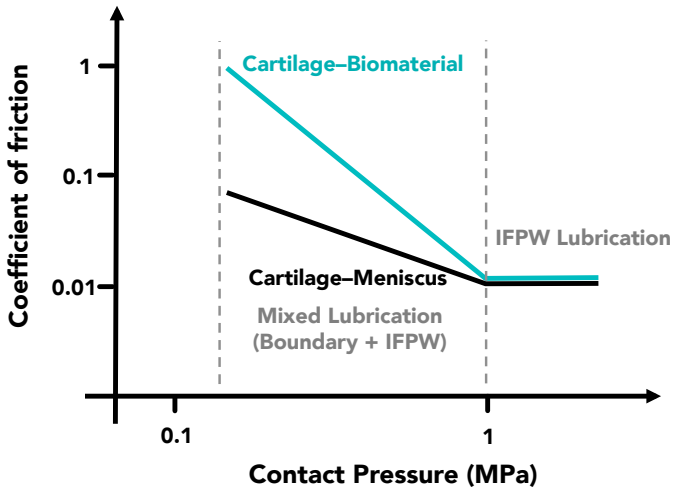

Figure 2. A schematic plot of the COF versus the contact pressure, indicating different lubrication mechanisms at the cartilage–meniscus interface (black line) and the cartilage–biomaterials interface (blue line).

that are deep enough to help this lubrication mechanism, but not so deep that affect the mechanical properties. Another approach can be texturing the surface of the biomaterial to achieve similar surface texture and roughness as meniscus. Further macro-scale studies are required with a wider range of contact pressures and sliding velocities, and the biomaterial has to be tested for longer sliding durations, e.g., a knee joint simulator can be of great help. In addition, experiments in the presence of the whole synovial fluid are recommended. *In vivo* studies are also essential to reveal how the biomaterial behaves while being implanted and study the possible wear and damage to the articular cartilage.

Bibliography

[1] Dowson, D., Bio-tribology. *Faraday Discussions*. **2012**, *156*, 9–30.

[2] Lee, S.; Spencer, N. D., Sweet, hairy, soft, and slippery. *Science*. **2008**, *319*, 575–576.

[3] Dejak, B.; Młotkowski, A.; Romanowicz, M., Finite element analysis of stresses in molars during clenching and mastication. *The Journal of Prosthetic Dentistry*. **2003**, *90*, 591–597.

[4] Trutoiu, L. C.; Carter, E. J.; Matthews, I.; Hodgins, J. K., Modeling and animating eye blinks. *ACM Transactions on Applied Perception*. **2011**, *8*, 1–17.

[5] Charnley, J., The lubrication of animal joints in relation to surgical reconstruction by arthroplasty. *Annals of the Rheumatic Diseases*. **1960**, *19*, 10–19.

[6] Klein, T. J.; Schumacher, B. L.; Blewis, M. E.; Schmidt, T. A.; Voegtline, M. S.; Thonar, E. J.; Masuda, K.; Sah, R. L., Tailoring secretion of proteoglycan 4 (PRG4) in tissue-engineered cartilage. *Tissue Engineering*. **2006**, *12*, 1429–1439.

[7] Dėdinaitė, A., Biomimetic lubrication. *Soft Matter*. **2012**, *8*, 273–284.

[8] Han, L.; Grodzinsky, A. J.; Ortiz, C., Nanomechanics of the Cartilage Extracellular Matrix. *Annual Review of Materials Research*. **2011**, *41*, 133–168.

[9] Athanasiou, K. A.; Darling, E. M.; Hu, J. C.; DuRaine, G. D.; Reddi, A. H., *Articular Cartilage*. CRC Press, **2013**.

[10] Ng, L.; Grodzinsky, A. J.; Patwari, P.; Sandy, J.; Plaas, A.; Ortiz, C., Individual cartilage aggrecan macromolecules and their constituent glycosaminoglycans visualized via atomic force microscopy. *Journal of Structural Biology*. **2003**, *143*, 242–257.

[11] Peters, T. J., *All About Albumin: Biochemistry, Genetics, and Medical Applications*. Academic Press, **1995**.

[12] Greene, G. W.; Banquy, X.; Lee, D. W.; Lowrey, D. D.; Yu, J.; Israelachvili, J. N., Adaptive mechanically controlled lubrication mechanism found in articular joints. *Proceedings of the National Academy of Sciences of the United States of America*. **2011**, *108*, 5255–5259.

[13] Dahl, L. B.; Dahl, I. M. S.; Engstrom-Laurent, A.; Granath, K., Concentration and molecular weight of sodium hyaluronate in synovial fluid from patients with rheumatoid arthritis and other arthropathies. *Annals of the Rheumatic Diseases*. **1985**, *44*, 817–822.

[14] Slack, S. M., Appendix A—Properties of Biological Fluids. In *Biomaterials Science: An Introduction to Materials in Medicine*, Ratner, B. D.; Hoffman, A. S.; Schoen, F. J.; Lemons, J. E., eds., 3rd ed., Elsevier, **2013**, p. 1479−1482.

[15] Jay, G. D., Lubricin and surfacing of articular joints. *Current Opinion in Orthopaedics*. **2004**, *15*, 355−359.

[16] Steele, B. L.; Alvarez-Veronesi, M. C.; Schmidt, T. A., Molecular weight characterization of PRG4 proteins using multi-angle laser light scattering (MALLS). *Osteoarthritis and Cartilage*. **2013**, *21*, 498−504.

[17] Yu, J.; Banquy, X.; Greene, G. W.; Lowrey, D. D.; Israelachvili, J. N., The boundary lubrication of chemically grafted and cross-linked hyaluronic acid in phosphate buffered saline and lipid solutions measured by the surface forces apparatus. *Langmuir*. **2012**, *28*, 2244−2250.

[18] Hills, B.; Crawford, R., Normal and prosthetic synovial joints are lubricated by surface-active phospholipid A Hypothesis. *The Journal of Arthroplasty*. **2003**, *18*, 499−505.

[19] Wise, C. M.; White, R. E.; Agudelo, C. A., Synovial fluid lipid abnormalities in various disease states: review and classification. *Seminars in Arthritis and Rheumatism*. **1987**, *16*, 222−230.

[20] Dumbleton, J., *Tribology of Natural and Artificial Joints*. Elsevier, **1981**.

[21] Makris, E. A.; Hadidi, P.; Athanasiou, K. A., The knee meniscus: structure-function, pathophysiology, current repair techniques, and prospects for regeneration. *Biomaterials*. **2011**, *32*, 7411−7431.

[22] Proctor, C. S.; Schmidt, M. B.; Whipple, R. R.; Kelly, M. A.; Mow, V. C., Material properties of the normal medial bovine meniscus. *Journal of Orthopaedic Research*. **1989**, *7*, 771−782.

[23] Gupte, C. M.; Bull, A. M. j.; Thomas, R. D.; Amis, A. A., A review of the function and biomechanics of the meniscofemoral ligaments. *Arthroscopy*. **2003**, *19*, 161−171.

[24] Arnoczky, S. P.; Warren, R. F., Microvasculature of the human meniscus. *The American Journal of Sports Medicine*. **1982**, *10*, 90−95.

[25] Seror, J.; Merkher, Y.; Kampf, N.; Collinson, L.; Day, A. J.; Maroudas, A.; Klein, J., Articular cartilage proteoglycans as boundary lubricants: structure and frictional interaction of surface-attached hyaluronan and hyaluronan-aggrecan complexes. *Biomacromolecules*. **2011**, *12*, 3432−3443.

[26] Schmidt, T. A.; Gastelum, N. S.; Nguyen, Q. T.; Schumacher, B. L.; Sah, R. L., Boundary lubrication of articular cartilage: role of synovial fluid constituents. *Arthritis and Rheumatism*. **2007**, *56*, 882−891.

[27] Katta, J.; Jin, Z.; Ingham, E.; Fisher, J., Biotribology of articular cartilage-A review of the recent advances. *Medical Engineering & Physics*. **2008**, *30*, 1349−1363.

[28] MacConaill, M. A., The function of intra-articular fibrocartilages, with special reference to the knee and inferior radio-ulnar joints. *Journal of Anatomy*. **1932**, *66*, 210−227.

[29] Jones, E., Joint lubrication. *The Lancet*. **1936**, *227*, 1043−1045.

[30] Dowson, D., Modes of lubrication in human joints. *Proceedings of the Institution of Mechanical Engineers, Conference Proceedings*. **1966**, *181*, 45−54.

[31] Gleghorn, J. P.; Bonassar, L. J., Lubrication mode analysis of articular cartilage using Stribeck surfaces. *Journal of Biomechanics*. **2008**, *41*, 1910−1918.

[32] L. Dintenfass, Lubrication in synovial joints: A theoretical analysis. *The Journal of Bone & Joint Surgery*. **1963**, *45*, 1241−1256.

[33] Zhu, D., *Encyclopedia of Tribology*. Springer US, Boston, MA, **2013**.

[34] McCutchen, C. W., The frictional properties of animal joints. *Wear*. **1962**, *5*, 1−17.

[35] Forster, H.; Fisher, J., The influence of loading time and lubricant on the friction of articular cartilage. *Proceedings of the Institution of Mechanical Engineers, Part H: Journal of Engineering in Medicine*. **1996**, *210*, 109−119.

[36] Ateshian, G. A.; Lai, W. M.; Zhu, W. B.; Mow, V. C., An asymptotic solution for the contact of two biphasic cartilage layers. *Journal of Biomechanics*. **1994**, *27*, 1347−1360.

[37] Caligaris, M.; Ateshian, G. A., Effects of sustained interstitial fluid pressurization under migrating contact area, and boundary lubrication by synovial fluid, on cartilage friction. *Osteoarthritis and Cartilage*. **2008**, *16*, 1220−7.

[38] Swann, D. A.; Radin, E. L., The Molecular Basis of Articular Lubrication. I. Purification and Properties of a Lubricating Fraction from Bovine Synovial Fluid. *Journal of Biological Chemistry*. **1972**, *247*, 8069−8073.

[39] Hills, B. A.; Butler, B. D., Surfactants identified in synovial fluid and their ability to act as boundary lubricants. *Annals of the Rheumatic Diseases*. **1984**, *43*, 641–648.

[40] Ateshian, G. A., A Theoretical Formulation for Boundary Friction in Articular Cartilage. *Journal of Biomechanical Engineering*. **1997**, *119*, 81–86.

[41] Hills, B. A., Boundary lubrication in vivo. *Proceedings of the Institution of Mechanical Engineers, Part H: Journal of Engineering in Medicine*. **2000**, *214*, 83–94.

[42] Unsworth, A., Tribology of human and artificial joints. *Proceedings of the Institution of Mechanical Engineers, Part H: Journal of Engineering in Medicine*. **1991**, *205*, 163–172.

[43] Maroudas, A., Hyaluronic acid films. *Proceedings of the Institution of Mechanical Engineers, Conference Proceedings*. **1966**, *181*, 122–124.

[44] Walker, P. S.; Dowson, D.; Longfield, M. D.; Wright, V., "Boosted lubrication" in synovial joints by fluid entrapment and enrichment. *Annals of the Rheumatic Diseases*. **1968**, *27*, 512–520.

[45] Fein, R. S., Are synovial joints squeeze-film lubricated? *Proceedings of the Institution of Mechanical Engineers, Conference Proceedings*. **1966**, *181*, 125–128.

[46] Higginson, G. R.; Norman, R., A model investigation of squeeze-film lubrication in animal joints. *Physics in Medicine and Biology*. **1974**, *19*, 785–792.

[47] Dowson, D.; Jin, Z. M., Micro-elastohydrodynamic lubrication of synovial joints. *Engineering in Medicine*. **1986**, *15*, 63–65.

[48] Murakami, T.; Higaki, H.; Sawae, Y.; Ohtsuki, N.; Moriyama, S.; Nakanishi, Y., Adaptive multimode lubrication in natural synovial joints and artificial joints. *Proceedings of the Institution of Mechanical Engineers, Part H: Journal of Engineering in Medicine*. **1998**, *212*, 23–35.

[49] Chan, S. M. T.; Neu, C. P.; DuRaine, G.; Komvopoulos, K.; Reddi, A. H., Atomic force microscope investigation of the boundary-lubricant layer in articular cartilage. *Osteoarthritis and Cartilage*. **2010**, *18*, 956–963.

[50] Schumacher, B.; Block, J.; Schmid, T.; Aydelotte, M.; Kuettner, K., A novel proteoglycan synthesized and secreted by chondrocytes of the superficial zone of articular cartilage. *Archives of Biochemistry and Biophysics*. **1994**, *311*, 144–152.

[51] Seror, J.; Sorkin, R.; Klein, J., Boundary lubrication by macromolecular layers and its relevance to synovial joints. *Polymers for Advanced Technologies*. **2014**, *25*, 468−477.

[52] McDermott, I. D.; Amis, A. A., The consequences of meniscectomy. *The Journal of Bone & Joint Surgery (British Volume)*. **2006**, *88-B*, 1549−1556.

[53] Andrews, S.; Shrive, N.; Ronsky, J., The shocking truth about meniscus. *Journal of Biomechanics*. **2011**, *44*, 2737−2740.

[54] Vrancken, A. C. T.; Buma, P.; van Tienen, T. G., Synthetic meniscus replacement: a review. *International Orthopaedics*. **2013**, *37*, 291−299.

[55] Baker, B. E.; Peckham, A. C.; Pupparo, F.; Sanborn, J. C., Review of meniscal injury and associated sports. *The American Journal of Sports Medicine*. **1985**, *13*, 1−4.

[56] Keene, G. C. R.; Bickerstaff, D.; Rae, P. J.; Paterson, R. S., The natural history of meniscal tears in anterior cruciate ligament insufficiency. *The American Journal of Sports Medicine*. **1993**, *21*, 672−679.

[57] Allen, P. R.; Denham, R. A.; Swan, A. V., Late degenerative changes after meniscectomy. Factors affecting the knee after operation. *The Journal of Bone & Joint Surgery (British Volume)*. **1984**, *66-B*, 666−671.

[58] Englund, M.; Lohmander, L. S., Risk factors for symptomatic knee osteoarthritis fifteen to twenty-two years after meniscectomy. *Arthritis and Rheumatism*. **2004**, *50*, 2811−2819.

[59] Fairbank, T. J., Knee joint changes after menisectomy. *The Journal of Bone & Joint Surgery (British Volume)*. **1948**, *30-B*, 664−670.

[60] Zur, G.; Linder-Ganz, E.; Elsner, J. J.; Shani, J.; Brenner, O.; Agar, G.; Hershman, E. B.; Arnoczky, S. P.; Guilak, F.; Shterling, A., Chondroprotective effects of a polycarbonate-urethane meniscal implant: histopathological results in a sheep model. *Knee Surgery, Sports Traumatology, Arthroscopy*. **2011**, *19*, 255−263.

[61] Verdonk, P. C. M.; Demurie, A.; Almqvist, K. F.; Veys, E. M.; Verbruggen, G.; Verdonk, R., Transplantation of viable meniscal allograft. Survivorship analysis and clinical outcome of one hundred cases. *The Journal of Bone & Joint Surgery*. **2005**, *87*, 715−724.

[62] Verdonk, P. C. M.; Demurie, A.; Almqvist, K. F.; Veys, E. M.; Verbruggen, G.; Verdonk, R., Transplantation of viable meniscal allograft. Surgical technique. *The Journal of Bone & Joint Surgery*. **2006**, *88*, 109−118.

[63] Milachowski, K.; Weismeier, K.; Wirth, C., Homologous meniscus transplantation. *International Orthopaedics*. **1989**, *13*, 1−11.

[64] Cole, B. J.; Carter, T. R.; Rodeo, S. A., Allograft Meniscal Transplantation. *The Journal of Bone & Joint Surgery*. **2002**, *84*, 1236−1250.

[65] Stone, K. R.; Rodkey, W. G.; Webber, R.; McKinney, L.; Steadman, J. R., Meniscal regeneration with copolymeric collagen scaffolds. In vitro and in vivo studies evaluated clinically, histologically, and biochemically. *The American Journal of Sports Medicine*. **1992**, *20*, 104−111.

[66] Klompmaker, J.; Veth, R.; Jansen, H.; Nielsen, H.; De Groot, J.; Pennings, A., Meniscal replacement using a porous polymer prosthesis: a preliminary study in the dog. *Biomaterials*. **1996**, *17*, 1169−1175.

[67] Tienen, T. G.; Heijkants, R. G. J. C.; de Groot, J. H.; Pennings, A. J.; Schouten, A. J.; Veth, R. P. H.; Buma, P., Replacement of the knee meniscus by a porous polymer implant. A study in dogs. *The American Journal of Sports Medicine*. **2006**, *34*, 64−71.

[68] Kang, S.-W.; Son, S.-M.; Lee, J.-S.; Lee, E.-S.; Lee, K.-Y.; Park, S.-G.; Park, J.-H.; Kim, B.-S., Regeneration of whole meniscus using meniscal cells and polymer scaffolds in a rabbit total meniscectomy model. *Journal of Biomedical Materials Research. Part A*. **2006**, *77A*, 659−671.

[69] Mandal, B. B.; Park, S.-H.; Gil, E. S.; Kaplan, D. L., Multilayered silk scaffolds for meniscus tissue engineering. *Biomaterials*. **2011**, *32*, 639−651.

[70] Balint, E.; Gatt, C. J.; Dunn, M. G., Design and mechanical evaluation of a novel fiber-reinforced scaffold for meniscus replacement. *Journal of Biomedical Materials Research. Part A*. **2012**, *100A*, 195−202.

[71] Kon, E.; Filardo, G.; Tschon, M.; Fini, M.; Giavaresi, G.; Reggiani, L. M.; Chiari, C.; Nehrer, S.; Martin, I.; Salter, D. M.; Ambrosio, L.; Marcacci, M., Tissue Engineering for Total Meniscal Substitution: Animal Study in Sheep Model—Results at 12 Months. *Tissue Engineering. Part A*. **2012**, *18*, 1573−1582.

[72] Toyonaga, T.; Uezaki, N.; Chikama, H., Substitute Meniscus of Teflon-net for the Knee Joint of Dogs. *Clinical Orthopaedics and Related Research*. **1983**, *179*, 291−297.

[73] Sommerlath, K.; Gallino, M.; Gillquist, J., Biomechanical characteristics of different artificial substitutes for rabbit medial meniscus and effect of prosthesis size on knee cartilage. *Clinical Biomechanics*. **1992**, *7*, 97–103.

[74] Messner, K., Meniscal substitution with a Teflon-periosteal composite graft: a rabbit experiment. *Biomaterials*. **1994**, *15*, 223–230.

[75] Kobayashi, M.; Chang, Y.-S.; Oka, M., A two year in vivo study of polyvinyl alcohol-hydrogel (PVA-H) artificial meniscus. *Biomaterials*. **2005**, *26*, 3243–3248.

[76] Elsner, J. J.; Portnoy, S.; Zur, G.; Guilak, F.; Shterling, A.; Linder-Ganz, E., Design of a free-floating polycarbonate-urethane meniscal implant using finite element modeling and experimental validation. *Journal of Biomechanical Engineering*. **2010**, *132*, 095001.

[77] De Coninck, T.; Elsner, J. J.; Linder-Ganz, E.; Cromheecke, M.; Shemesh, M.; Huysse, W.; Verdonk, R.; Verstraete, K.; Verdonk, P., In-vivo evaluation of the kinematic behavior of an artificial medial meniscus implant: A pilot study using open-MRI. *Clinical Biomechanics*. **2014**, *29*, 898–905.

[78] Condello, V.; Arbel, R.; Agar, G.; Rozen, N.; Angele, P.; Victor, J.; Brittberg, M.; Verdonk, P., A novel synthetic meniscus implant for the treatment of middle aged patients: results of 118 patients in a prospective, multi-center study. In *European Federation of National Associations of Orthopaedics and Traumatology Meeting*, London, United Kingdom, **2014**.

[79] Condello, V.; Ronga, M.; Linder-Ganz, E.; Zorzi, C., Alternatives to Meniscus Transplantation Outside the United States. In *Cartilage Restoration*, Farr, J.; Gomoll, A. H., eds., chap. 19, Springer New York, New York, NY, **2013**, p. 223–249.

[80] Rongen, J. J.; van Tienen, T. G.; van Bochove, B.; Grijpma, D. W.; Buma, P., Biomaterials in search of a meniscus substitute. *Biomaterials*. **2014**, *35*, 3527–3540.

[81] Klein, J., Molecular mechanisms of synovial joint lubrication. *Proceedings of the Institution of Mechanical Engineers, Part J: Journal of Engineering Tribology*. **2006**, *220*, 691–710.

[82] Dowson, D., Elastohydrodynamic and micro-elastohydrodynamic lubrication. *Wear*. **1995**, *190*, 125–138.

[83] Jay, G. D.; Tantravahi, U.; Britt, D. E.; Barrach, H. J.; Cha, C.-J., Homology of lubricin and superficial zone protein (SZP): products of megakaryocyte stimulating factor (MSF) gene expression by human synovial fibroblasts and articular chondrocytes localized to chromosome 1q25. *Journal of Orthopaedic Research*. **2001**, *19*, 677−687.

[84] McNary, S. M.; Athanasiou, K. A.; Reddi, A. H., Engineering Lubrication in Articular Cartilage. *Tissue Engineering: Part B*. **2012**, *18*, 1−13.

[85] Das, S.; Banquy, X.; Zappone, B.; Greene, G. W.; Jay, G. D.; Israelachvili, J. N., Synergistic interactions between grafted hyaluronic acid and lubricin provide enhanced wear protection and lubrication. *Biomacromolecules*. **2013**, *14*, 1669−1677.

[86] Kuijer, R.; Van De Stadt, R. J.; De Koning, M. H. M. T.; Van Der Korst, J. K., Influence of Constituents of Proteoglycans on Type II Collagen Fibrillogenesis. *Collagen and Related Research*. **1985**, *5*, 379−391.

[87] Köwitsch, A.; Yang, Y.; Ma, N.; Kuntsche, J.; Mäder, K.; Groth, T., Bioactivity of immobilized hyaluronic acid derivatives regarding protein adsorption and cell adhesion. *Biotechnology and Applied Biochemistry*. **2011**, *58*, 376−389.

[88] Ludwig, T. E.; McAllister, J. R.; Lun, V.; Wiley, J. P.; Schmidt, T. A., Diminished cartilage-lubricating ability of human osteoarthritic synovial fluid deficient in proteoglycan 4: Restoration through proteoglycan 4 supplementation. *Arthritis and Rheumatism*. **2012**, *64*, 3963−3971.

[89] Höök, F.; Rodahl, M.; Brzezinski, P.; Kasemo, B., Energy dissipation kinetics for protein and antibody−antigen adsorption under shear oscillation on a quartz crystal microbalance. *Langmuir*. **1998**, *14*, 729−734.

[90] Veeregowda, D. H.; Kolbe, A.; van der Mei, H. C.; Busscher, H. J.; Herrmann, A.; Sharma, P. K., Recombinant supercharged polypeptides restore and improve biolubrication. *Advanced Materials*. **2013**, *25*, 3426−3431.

[91] Veeregowda, D. H.; van der Mei, H. C.; de Vries, J.; Rutland, M. W.; Valle-Delgado, J. J.; Sharma, P. K.; Busscher, H. J., Boundary lubrication by brushed salivary conditioning films and their degree of glycosylation. *Clinical Oral Investigations*. **2012**, *16*, 1499−1506.

[92] Ducker, W. A.; Senden, T. J.; Pashley, R. M., Direct measurement of colloidal forces using an atomic force microscope. *Nature*. **1991**, *353*, 239−241.

[93] Ralston, J.; Larson, I.; Rutland, M. W.; Feiler, A. A.; Kleijn, M., Atomic force microscopy and direct surface force measurements (IUPAC Technical Report). *Pure and Applied Chemistry*. **2005**, *77*, 2149–2170.

[94] Pettersson, T.; Nordgren, N.; Rutland, M. W.; Feiler, A., Comparison of different methods to calibrate torsional spring constant and photodetector for atomic force microscopy friction measurements in air and liquid. *The Review of Scientific Instruments*. **2007**, *78*, 093702(1–8).

[95] Jay, G. D.; Torres, J. R.; Warman, M. L.; Laderer, M. C.; Breuer, K. S., The role of lubricin in the mechanical behavior of synovial fluid. *Proceedings of the National Academy of Sciences of the United States of America*. **2007**, *104*, 6194–6199.

[96] Chang, D. P.; Guilak, F.; Jay, G. D.; Zauscher, S., Interaction of lubricin with type II collagen surfaces: adsorption, friction, and normal forces. *Journal of Biomechanics*. **2014**, *47*, 659–566.

[97] Chang, D. P.; Abu-Lail, N. I.; Coles, J. M.; Guilak, F.; Jay, G. D.; Zauscher, S., Friction force microscopy of lubricin and hyaluronic acid between hydrophobic and hydrophilic surfaces. *Soft Matter*. **2009**, *5*, 3438–3445.

[98] Zappone, B.; Ruths, M.; Greene, G. W.; Jay, G. D.; Israelachvili, J. N., Adsorption, lubrication, and wear of lubricin on model surfaces: polymer brush-like behavior of a glycoprotein. *Biophysical Journal*. **2007**, *92*, 1693–1708.

[99] Dumont, G. D.; Hogue, G. D.; Padalecki, J. R.; Okoro, N.; Wilson, P. L., Meniscal and chondral injuries associated with pediatric anterior cruciate ligament tears: relationship of treatment time and patient-specific factors. *The American Journal of Sports Medicine*. **2012**, *40*, 2128–2133.

[100] Jacobson, A., Biotribology: the tribology of living tissues. *Tribology & Lubrication Technology*. **2003**, *59*, 32–38.

[101] Zreiqat, H.; Dunstan, C. R.; Rosen, V., *A Tissue Regeneration Approach to Bone and Cartilage Repair*. Mechanical Engineering Series, Springer, Cham, **2015**.

[102] Buma, P.; van Tienen, T.; Veth, R., The collagen meniscus implant. *Expert Review of Medical Devices*. **2007**, *4*, 507–516.

[103] Chiari, C.; Koller, U.; Dorotka, R.; Eder, C.; Plasenzotti, R.; Lang, S.; Ambrosio, L.; Tognana, E.; Kon, E.; Salter, D.; Nehrer, S., A tissue engineering approach to meniscus regeneration in a sheep model. *Osteoarthritis and Cartilage*. **2006**, *14*, 1056–1065.

[104] Kobayashi, M.; Toguchida, J.; Oka, M., Preliminary study of polyvinyl alcohol-hydrogel (PVA-H) artificial meniscus. *Biomaterials*. **2003**, *24*, 639–647.

[105] Majd, S. E.; Kuijer, R.; Köwitsch, A.; Groth, T.; Schmidt, T. A.; Sharma, P. K., Both Hyaluronan and Collagen Type II Keep Proteoglycan 4 (Lubricin) at the Cartilage Surface in a Condition That Provides Low Friction during Boundary Lubrication. *Langmuir*. **2014**, *30*, 14566–14572.

[106] Wang, A.; Essner, A.; Schmidig, G., The effects of lubricant composition on in vitro wear testing of polymeric acetabular components. *Journal of Biomedical Materials Research. Part B, Applied Biomaterials*. **2004**, *68*, 45–52.

[107] Blewis, M. E.; Nugent-Derfus, G. E.; Schmidt, T. A.; Schumacher, B. L.; Sah, R. L., A model of synovial fluid lubricant composition in normal and injured joints. *European Cells & Materials*. **2007**, *13*, 26–39.

[108] Harsha, A. P.; Joyce, T. J., Challenges associated with using bovine serum in wear testing orthopaedic biopolymers. *Journal of Engineering in Medicine*. **2011**, *225*, 948–958.

[109] Feiler, A. A.; Sahlholm, A.; Sandberg, T.; Caldwell, K. D., Adsorption and viscoelastic properties of fractionated mucin (BSM) and bovine serum albumin (BSA) studied with quartz crystal microbalance (QCM-D). *Journal of Colloid and Interface Science*. **2007**, *315*, 475–481.

[110] Chang, D. P.; Abu-Lail, N. I.; Guilak, F.; Jay, G. D.; Zauscher, S., Conformational mechanics, adsorption, and normal force interactions of lubricin and hyaluronic acid on model surfaces. *Langmuir*. **2008**, *24*, 1183–1193.

[111] Indest, T.; Laine, J.; Kleinschek, K. S.; Zemljič, L. F., Adsorption of human serum albumin (HSA) on modified PET films monitored by QCM-D, XPS and AFM. *Colloids and Surfaces A: Physicochemical and Engineering Aspects*. **2010**, *360*, 210–219.

[112] Mate, C. M., *Tribology on the Small Scale: A Bottom Up Approach to Friction, Lubrication, and Wear*. Oxford University Press, **2008**.

[113] Coles, J. M.; Chang, D. P.; Zauscher, S., Molecular mechanisms of aqueous boundary lubrication by mucinous glycoproteins. *Current Opinion in Colloid & Interface Science*. **2010**, *15*, 406–416.

[114] Nejadnik, M. R.; Olsson, A. L. J.; Sharma, P. K.; van der Mei, H. C.; Norde, W.; Busscher, H. J., Adsorption of pluronic F-127 on surfaces with different hydrophobicities probed by quartz crystal microbalance with dissipation. *Langmuir*. **2009**, *25*, 6245–62459.

[115] Pettersson, T.; Naderi, A.; Makuska, R.; Claesson, P. M., Lubrication properties of bottle-brush polyelectrolytes: an AFM study on the effect of side chain and charge density. *Langmuir*. **2008**, *24*, 3336−3347.

[116] Veeregowda, D. H.; Busscher, H. J.; Vissink, A.; Jager, D.-J.; Sharma, P. K.; van der Mei, H. C., Role of structure and glycosylation of adsorbed protein films in biolubrication. *PLoS ONE*. **2012**, *7*, e42600.

[117] Venus Trial. `https://www.meniscus-study.com/home`. **2016**. Accessed: April 2016.

[118] Hirsh, S. L.; McKenzie, D. R.; Nosworthy, N. J.; Denman, J. A.; Sezerman, O. U.; Bilek, M. M. M., The Vroman effect: competitive protein exchange with dynamic multilayer protein aggregates. *Colloids and Surfaces B: Biointerfaces*. **2013**, *103*, 395−404.

[119] Bionate® Thermoplastic Polycarbonate Polyurethane (PCU). `http://www.dsm.com/content/dam/dsm/medical/en_US/documents/bionate(r)-pcu-product-sheet.pdf`. **2012**. Accessed: April 2016.

[120] Moazzez, B.; O'Brien, S. M.; Merschrod S, E. F., Improved adhesion of gold thin films evaporated on polymer resin: applications for sensing surfaces and MEMS. *Sensors*. **2013**, *13*, 7021−7032.

[121] Nakanishi, K.; Sakiyama, T.; Imamura, K., On the adsorption of proteins on solid surfaces, a common but very complicated phenomenon. *Journal of Bioscience and Bioengineering*. **2001**, *91*, 233−244.

[122] McClellan, S. J.; Franses, E. I., Adsorption of bovine serum albumin at solid/aqueous interfaces. *Colloids and Surfaces A: Physicochemical and Engineering Aspects*. **2005**, *260*, 265−275.

[123] Shiboski, S. C.; Shiboski, C. H.; Criswell, L. A.; Baer, A. N.; Challacombe, S.; Lanfranchi, H.; Schiødt, M.; Umehara, H.; Vivino, F.; Zhao, Y.; Dong, Y.; Greenspan, D.; Heidenreich, A. M.; Helin, P.; Kirkham, B.; Kitagawa, K.; Larkin, G.; Li, M.; Lietman, T.; Lindegaard, J.; McNamara, N.; Sack, K.; Shirlaw, P.; Sugai, S.; Vollenweider, C.; Whitcher, J.; Wu, A.; Zhang, S.; Zhang, W.; Greenspan, J. S.; Daniels, T. E., American College of Rheumatology classification criteria for Sjögren's syndrome: A data-driven, expert consensus approach in the Sjögren's International Collaborative Clinical Alliance Cohort. *Arthritis Care & Research*. **2012**, *64*, 475−487.

[124] Manson, T. T.; Cosgarea, A. J., Meniscal injuries in active patients. *Advanced Studies in Medicine*. **2004**, *4*, 545−552.

[125] Jones, J. C.; Burks, R.; Owens, B. D.; Sturdivant, R. X.; Svoboda, S. J.; Cameron, K. L., Incidence and risk factors associated with meniscal injuries among active-duty US military service members. *Journal of Athletic Training*. **2012**, *47*, 67−73.

[126] Majewski, M.; Susanne, H.; Klaus, S., Epidemiology of athletic knee injuries: A 10-year study. *The Knee*. **2006**, *13*, 184−188.

[127] Verdonk, P. C. M.; Forsyth, R. G.; Wang, J.; Almqvist, K. F.; Verdonk, R.; Veys, E. M.; Verbruggen, G., Characterisation of human knee meniscus cell phenotype. *Osteoarthritis and Cartilage*. **2005**, *13*, 548−60.

[128] Ateshian, G. A., The role of interstitial fluid pressurization in articular cartilage lubrication. *Journal of Biomechanics*. **2009**, *42*, 1163−1176.

[129] Abraham, G.; Frank, R.; Gupta, A.; Harris, J.; McCormick, F.; Cole, B., Trends in Meniscus Repair and Meniscectomy in the United States, 2005-2011. *American Journal of Sports Medicine*. **2013**, *41*, 2333−2339.

[130] Vrancken, A. C. T.; Madej, W.; Hannink, G.; Verdonschot, N.; van Tienen, T. G.; Buma, P., Short Term Evaluation of an Anatomically Shaped Polycarbonate Urethane Total Meniscus Replacement in a Goat Model. *PLoS ONE*. **2015**, *10*, e0133138.

[131] Majd, S. E.; Kuijer, R.; Schmidt, T. A.; Sharma, P. K., Role of hydrophobicity on the adsorption of synovial fluid proteins and biolubrication of polycarbonate urethanes: Materials for permanent meniscus implants. *Materials & Design*. **2015**, *83*, 514−521.

[132] Zhu, T. F.; Budin, I.; Szostak, J. W., Vesicle extrusion through polycarbonate track-etched membranes using a hand-held mini-extruder. *Methods in Enzymology*. **2013**, *533*, 275−282.

[133] Horvath, S. M.; Hollander, J. L., Intra-articular tempreture as a measure of joint reaction. *The Journal of Clinical Investigation*. **1949**, *28*, 469−473.

[134] Khoshgoftar, M.; Vrancken, A. C. T.; van Tienen, T. G.; Buma, P.; Janssen, D.; Verdonschot, N., The sensitivity of cartilage contact pressures in the knee joint to the size and shape of an anatomically shaped meniscal implant. *Journal of Biomechanics*. **2015**, *48*, 1427−1435.

Summary

Samenvatting

Summary

Clinical studies have shown that meniscal lesions are one of the most frequent knee injuries. Loss of the meniscus function due to the injury changes the load distribution on the articular cartilage of femur and tibia, resulting in degenerative arthritis. Therefore, the cartilage needs to be protected before it gets degenerated by the malfunctioning meniscus. Considering the currently available treatments, replacing an injured meniscus with a meniscus implant is a promising solution. The main theme of this thesis is the biotribology of the knee joint—the study of the involved mechanisms and molecules—and its role on developing a new meniscus implant. This thesis provides *in vitro* studies of tribology of different biomaterials and surfaces in the presence of different (lubricant) molecules both at nano- (**Chapters 2** and **3**) and macro-scale (**Chapter 4**).

At a more fundamental level, **Chapter 2** aims to clarify the not yet fully understood role of synovial fluid and articular cartilage molecules in the lubrication of the native joint. In particular, the roles of hyaluronan (HA) and type II collagen in binding PRG4 to the cartilage surface were studied, in the presence and absence of albumin. These *in vitro* molecular-level characterizations were done using quartz crystal microbalance with dissipation (QCM-D). Additionally, the changes in the coefficient of friction (COF) brought about by these molecules were studied using atomic force microscopy (AFM) with colloidal probe. QCM-D revealed an interaction between the freely floating PRG4 and surface-bound HA through the C and N termini of PRG4. Other interesting interactions include the observed irreversible PRG4–albumin interaction and reversible albumin–HA interaction. Due to these interactions, PRG4 did not interact with HA in the presence of albumin molecules. Surface-bound type II collagen, on the other hand, interacted very well with PRG4, irrespective of the presence of albumin. In the following step the superficial zone (SZ) of the articular cartilage was mimicked through mechanical entanglement of type II collagen fibrils into surface-bound HA loops. PRG4 adsorbed very well on this layer and albumin was not able to block this interaction. These results underscore the strong contribution of type II collagen fibrils in keeping PRG4 molecules in the SZ during cartilage articulation. Furthermore, PRG4 adsorption on the soft surface of the mimicked SZ provided a COF of 0.010 ± 0.004, the same order of magnitude as the COF of natural cartilage. To conclude, this study proposes that in the SZ of the articular cartilage, not one single molecule but, dependent on the mechanical conditions, different combinations of molecules provide the unique lubrication mechanism of the synovial joints.

The second aim of this thesis, presented in **Chapters 3** and **4**, is to provide comprehensive studies of the friction and wear of a set of polycarbonate urethane (PCU) materials (with or without C18 chains, mono-functional PDMS groups or mono-functional PTFE groups, as surface modifications) considered for use as a meniscus implant.

While the lubrication of the natural meniscus is provided by both absorption and release of the synovial fluid components through its pores, the non-porous PCU meniscus implant can only be lubricated through the adsorption of these lubricating components on its surfaces. Therefore, **Chapter 3** focuses on understanding the adsorption characteristics of PRG4 and albumin on biomaterials and relating it to the nano-tribology of the materials, using QCM-D and AFM with colloidal probe. PCU and PCU modified with surface-tethered C18 chains (mPCU-c) were spin-coated on QCM gold crystals to make this study possible. Both hydrophobic and hydrophilic self-assembled monolayers (SAM) on gold were used as substrates, to study a wider wettability range. PRG4 adsorbed in high amounts and formed a highly hydrated viscoelastic layer on all the surfaces, as opposed to the thin, rigid layer formed by albumin. PRG4 adsorption on hydrophobic surfaces was significantly higher than its adsorption on the hydrophilic surfaces, while albumin adsorption did not show sensitivity to the surface hydrophobicity. The adsorption of PRG4 on the soft surfaces of PCU and mPCU-c significantly decreased the measured COF values, as compared to the COFs measured on the bare surfaces of PCU and mPCU-c. An exceptionally low COF of 0.024 ± 0.018 was measured on mPCU-c, which is on the same order of magnitude as the COF of natural cartilage. Unfortunately, when simultaneously added, albumin completely blocked PRG4 adsorption on either PCU or mPCU-c, and the measured COF values increased. Another interesting observation was that albumin adsorption on hydrophobic substrates (water contact angle ≥70° ± 4°) dramatically increased the measured COF, possibly due to the altered orientation and configuration of the adsorbed albumin. This result indicates tribological risks of increased hydrophobicity through hydrocarbon surface modification of PCU.

Additional QCM-D experiments were performed (**Chapter 4**, supplementary data) to study the adsorption mechanisms of PRG4 and albumin on mPCU-s (modified PCU with mono-functional PDMS groups) and mPCU-f (modified PCU with mono-functional PTFE groups). The adsorption of PRG4 and albumin followed a similar trend to that observed on PCU and mPCU-c, with albumin also blocking the adsorption of PRG4. In the same chapter it is also shown that phospholipids in the form of POPC vesicles did not adsorb on any of the biomaterials.

Chapter 4 addresses the macro-tribology of PCU, mPCU-c, mPCU-s and

mPCU-f, in the presence of the synovial fluid molecules (HA, albumin, POPC and PRG4), thus complementing the molecular-level approach of the previous chapters. A reciprocating, sliding set-up was developed to measure the COF between cartilage and the PCU materials, in which the stance and swing phases of the gait cycle were mimicked by applying specific loading conditions. The contact pressure during swing was 0.4 MPa and the contact pressure during stance was 1 or 4.5 MPa. At the end, the wear and damage of the cartilage due to the articulation against the PCU materials were evaluated using histological techniques. Results were compared to the tribology of an intact knee joint by studying the cartilage–meniscus tribological properties in the same model. The COF measured between cartilage and the native meniscus was low during both stance and swing phases ($0.01 < COF < 0.12$). Cartilage and meniscus are both porous; upon compression the interstitial fluid becomes pressurized and weeps out of their pores to create a thick fluid film at the interface, which lubricates the articulating surfaces, resulting in low COFs. At low contact pressures, i.e., the swing phase, on the other hand, not enough interstitial fluid weeps out to give rise to a sufficiently thick fluid film. In spite of this interpretation, low and high contact pressures applied to mimic the stance and swing phases did not cause a significant difference between COFs measured on meniscus. The PCUs, on the other hand, behaved differently: although the COFs were similar to those measured on meniscus during the stance phase, the COF increased drastically during the swing phase. Therefore, PCU materials behaved worse than meniscus during swing, which indicated complete breakdown of the interstitial fluid pressurization and weeping (IFPW) lubrication mechanism due to their non-porous structure. Under these conditions, the boundary lubrication due to the lubricating molecules could have taken over and facilitated the sliding process. If so, the surface modifications of PCU could have shown an effect during the swing phase. But the surface modifications included in this study did not decrease the COF. Considering the results of **Chapter 3**, the reason probably is the presence of albumin, which blocks the adsorption of the most important boundary lubricant, i.e., PRG4, on the PCU surfaces. Another outcome of this research was the relation between the contact pressures and COF. The COF decreased with increasing the contact pressure according to a power equation up to ~1 MPa, i.e., the IFPW lubrication mechanism no longer decreased the COF and improved the bio-lubrication on either meniscus or biomaterials. The sliding duration mimicked 9 and 36 hours of normal activity. The COF increased with increasing the sliding duration. Changes in the lubricant solution or surface modification of PCU did not affect PCU's tribological performance. The histology showed that PCU materials and meniscus damaged cartilage occasionally, yet no systematic correlation was found between the damage and the experimental condition. The wear of cartilage after articulation against meniscus was low (scores < 1). To be concluded, perma-

nent meniscus implants made of PCU, which show high COF in the swing phase of the gait cycle, can result in patient discomfort and wear of cartilage in the long term.

In this thesis tribological properties of biomaterials for meniscus implant were evaluated through a multiscale approach *in vitro*. The nanoscopic approach of **Chapters 2** and **3** provide information on fundamental level, adsorption mechanism of the molecules and the consequent boundary lubrication, using QCM-D and AFM. The macroscopic approach of **Chapter 4** provides a wider overview of the lubrication mechanisms on the substrate and revealed that boundary lubrication and IFPW lubrication are the operative lubrication mechanisms. Studying the mechanisms within such complex systems as synovial joints asks for such multiscale and comprehensive methods.

Samenvatting

Klinische studies hebben aangetoond dat een laesie van de meniscus een van de meest voorkomende soorten van knieletsel is. Verlies van de meniscus functie ten gevolge van letsel veranderd de distributie van krachten op het kraakbeen in het gewricht van de femur en tibia, resulterend in degeneratieve artritis. Om deze reden moet het kraakbeen beschermd worden vóórdat het beschadigd raakt door een disfunctionerende meniscus. Met inachtneming van de huidige beschikbare behandelingen, is het vervangen van de beschadigde meniscus door een implantaat een veelbelovend alternatief. Het hoofd thema van dit proefschrift is de biotribologie van het kniegewricht—de betrokken mechanismen en moleculen—en de rol ervan in het ontwerpen van een nieuw meniscus implantaat. Dit proefschrift bevat een *in vitro* studie die de tribologie van verschillende biomaterialen en oppervlakken in de aanwezigheid van verschillende (lubricerende) moleculen behandeld, zowel op nano- (**Hoofdstukken 2** en **3**) als macro-niveau (**Hoofdstuk 4**).

Op een meer fundamenteel niveau, is het doel van **Hoofdstuk 2** om de nog niet volledig begrepen rol die synoviaal vocht moleculen in het gewrichtskraakbeen spelen in natuurlijke smering van het gewricht, beter te begrijpen. Meer specifiek werd er met behulp van een *in vitro* model gekeken naar de rol van hyaluronan (HA) en type II collageen in het binden van PRG4 aan het kraakbeen oppervlak op moleculair niveau, in de aan- en afwezigheid van albumine, gebruikmakend van quartz crystal microbalans met dissipatie (QCM-D). De veranderingen op de frictie coëfficiënt (COF) werden onderzocht met behulp van atomic force microscopy (AFM) met een colloïdale probe. QCM-D liet een interactie zien tussen losse PRG4 en oppervlakte gebonden HA door de C en N eindgroepen van PRG4. Andere interessante interacties die werden gezien waren irreversibele interacties tussen PRG4 en albumine en reversibele albumine–HA interacties. Door deze laatste interacties was er geen interactie tussen PRG4 en HA in de aanwezigheid van albumine moleculen. Oppervlakte gebonden type II collageen, echter, liet juist wel interacties zien met PRG4, in aan- én afwezigheid van albumine. De volgende stap was het simuleren van de superficiële zone (SZ) van gewrichtskraakbeen door het mechanisch verwikkelen van type II collageen fibrillen met oppervlakte gebonden HA loops. PRG4 adsorbeerde erg goed op deze laag en albumine was niet in staat om deze interactie te blokkeren. Deze resultaten laten een sterke bijdrage zien van type II collageen in het op het SZ aanwezig houden van PRG4 tijdens bewegingen in het gewricht. Daarnaast liet geadsorbeerd PRG4 op SZ een COF zien van 0.010 ± 0.004, dezelfde orde van grootte als de COF van natuurlijk kraakbeen.

Tenslotte stelt deze studie dat in de SZ van gewrichtskraakbeen, niet één, maar afhankelijk van de mechanische condities, verschillende combinaties van meerdere moleculen verantwoordelijk zijn in het voorzien van het unieke smeringssysteem van synoviale gewrichten.

Het tweede doel van dit proefschrift, gepresenteerd in **Hoofstukken 3** en **4**, was het voorzien in uitgebreide studies naar de wrijving en slijtage van een set polycarbonaat urethaan (PCU) materialen (met of zonder oppervlakte gebonden C18 ketens, mono-functionele PDMS groepen of mono-functionele PTFE groepen als oppervlakte modificaties), die overwogen worden voor gebruik als meniscus implantaat.

Terwijl de smering van de natuurlijke meniscus verzorgd wordt door zowel absorptie als release van synoviaal vocht componenten door de poriën, kan de niet poreuze PCU meniscus alleen gesmeerd worden door adsorptie van deze smerende componenten op het oppervlak. Vandaar dat **Hoofdstuk 3** gericht is op het begrijpen van de adsorptie karakteristieken van PRG4 en albumine op biomaterialen en deze relateert aan de nano-tribologie van de materialen, door middel van QCM-D en AFM met colloïdale probe. PCU en PCU met oppervlakte gebonden C18 ketens (mPCU-c) werden op QCM kristallen gespincoat om dit onderzoek mogelijk te maken. Hydrofobe en hydrofiele self-assembled monolayers (SAM) op goud werden gebruikt om een groter bereik van bevochtigingseigenschappen te verkrijgen. PRG4 moleculen adsorbeerden in grote hoeveelheden en vormden een zeer gehydrateerde viscoelastische laag op alle oppervlakken, in tegenstelling tot albumine dat een dunne starre laag vormde. PRG4 adsorptie op hydrofobe oppervlakken was significant hoger dan op hydrofiele oppervlakken, terwijl albumine adsorptie geen verschil liet zien tussen hydrofiele en hydrofobe oppervlakken. De adsorptie van PRG4 op de zachte oppervlakken van PCU en mPCU-c zorgde voor een significante daling van de gemeten COF waarden, vergeleken met schoon PCU en mPCU-c. Een uitzonderlijk lage COF van 0.024 ± 0.018 werd gemeten op mPCU-c, in dezelfde orde van grootte als de COF van natuurlijk kraakbeen. Helaas blokkeerde albumine, wanneer tegelijkertijd toegevoegd, de adsorptie van PRG4 op PCU en mPCU-c waardoor de gemeten COF waarden toenamen. Een andere interessante observatie was dat albumine adsorptie op hydrofobe substraten (waterrandhoek ≥70° ± 4°) de COF dramatisch liet toenemen, mogelijk door de veranderde oriëntatie en configuratie van de geadsorbeerde albumine. Dit resultaat laat de aan tribologie gerelateerde risico's van een verhoogde hydrofobiciteit zien door hydrocarbon modificatie van PCU.

Extra experimenten werden uitgevoerd om de adsorptie mechanismen te bestuderen van PRG4 en albumine op mPCU-s (gemodificeerd met mono-functio-

nele PDMS groepen) en mPCU-f (gemodificeerd met mono-functionele PTFE groepen) met behulp van QCM-D (**Hoofdstuk 4**, supplementary data). De adsorptie van moleculen was vergelijkbaar met die op PCU en mPCU-c en albumine blokkeerde de adsorptie van PRG4 eveneens. In hetzelfde hoofdstuk is ook te zien dat lipiden in de vorm van POPC vesicles op geen van de biomaterialen adsorberen.

Om het perspectief volledig te maken hebben we in **Hoofdstuk 4** de macrotribologie van PCU, mPCU-c, mPCU-s en mPCU-f bestudeerd, in de aanwezigheid van synoviaal vocht moleculen (HA, albumine, POPC en PRG4). Een reciprocerend glijdend model was ontwikkeld om de COF te meten tussen kraakbeen en PCU materialen, waarin de stand en zwaaifase van de loopcyclus werden nagebootst door specifieke belasting. De belasting gedurende de zwaaifase was 0.4 MPa en de belasting tijdens de stand was 1 of 4.5 MPa. Uiteindelijk werd de schade en slijtage van het kraakbeen ten gevolge van het contact met de PCU materialen geëvalueerd met behulp van histologie. De resultaten werden vergeleken met de tribologie van een intacte knie door middel van het bestuderen van de kraakbeen–meniscus tribologie in hetzelfde model. De gemeten COF op de intacte meniscus was laag, zowel tijdens stand als in de zwaaifase ($0.01 < COF < 0.12$). Kraakbeen en meniscus zijn beiden poreus en wanneer ze samengedrukt worden wordt de druk op de interstitiële vloeistof verhoogd, waardoor deze uit de poriën komt en een film vormt op het oppervlak die een smerende werking heeft, resulterend in lage COFs. Bij een lage druk, i.e. tijdens de zwaaifase, wordt niet genoeg interstitiële vloeistof door de poriën geperst waardoor de smerende film niet gevormd wordt. Echter, dit verschil leidt niet tot significante verschillen in COFs gemeten op de meniscus tijdens stand en zwaaifases. PCUs gedroegen zich anders, hoewel de COFs gemeten tijdens de stand fase vergelijkbaar waren, was de COF tijdens de zwaaifase aanzienlijk hoger dan op de meniscus. Vandaar dat PCU materialen veel slechter presteerden dan de meniscus tijdens de zwaaifase, wat een aanwijzing is voor een absentie van het door de interstitiële vloeistofdruk (IFPW) veroorzaakte smeringsmechanisme. Onder deze omstandigheden kan het type smering veranderd zijn in grenssmering en zo het glijden hebben gefaciliteerd. In dit geval zouden de oppervlakte modificaties van PCU een effect hebben laten zien tijdens de zwaaifase, maar de bestudeerde modificaties verlaagden de COF niet. Met inachtneming van de resultaten in **Hoofdstuk 3** is de reden daarvoor waarschijnlijk de aanwezigheid van albumine, die de adsorptie van PRG4, het belangrijkste molecuul voor adequate smering, op de PCU blokkeert. Een andere uitkomst van dit onderzoek was de relatie tussen de contact druk en COF. De COF werd lager met stijgende druk volgens een machtsverband, maar dit stopte boven ~1 MPa, i.e., het IFPW smeringsmechanisme verlaagde de COF niet langer en verbeterde de bio-lubricatie op zowel meniscus als biomateriaal. De duur van het experiment

bootste 9 en 36 uur van normale patiënt activiteit na. De COF werd hoger naarmate de duur van het experiment langer werd. Veranderingen in de smeringsvloeistof of oppervlakte functionalisatie van PCU hadden geen effect op de tribologische eigenschappen van PCU. Histologie liet zien dat de biomaterialen en meniscus in sommige gevallen beschadigd kraakbeen lieten zien, maar er werd geen correlatie gevonden tussen de schade en de experimentele condities. Kraakbeen slijtage na wrijving tegen de meniscus was laag (scores <1). Concluderend betekent dit dat permanente meniscus implantaten van PCU die een hoge COF in de zwaaifase laten zien kunnen resulteren in ongemak voor de patiënt en slijtage van het kraakbeen op lange termijn.

In dit proefschrift zijn de tribologische eigenschappen van biomaterialen als meniscus implantaat geëvalueerd door middel van een uitgebreide *in vitro* experimentele aanpak. De nanoscopische aanpak van **Hoofdstukken 2** en **3** leverde informatie op een fundamenteel niveau, adsorptie mechanismen van de moleculen en de daarop volgende grenssmering, door het gebruik van QCM-D en AFM. De macroscopische aanpak van **Hoofdstuk 4** resulteerde in een uitgebreider overzicht van de smeringsmechanismen op het substraat en onthulde dat grenssmering en IFPW smering aan de orde zijn. Het bestuderen van de mechanismen van zulke complexe systemen als de synoviale gewrichten vraagt om een zeer uitgebreide aanpak en gebruik van diverse methoden.

Abbreviations

AFM:	atomic force microscope
AR:	aspect ratio
BSA:	bovine serum albumin
COF:	coefficient of friction
ECM:	extra-cellular matrix
GAG:	glycosaminoglycans
HA:	hyaluronan
IFPW:	interstitial fluid pressurization and weeping
PBS:	phosphate-buffered saline
PCU:	polycarbonate urethane
PDMS:	polydimethylsiloxane
POPC:	1-palmitoyl-2-oleoyl-sn-glycero-3-phosphocholine
PRG4:	proteoglycan 4
PTFE:	polytetrafluoroethylene
QCM-D:	quartz crystal microbalance with dissipation
SAM:	self-assembled monolayer
SAPL:	surface-active phospholipid
SZ:	superficial zone
SZP:	superficial zone protein
THF:	tetrahydrofuran
UHMWPE:	ultrahigh molecular weight polyethylene
UMT:	universal mechanical tester
M_w:	molecular weight
P_c:	contact pressure
mPCU-c:	modified polycarbonate urethane with C18 chains
mPCU-f:	modified polycarbonate urethane with PTFE groups
mPCU-s:	modified polycarbonate urethane with PDMS groups
t-HA 25:	25% thiolated hyaluronan
t-HA 5:	5% thiolated hyaluronan
t-HA:	thiolated hyaluronan

Acknowledgments

Henk, **Prashant** and **Roel**, words cannot express how grateful I am for the opportunity you gave me here at BME.

Prashant, thank you for being my supervisor, you have been a valuable one! Further, I am thankful for the opportunity you gave me to pursue my PhD, not only in a relatively new scientific field but also in a new country, both of which has enriched me more than words can express. Together, of course with the dear help of others, I feel we have accomplished quite a bit in the field of biotribology. We have published two papers and a third one is recently submitted, which makes me feel proud and happy. Moreover, I feel that our many lively discussions, your insights during our meetings, hours spent in the lab, days spent analyzing the data, months writing on manuscripts have given me the correct set of tools to continue my career in this particular field. On a more personal note, **Prashant**, irrespective of the fact that we did not constantly see eye to eye on some aspects of my work, I always felt I could come to you and share personal things going on in my life, and you were never shy in handing out a Kleenex or two. For this I am ever so thankful.

Roel, it has been a true pleasure having you as one of my supervisors. Most of all it has been interesting working across disciplines and learning from you in respect to your extensive background in the physiology of cartilage and orthopedics. I always felt comfortable picking your brain, so to speak, about these subjects less known to me. I have enjoyed our meetings, and even though we might not have agreed all the time on where to take my manuscripts and/or experiments, I feel that after comparing thoughts and ideas it all became better in the end. Thank you for that and happy retirement!

Henk, I truly appreciate what you have done for the realization of this thesis. Although you were not directly involved in my PhD project in the beginning, having you as the head of the department and a valuable mentor and guider has been a great help and pleasure, thank you! It would only be appropriate to end this acknowledgment to you with a Chinese proverb that made me think of you (I will write it in English but I am sure you would be able to read it back to me in Chinese): *Teachers open the doors, but you must enter yourself*.

My sincere gratitude to the members of the reading committee, **Prof. Emile van der Heide**, **Prof. Nico Verdonschot** and **Prof. Sjoerd K. Bulstra**, for taking your

time to assess my thesis. It has been an honor to have you approve my dissertation.

Next, I would like to thank the dear members of the **TRAMMPOLIN** consortium, including but not limited to **Jac Koenen**, **Pieter Buma**, **Tonny van Tienen**, **Nico Verdonschot**, **René van Donkelaar**, **Keita Ito** and **Detlef Schumann**. It was a pleasure to work with you. I appreciate all the valuable feedback and discussions during the project meetings.

I am also much obliged to my collaborators and co-authors. The quality of this thesis would not be the same without their contribution. Dear **Prof. Tannin Schmidt**, this work would not be possible without you and the PRG4 you provided, and I sincerely appreciate all the valuable comments on the manuscripts. Dear **Prof. Thomas Groth**, I would also like to express my sincere gratitude to you for providing t-HA, which made the publication of the first article possible.

All the students I supervised over these years, **Aditya**, **Simone**, **Otmar**, **Frank**, **Erik-Jan**, **Philippine**, **Nikki**, Fabian, Suzanne, Merel, Eef, Chantal, Astrid and Maarten, your contribution to this work is truly appreciated.

I would also like to express my appreciations to all the academic staff at BME: **Henny van der Mei**, **Willem Norde**, **Theo van Kooten**, **Jelmer Sjollema**, **Sarthak Misra**, **Patrick van Rijn**, **Romana Schirhagl**, **Dirk Grijpma** and **Danielle Neut**.

Wya, **Ina** and **Willy**, you were always ready to help; thank you for all the financial paper works and the administrative affairs. **Betsy**, thank you for being my lab coach and showing me around in the lab. **Joop**, thank you for teaching me how to operate the AFM; without you a big part of this work would be impossible. **Hans**, thank you for all the help especially with UMT and DLS. **Marianne**, thank you for always readily helping with ordering chemicals and whatever was missing. **Ed**, thanks for all the computer-related support. **Willem**, **Gesinda**, **René**, **Jelly**, **Minnie**, **Corien** and **Chris**, thank you all for your help and making lab a pleasant place to work in.

Colleagues/friends at BME: **Akshay**, **Anna**, **Bart**, **Brandon**, **Edward**, **Ferdi**, **Hilde**, **Mark**, **Mihaela**, **Niar**, **Nina**, **Jenny**, **Jiapeng**, **Philipp**, **Qihui**, **Raquel**, **René**, **Simon**, **Song**, **Stefan**, **Vera**, **Willem** and **Yi Wang**, your presence made my days at BME much more enjoyable. Thanks for all the fun moments we shared during coffee/tea/lunch breaks, Kolff days, parties and drinks.

Jan and **Rebecca**, will I ever find office-mates as great as you again? **Jan**, thank you for taking your time to translate the thesis summary into Dutch. **Rebecca**, thank you for teaching me how to work with POPC. My previous office-mates, **Arina**,

Bu, **Helen**, **Jesse**, **Joana**, **Victor** and **Yun**, thanks for all the conversations, dinners and traveling.

Katya and **Rebecca**, my dear paranimfen, nothing can replace your endless support through all these years. Thank you for standing next to me on this important day of my life as well.

To be far from family is difficult. Strangers who became good friends of mine in Groningen made that easier and smoother. To all of you at the BME, UMCG, Zernike Campus or Rob&Inez Tango School: **Katia**, **Victoria**, **Riccardo**, **Agnieszka**, **Deepak**, **Barbara**, **Jan**, **Yiwen**, **Fabiola**, **Susan**, **Genia**, **Marta**, **Jelena**, **Henry**, **Milica**, **Solmaz**, **Thomas**, **Gemma**, **Edu**, **Wenjun**, **Tao**, **Rob**, **Inez**; and all the amazing people of the **Molecular Dynamics Group** especially **Clément**, **Helgi**, **Floris**, **Pim**, and **Ignacio**; What would life be without friends? Thanks for all the sightseeing, dinners, lunches, brunches, BBQs, drinks, parties, game nights, …!

I met very special people in Groningen who became my "family" here, **Rebecca**, **Katya**, **Ghazaleh**, **Gülcan** and **Manel**, I cannot imagine my life here without you. How many new cities/places discovered together, how many great moments engraved in my memories, how much I truly enjoyed you and your company …

Rebecca, nothing brings two people together more than running around shouting "bananaaa" and "fin" for no apparent reason and then laugh uncontrollably. We have shared many extremely funny moments together as well as tough ones. I am ever grateful for the three years we have been by each other's side, emotionally as well as physically (being my office mate and all!!!). Thanks for letting me be who I am in front of you. Azizam, I hope that wherever the future brings us, there will always be time for us to meet and catch up, because you know, *a friendship is not a big thing, it is a million little things*…

Katya, at first our shared passion for traveling and fashion brought us together; later your great personality kept us together. You are such an amazing friend and a dedicated scientist who is always ready to give wise and short-to-the-point advice. I learned a lot from you. Thank you for making me a better person because, as you quote from Terry Pratchett, *I'm made up of everyone I've ever met who's changed the way I think*. Also thanks for proof-reading my thesis.

Gülcan, you took a piece of my heart with yourself to Ankara. I miss you every day since you left Groningen. You are such a positive, kind human being. Bebisim, we proved that a true friendship is not a matter of time, but of quality. I believe this proverb explains our current condition to the point *Gülü seven dikenine katlanır*.

Ghazaleh, I would never think I would find you again, definitely not in Groningen! When living far from home, sometimes it's very relaxing to talk in your mother tongue and analyze all the world's problems with an old friend. I always enjoyed your cozy place and your company. May you continue making coffee for me!

Manel, thanks for introducing me to the Portuguese culture, landscape, *fado*, *Saramago*, food, food, food, …! You are such an honest, caring, passionate friend and a persistent, natural scientist. I am always amazed by your ability of finding solutions for all the problems in one (or two) blink(s) of an eye. I cannot express how grateful I am for your motivation and optimism, and everything you taught me (including Python!). I am happy to have you in my life. I also like to thank your amazing mom and grandma and Bruna for their great company and an incredible time I had in Lisbon. I am ever so grateful for the time and energy you spent on making a perfect cover and layout for this book.

My dearest **Yasser** and **Samaneh**, although we couldn't meet as much as we wanted to after I moved to Groningen (because of the tough lives of a PhD, a professor and an architect), the distance didn't change anything. **Yasser**, you are such an amazing teacher, brilliant scientist and great friend. I learned so much from you and you influenced my life a lot. **Samaneh**, I am always stunned with your energy and can never keep up with that. You are one of the most lovely, kindest and strongest people I know. Next to you I am so comfortable and everything feels so right/great. Thank you both for your never-ending support and concern, throughout my journey from Stockholm to Trondheim to Groningen.

The most important people in my life, my **mom** and **dad**; without your endless and unconditional love and support (and I know how difficult it is for you having your only child living thousands of kilometers away) it wouldn't be possible for me to achieve all of this. Your presence and encouragement have been my greatest source of motivation. Since January 2009 the most unbearable part of my new life outside my country was and is saying goodbye to you at the airport to fly to Stockholm/Amsterdam. It breaks my heart into pieces each and every time. Thank you for always being there for me like nobody else can. Words cannot express how much I love you. همیشه شاد، سلامت و امیدوار باشید. بی نهایت دوستتون دارم.